Effect of reduced expression of sorcin on Ca^{2+} handling, *in vivo* heart function and transcriptional regulation

Inaugural-Dissertation

zur Erlangung des Doktorgrades

der Mathematisch-Naturwissenschaftlichen Fakultät

der Universität zu Köln

vorgelegt von
Malik Alock Suchitra
aus Muzaffar Nagar, India

im Dezember 2005

Berichterstatter: Herr Prof. Dr. Jens Brüning

Frau Prof. Dr. A.A. Noegel

Herr Prof. Dr. Robert H. G. Schwinger

Tag der mündlichen Prüfung: 10 February 2006

To My Parents

TABLE OF CONTENTS

Abbreviations

Abstract

Zusammenfassung

1 Introduction

2 Materials and methods

3   Results

4   Discussion

Abbreviations

(m/m)	Mass/Mass
°C	Degree Celsius
A, mA	Ampere, Milliampere
Ad	Adenovirus
Ad.as.Sor.GFP	Adenovirus antisense sorcin vector expressing Green fluoresecent protein
Ad.GFP	Adenoviral vector expressing Green fluorescent protein
Amp	Ampicillin
ANF	Atrial natriuretic factor
AP	Action potential
ATP	Adenosine triphosphate
ARC	Adult rat cardiomyocyte
β-AR	β-Adrenergic receptor
β-MHC	β-Myosin heavy chain
BNP	B-type natriuretic peptide
BSA	Bovine serum albumin
Ca^{2+}	Calcium ions
cAMP	cyclic Adenosine monophosphate
cDNA	complementary DNA
cGMP	cyclic Guanosine monophosphate
CICR	Calcium induced calcium release
Ci	Curie
CMV	Cytomegalovirus
cpm	Counts per minute
CSQ	Calsequestrin
DAPI	4',6-Diamidino-2-phenylindole dihydrochloride
DCM	Dilated cardiomyopathy
DEPC	Diethylpyrocarbonate
DHPR	Dihydropyridine receptor
DMSO	Dimethylsulfoxide
dNTP	Deoxyribonucleotide triphosphate
DTT	1,4-dithiothreitol
DU	Densitometric units

E-C coupling	Excitation contraction coupling
ECL	Enhanced chemiluminiscence reaction
EDTA	Ethylenedinitrilotetraaceticacid disodiumdihydrate
EGTA	Ethylene glycol-bis (β-Aminoethyl ether) tetracetic acid
FKBP12.6	FK binding protein 12.6
g, mg, μg	Gram, Milligram, Mikrogram
GAPDH	Glyseraldehyde-3-phosphate dehydrogenase
GATA4	GATA binding protein 4
GFP	Green fluorescent protein
h	Hour
HEPES	2-[4-(2-Hydroxyethyl)-1-piperazinyl]-ethane-sulfonic acid
HRP	Horse radish peroxidase
Hz	Hertz [1/s]
IgG	Immunoglobulin G
kb	Kilobase
K_D	Dissociation constant
kDa	Kilodalton
l, ml, μl	Liter, Milliliter, Microliter
LB	Luria bertani medium
LTCC	L-Type calcium channel
mm, μm, nm	Millimeter, Micrometer, Nanometer
mM, μM, nM	Millimol(ar), Micromol(ar), Nanomol(ar)
Mean	Arithmatic mean
MG	Molecular weight in g/mol
MOI	Moieties of infection or Multiplicity of infection (Virus/Cell)
MOPS	3-(N-Morpholino)propanesulfonic acid
mRNA	Messenger ribonucleic acid
n	Number
NCX	$Na^+ Ca^{2+}$-exchanger
NF-AT	Nuclear factor of activated T cells
NFU	Normalised fluorescent units
NGS	Normal goat serum
OD	Optical density
PAGE	Polyacrylamide gel electrophoresis

PBS	Phosphate buffered saline
pCa	Negative logarithm of the calcium ion concentration
pfu	Plaque forming units
pH	Negative log of the H^+ concentration
PKA	Proteinkinase A
PLB	Phospholamban
PMSF	Phenylmethylsulphonylfluoride
PNPP	p-Nitrophenyl phosphate
PVDF	Polyvinyldifluoride
RT	Room temperature
RyR2	Ryanodine Receptor
s, ms	Second, Millisecond
SDS	Sodium dodecyl sulphate
SEM	Standard Error Mean
SERCA 2a	Sarcoplasmic reticulum Ca^{2+}-ATPase Isoform 2a
SR	Sarcoplasmic reticulum
TAE	Tris acetate EDTA
TBS	Tris buffered NaCl
TBST	Tris buffered NaCl with tween
TEMED	N,N,N`,N`Tetramethylendiamine
Tris	Tris(hydroxymethyl)-aminomethane
TTCC	T-type calcium channel
T to peak	Time to peak
U	Enzymatic activity
U/min	Units per minute
V, mV	Volt, Millivolt
vs.	versus

Abstract

An adequate and efficient Ca^{2+} handling is the essential condition for effective functioning of the heart. Decreased peak systolic Ca^{2+} with prolongation of the duration of Ca^{2+} transient, slower rates of SR Ca^{2+} uptake and various other alterations in Ca^{2+} efflux leading to elevation in diastolic Ca^{2+} are the key features of the failing heart. These key alterations in heart failure necessitate further evaluation of proteins involved in these regulatory mechanisms. Sorcin, a penta E-F hand family protein associates with cardiac ryanodine receptors, L-type Ca^{2+} channel as well as SR Ca^{2+} ATPase and modulates excitation-contraction coupling in the heart. The present thesis aims at understanding the role of sorcin in calcium handling, the effect of decreased level of sorcin on remodeling of the heart and subsequent transcriptional regulation, by using the adenoviral antisense RNA approach.

A decrease in the endogenous sorcin expression (75% on the mRNA level and 53% on the protein level) was obtained in the adult rat cardiomyocytes. The decreased amount of sorcin resulted in reduced cell contractility and significantly depressed Ca^{2+} transient amplitude accompanied with the decreased rate of relaxation in the transfected cardiomyocytes. The increase in stimulation frequency was associated with a negative force-frequency relationship in cardiomyocytes with depressed sorcin, mimicking the behavior exhibited by the failing human cardiomyocytes. However, the β-adrenergic stimulation was unaltered. An oxalate facilitated Ca^{2+} uptake assay indicated decreased Ca^{2+} uptake by the sarcoplasmic reticulum in the cardiomyocytes with decreased expression of sorcin. Moreover, incubating the sarcoplasmic reticulum vesicle preparations with recombinant sorcin (1 μM) enhanced the SR Ca^{2+} uptake and brought it back to the control level. The depressed expression of SR Ca^{2+} ATPase on the mRNA as well as protein level was also observed. The expression of ryanodine receptors, triadin and phospholamban was unaltered, while a mild increase in the expression of FKBP12.6 was observed. *In vivo* downregulation of sorcin, achieved by the catheter based cardiac specific gene delivery resulted in severe chamber dilation. Echocardiography revealed ventricular enlargement, decreased heart rate and increased chamber dimension indicating dilated cardiomyopathy in the hearts with depleted levels of sorcin. After 14 days the animals were sacrificed and an increase in the heart weight was observed. In addition, upregulation of calcineurin expression and higher phosphatase activity was observed which was accompanied with increased dephosphorylation of NF-AT$_{C3}$. GATA4 expression was significantly upregulated in the antisense sorcin transfected cardiomyocytes. The mRNA expression of hypertrophic marker gene β-myosin heavy chain was upregulated, while expression of atrial natriuretic factor and B-type natriuretic peptide was unaltered.

In conclusion, using the antisense mRNA approach for sorcin it can be concluded that downregulation of sorcin diminishes the cardiac contractile performance and leads to the ventricular remodeling of the heart. This process is at least partially due to the activation of calcineurin-NFAT signaling pathway. The antisense approach proves to be a valuable tool to identify targets that modulate cardiac contractility and may open new avenues for the treatment of myocardial diseases with diminished cardiac output such as heart failure.

Zusammenfassung

Für eine effektive Herzfunktion ist eine effiziente Ca^{2+}-Homöostase wesentlich. Vermindert systolisch freigesetztes Ca^{2+}, eine Verlängerung des Ca^{2+}-Transienten und eine reduzierte Aufnahmerate des sarkoplasmatischen Retikulums (SR) sind wesentliche Veränderungen einer Herzinsuffizienz. Diese Störungen machen eine weitere Untersuchung von Proteinen notwendig, die die myokardiale Ca^{2+}-Homöostase regulieren. Sorcin ist ein EF-Hand Protein, dass mit dem kardialen Ryanodin-Rezeptor, dem L-Typ Ca^{2+}-Kanal sowie mit der SR Ca^{2+}-ATPase assoziiert ist und die elektromechanische Kopplung am Herzen mitreguliert. Die vorliegende Doktorarbeit hatte zum Ziel, die Rolle von Sorcin für die Ca^{2+}-Homöostase, die Bedeutung einer verminderten Expression von Sorcin auf die Herzentwicklung und die transkriptionale Regulation mit Hilfe von adenoviralem Antisense Sorcin zu untersuchen.

Eine Reduktion der endogenen Sorcin Expression (74% der mRNA Expression und 53% der Proteinexpression) konnte mit Hilfe dieses adenoviralen antisense Ansatzes in isolierten Rattenkardiomyozten erzielt werden. Die verminderte Sorcin Expression führte zu einer reduzierten Zellkontraktion, einer verminderten Amplitude des Ca^{2+}-Transienten und einer Verlängerung der Relaxationsrate. Erhöhung der Stimulationsfrequenz zeigte eine negative Kraft-Frequenz-Beziehung (KFB) in Kardiomyozyten mit verminderter Sorcin Expression, die mit der KFB an insuffizienten, menschlichen Kardiomyozyten vergleichbar ist. Die β-adrenerge Stimulation blieb erhalten. Der Ca^{2+}-Uptake mit Oxalat zeigte verminderte Aufnahmeraten des SR an Kardiomyozyten mit verminderter Sorcin Expression, Inkubation mit rekombinantem Sorcin (1µM) führten zu einer erhöhten SR Ca^{2+}-Aufnahmerate. Zudem wurde eine reduzierte Expression der SR Ca^{2+}-ATPase nachgewiesen. Die Expression des Ryanodin Rezeptors, von Triadin und Phospholamban blieb unverändert, während die Proteinexpressin von FKBP 12,6 erhöht war. Reduktion der Expression von Sorcin mit Hilfe eines katheterbasierten, intrakoronaren Applikationsweges in vivo führte zu einer schweren Herzdilatation. Echokardiographie der transfizierten Herzen zeigte eine ventrikuläre Herzvergrösserung, eine verminderte Herzfrequenz und einen erhöhten end-diastolische Durchmesser. Nach 14 Tagen Transfektion wurde morphologisch eine Zunahme des Herzgewichtes gesehen. Zudem wurden an Antisense Sorcin transfizierten Kardiomyozyten eine erhöhte Calcineurin Aktivität und Expression, verbunden mit einer höheren NF-AT$_{C3}$ Dephosphorylierung, und eine erhöhte Expression der GATA4 Expression gefunden. Das Hypertrophiemarker-Gene „β- Myosin Heavy Chain" war erhöht, während die Expression des atrialen, natiuretischen (ANP) und gehirnspezifischen, natiuretischen Peptiden (BNP) unverändert blieb.

Zusammenfassend werden durch eine Verminderung der Sorcin Expression mit Hilfe eines adenoviralen Anti-sense Ansatzes eine reduzierte kardiale Kontraktionskopplung und eine dilatative Kardiomypathie ausgelöst. Dieser Prozess beinhaltet Störungen der Ca^{2+}-Homöostase und Aktivierung des Calcineurin- NFAT Signaltransduktionsweges. Die adenovirale anti-sense Strategie kann dazu verwandt werden, um Zielproteine bei der Entstehung einer Herzinsuffizienz zu identifizieren, die die kardialen Kontraktilität und Leistung insbesondere bei verminderten kardialen Pumpleistung verbessern können. Dieser Ansatz kann in der Entwicklung neuer Therapieformen bei der menschlichen Herzinsuffizienz verwandt werden.

1. Introduction

1.1 Calcium cycling in the normal heart

Calcium (Ca^{2+}) ions function as ubiquitous intracellular messengers that regulate many different cellular processes in cardiac myocytes (Frank et al., 2003, Bers, 2005). Ca^{2+} plays a requisite role not only in the electromechanical and contractile activity in the excitation contraction coupling (E-C coupling) (Bers, 2002), but also in modulating E-C coupling by activation of kinases and phosphatases which can modulate gene expression responsible for hypertrophic signaling and heart failure (Chien et al., 2003).

The process ensuring contraction and relaxation through a series of events from electrical excitation of the myocyte to the contraction of the heart is termed as excitation contraction coupling. Depolarization of the plasma membrane during the cardiac action potential activates voltage gated L-type Ca^{2+} channels (LTCC or dihydropyridine receptors) leading to a mild Ca^{2+} influx into the cytosol which in turn triggers a massive release of Ca^{2+} from the sarcoplasmic reticulum through ryanodine receptors (RYR2), this phenomenon is termed as calcium induced calcium release (CICR) (Fabiato, 1985). The tremendous increase in cytoplasmic Ca^{2+} concentration (almost 10 fold) leads to the actin-myosin cross bridge formation, which is activated by Ca^{2+} binding to troponin C and ultimately results in the contraction of myocyte (Solaro et al., 2002, Brixius et al., 2002).

The increase in cytosolic Ca^{2+} concentration during the contraction is immediately followed by Ca^{2+} removal, which results in deactivation of contractile machinery and myocardial relaxation during diastole. Cytosolic Ca^{2+} is pumped back into the sarcoplasmic reticulum (SR) by sarcoplasmic reticulum Ca^{2+} ATPase (SERCA2a) (Bers, 2002, Frank et al., 2003). Activity of SERCA2a is under the control of phospholamban (PLB), which in the nonphosphorylated form inhibits SERCA2a activity while phosphorylation of PLB reverses this inhibition (Koss et al., 1996, Frank et al., 2000).
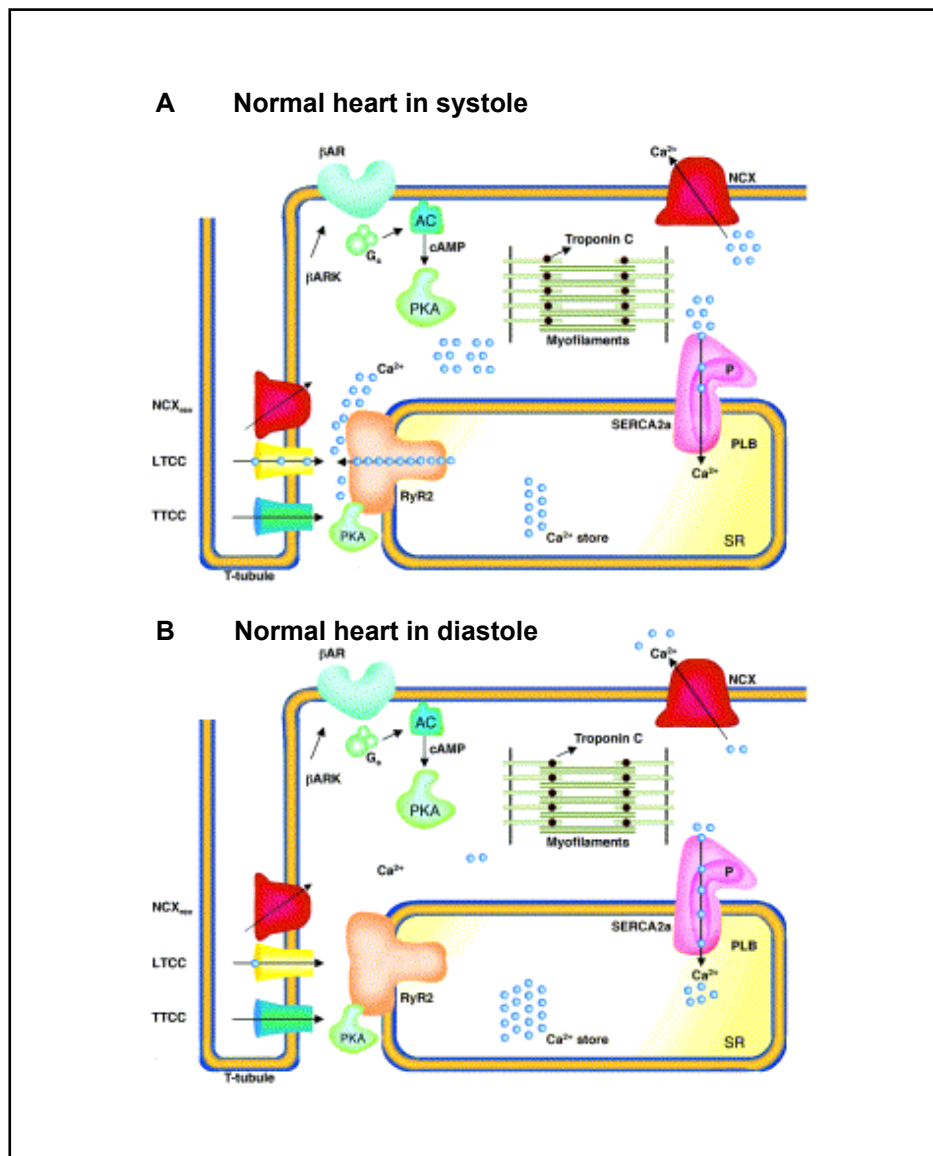
Fig. 1.1 Excitation contraction (E-C) coupling in normal heart

(**A**) Depolarization due to action potential activates voltage gated L-type Ca^{2+} channels in the transverse tubule (yellow) resulting in a mild Ca^{2+} influx (blue circles) into the cytosol, Ca^{2+} influx can also occur through T-type Ca^{2+} channels (blue) or reverse mode Na^+/Ca^+ exchanger (NCX_{rev}, red). The Ca^{2+} influx from LTCC triggers a profound Ca^{2+} release from sarcoplasmic reticulum (SR) via RYR2 (orange). During systole, there is a ten-fold increase in the intracellular Ca^{2+} reaching a concentration up to 1 μM. At this high concentration, free Ca^{2+} binds to troponin C (brown), inducing a conformational change that results in cross bridge formation in actin–myosin myofilaments (green) and muscle contraction. The β-adrenergic signaling pathway (green) is capable of increasing the E-C coupling gain. Agonist activation of β-adrenoceptors (β-AR) allows activation of adenylate cyclase (AC) by production of cyclic AMP (cAMP), which is responsible for the activation of protein kinase A (PKA, green). β-AR kinases regulate the β-AR agonist activation. (**B**) During diastole intracellular Ca^{2+} is pumped back from the cytosol to the SR via SR Ca^{2+} ATPase (SERCA2a, pink) and relaxation of the myocyte is achieved. SERCA2a is regulated by phospholamban (PLB, purple). Phosphorylated PLB (with 'P') does not inhibit SERCA2a under baseline conditions. A part of Ca^{2+} is extruded from the cytosol by sarcolemmal Na^+ / Ca^+ exchanger mode (NCX, red). Modified from: Wehrens and Marks (2003).

1.2 Altered Ca^{2+} cycling in the hypertrophied and failing heart

Abnormal and altered intracellular Ca^{2+} handling plays a crucial role in the development of cardiac hypertrophy, heart failure and fatal ventricular arrhythmias (Wehrens et al., 2003). Depressed systolic intracellular Ca^{2+} transients, increased diastolic intracellular Ca^{2+} concentration and the slow rate of diastolic decay of intracellular Ca^{2+} concentration are the key features of the failing human heart (Beuckelmann et al., 1992, Schwinger et al., 1995). Reduction in the SR Ca^{2+} content (Lindner et al., 2002) and a decreased E-C coupling gain have also been reported in the failing human myocardium (Gomez et al., 1997).

Chronic hyperactivity of the sympathetic nervous system is one of the main characteristic of congestive heart failure (Chidsey, 1962). The constantly elevated high adrenergic activity leads to maladaptive changes in the β-adrenergic signaling pathway and results in the decreased expression and coupling of the β-adrenoceptors (Bristow et al., 1984), reduction in the coupling of the β$_2$-adrenoceptors (Daaka et al., 1997), an increase in the expression of the inhibiting G protein G$_i$, an increase in the expression of the β-adrenoceptor kinases (Neumann et al., 1988, Ungerer et al., 1993) and depressed expression and function of adenylyl cyclases (Rockmann et al., 2002). Altered β-adrenergic signaling and depressed phosphatase activity in heart failure is responsible for hyperphosphorylation of L-type Ca^{2+} channels (Chen et al., 2002), NCX (Wie et al., 2003) and cardiac RYR2 (Reiken et al., 2003, Marx et al., 2002).

1.3 Role of Ca^{2+} cycling proteins in the altered calcium cycling

Periodic change in Ca^{2+} concentration in cardiomyocytes is the prerequisite for cardiac contraction and relaxation. Various proteins associated with the SR, integrally regulate the vital periodic change in intracellular Ca^{2+} concentration ensuring the smooth functioning of the myocardium. Abnormal cardiac E-C coupling is the result of altered function of Ca^{2+} proteins responsible for intracellular Ca^{2+} homeostasis. Altered expression and activity of SERCA2a (Schwinger et al., 1995,) phosphorylation of PLB (Dash et al., 2001), RYR2 (Marks et al., 2002), Na$^+$/Ca$^+$ exchanger and Na$^+$ K$^+$ ATPase (Schwinger et al., 1999) have been reportedly associated with various features of contractile dysfunction (Arai et al., 1993, Go et al., 1995, Hasenfuss 1994).

1.3.1 Ryanodine receptors – A macromolecular complex

Ryanodine receptors (RYR2), a 565 kDa homotetramer consisting of four monomeric subunits is the main SR Ca^{2+} release channel and plays a predominant role in E-C coupling (Marx et al., 2002). The subunit contains a high conductance Ca^{2+} selective pore, Ca^{2+} activation and inactivation sites, several phosphorylation sites and multiple binding sites for an array of endogenous regulators, which include ATP, Mg$^+$ and calmodulin. Knock out of RYR2 gene in mice proved to be fatal and the mice died at embryonic day 10 with morphological abnormalities. Prior to death the knock out cardiomyocytes showed structurally abnormal mitochondria, highly vacuolated SR with elevated concentrations of Ca^{2+}, suggesting that RYR2 is absolutely required for cellular Ca^{2+} homeostasis as a major Ca^{2+} release channel (Takeshima et al., 1998). RYR2 also functions as a scaffolding protein for various other proteins like FK binding proteins, Calmodulin (CaM), calsequestrin, triadin, junction, and several other proteins forming a macromolecular complex channel protein system (Bers, 2004) and alterations in these interacting proteins have been associated with the pathogenesis in the heart.

1.3.2 Proteins interacting with ryanodine receptors

(a) FK binding proteins

FKBP 12.6, a member of immunophilin family of proteins associates with the cytosolic domain of cardiac RYR2 with high affinity (Marx et al., 2002). Disruption of the FKBP12.6 gene in mice resulted in cardiac hypertrophy in male mice, but not in female mice. Female mice hearts were normal, despite the fact that male and female knockout mice displayed similar dysregulation of Ca^{2+} release, the amplitude, duration of Calcium sparks and calcium-induced calcium release gain (Xin et al., 2002). Another study reported consistent display of exercise-induced cardiac ventricular arrhythmias that cause sudden cardiac death due to the ablation of FKBP 12.6 (Wehrens et al., 2003). FKBP 12.6 stabilizes RYR2 channel activity and inhibits the aberrant activation of RYR2 during diastole, the protein kinase A based phosphorylation of FKBP 12.6 causes dissociation of FKBP 12.6 from the RYR2 resulting in unstable RYR2 channel which can induce life threatening arrhythmias (Wehrens et al., 2004).

(b) Calmodulin

Calmodulin (CaM is a 16.6 kDa Ca^{2+} binding protein with four E-F hands existing as pairs on the bi-globular structure (Strynadka et al., 1989). At high $[Ca]_i$ levels, CaM activates its targeting partners by binding to them with high affinity. It is suggested that under physiological conditions CaM bound to RYR2 may inhibit open basal probability and alter the Ca^{2+} dependent activation of the RYR (Yamaguchi et al., 2003).

(C) Protein Kinase A, Calmodulin dependent protein kinase II and phosphatases

Protein Kinase A (PKA) is anchored to cardiac RYR via protein kinase A anchoring protein (AKAP) in the cytosolic domain of RYR2. PKA dependent RYR2 phosphorylation alters RYR2 gating and reportedly speeds up the time course of release without affecting the amount of released Ca^{2+} (Valdiva et al., 2000). In the complex physiological system PKA activation also increases I_{Ca} trigger and SR calcium load in such a way that the amount of SR Ca^{2+} release during E-C coupling is greatly enhanced.

Calmodulin dependent protein kinase II (CaMKII) is mainly expressed as the δ isoform in the heart and is also known to phosphorylate RYR2 and alter RYR2 activity (Wichter et al., 1991). Endogenous CaMKII increases the amount of SR Ca^{2+} release for a given SR Ca^{2+} content and I_{Ca} trigger in intact voltage clamped ventricular cardiomyocytes (Li et al., 1997). Transgenic mice overexpressing CaMKII δ exhibited increased diastolic calcium spark frequency and fractional SR Ca^{2+} release during E-C coupling despite a reduced SR calcium content and diastolic $[Ca]_i$ (Maier et al., 2003).

In heart failure, despite the increased phosphatase expression there is less phosphatase associated with RYR2 that could possibly lead to enhanced RYR2 phosphorylation in heart failure resulting in increased diastolic calcium leak (Bers, 2003).

(d) Calsequestrin, junctin, triadin and histidine rich Ca^{2+} binding protein

Cardiac calsequestrin is a 45.2 kDa high capacity moderate affinity Ca^{2+} binding protein localized at lumen of

the junctional SR in cardiac muscle (Scott et al., 1988; Frank et al., 2001). Calsequestrin (CSQ) undergoes a structural transformation after binding to calcium. Transgenic mice overexpressing more than 10-fold CSQ developed cardiac hypertrophy and the cardiomyocytes showed increased amount of SR Ca^{2+} content (Jones et al., 1998, Sato et al., 1998) but the twitch Ca^{2+} transients and contractions were depressed. Adenoviral mediated moderate overexpression of CSQ (2-4 fold) resulted in enhanced Ca^{2+} transient amplitude and increased SR Ca^{2+} load (Terentyev et al., 2003).

Triadin and junctin are present at the junctional SR and they interact with each other, CSQ and RYR2. The interaction between triadin, junctin and CSQ is suggested to influence indirectly RYR2 gating and Ca^{2+} release (Gyoerke et al., 2004). A histidine rich Ca^{2+} binding protein (170 kDa) is also present in the SR lumen and has been reported to bind to triadin (Sacchetto et al., 2001) and may also influence Ca^{2+} handling (Fan et al., 2004).

1.3.3 Sarcoplasmic reticulum Ca^{2+} ATPase (SERCA2a)

SR Ca^{2+} ATPase is the prime regulator of the rate of Ca^{2+} reuptake during relaxation in the heart (Periasamy et al., 2001). Five distinct Ca^{2+} ATPase isoforms are found in skeletal, smooth and cardiac muscles and are encoded by three different mammalian genes (SERCA1, SERCA2 and SERCA3) (Arai et al., 1994, Loukianov et al., 1998). SERCA2a is the main isoform expressed in cardiac muscle. Transgenic mice overexpressing SERCA2a exhibited increased myocardial contractility and relaxation by increasing SR Ca^{2+} transport (He et al., 1997, Baker et al., 1998). Ablation of SERCA2a and SERCA2b resulted in the embryonic lethality (Periasamy et al., 1999). Heterozygous mutant hearts expressing 65% of the protein levels of SERCA2 as compared to the wild type, exhibited impaired cardiac contractility and relaxation (Ji et al., 2000). Ablation of SERCA2a specifically, resulted in increased incidence of neonatal mortality and structural malformations accompanied with mild cardiac hypertrophy with impaired cardiac contractility and relaxation (Van der Heyen et al., 2001).

1.3.4 Phospholamban

The calcium pumping activity of SERCA2a is primarily regulated by phospholamban (PLB), a low molecular weight (52 amino acid) integral SR membrane phosphoprotein that inhibits SERCA2a in its unphosphorylated state (Frank et al., 2000). Phospholamban is highly conserved and present in single copy in the genome of mammalian and avian species (Chu et al., 1998). Oligomeric phospholamban is a pentamer of five identical subunits (Luo and Kranias, 1998). Phosphorylation of PLB by cyclic-AMP dependent or calmodulin dependent protein kinases (PKA or CaMKII) relieves this inhibition, allowing faster twitch relaxation and decline of $[Ca]_i$ (Munch et al., 2000). Transgenic mice overexpressing two fold higher PLB in the heart displayed impaired cardiac contractility and relaxation but exhibited normal growth (Kadambi et al., 1996). However, 4 fold transgenic overexpression of PLB in mice resulted in development of overt heart failure and a premature mortality with aging (Dash et al., 2001). In contrast ablation of PLB was followed by increased force of

contraction, attenuated β-adrenergic responsiveness, increased relaxation rates and enhanced cardiac in vivo performance (Luo et al., 1994, Chu et al., 1996).
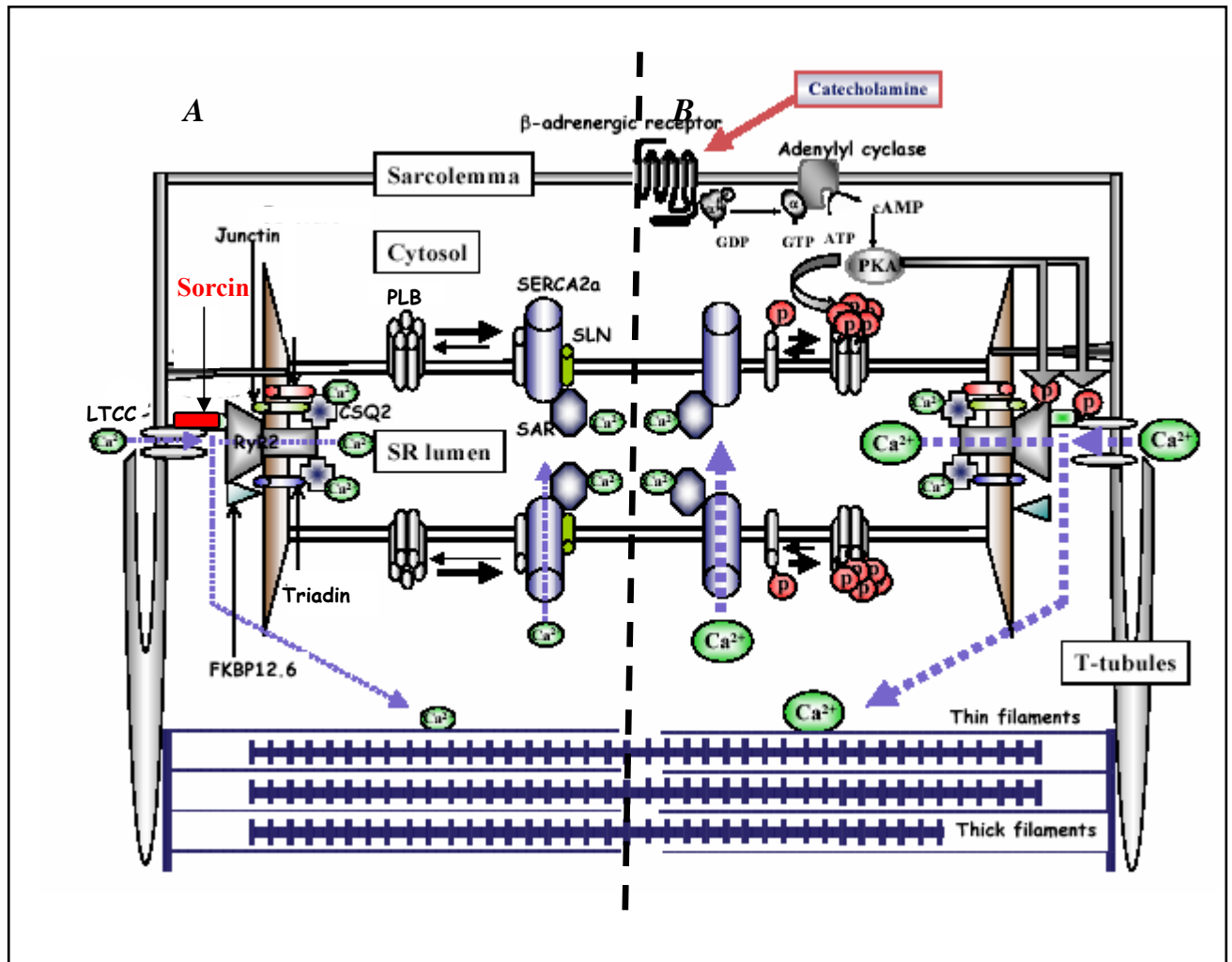
Fig 1.2 Regulation of intracellular calcium homeostasis by Ca^{2+} cycling proteins.

(A) During the action potential a small amount of extracellular Ca^{2+} enters the cardiomyocyte through the sarcolemmal L-type Ca^{2+} channels (LTCC), which in turn triggers the release of a larger amount of Ca^{2+} from the sarcoplasmic reticulum (SR) via ryanodine receptors (RYR2) into the cytosol. Phosphorylated PLB relieves its inhibition on SERCA2a activity, resulting in an increase in Ca^{2+} uptake into the SR. The RyR2 is also associated with cardiac calsequestrin (CSQ), triadin and junctin. Sorcin is a penta-EF hand Ca^{2+} binding protein that binds directly to both RyR2 and the LTCC. **(B)** β-adrenergic stimulation causes enhanced Ca^{2+} release and uptake by via cAMP-dependent PKA signal pathway. PKA phosphorylates L-type Ca^{2+} channels (LTCC), the cardiac ryanodine receptor (RyR2) and phospholamban (PLB). The phosphorylated RyR2 is dissociated from FKBP12.6, resulting in pronounced channel open probability. Phosphorylated PLB relieves its inhibition on SERCA2a activity, resulting in an increase in Ca^{2+} uptake into the SR. The Ca^{2+} movement is indicated with blue broken lines. Modified from: Minamisawa et al. (2004).

1.4 Sorcin and its role in calcium cycling

Sorcin (**so**luble **r**esistance-related **c**alcium-b**in**ding protein) is an evolutionary conserved, 21.6 kDa Ca^{2+} binding protein. Sorcin was originally isolated from multidrug resistant cells in which it was overexpressed as a result of amplification of the sorcin gene (Meyers et al, 1991). In recent years sorcin has emerged as a potential calcium cycling protein and growing literature has emphasised its role in the regulation of intracellular homeostasis and modulation of E-C coupling. However, the ambiguity associated to its function demands further research to fully understand the role played by sorcin in the regulation of calcium cycling in the heart.

1.4.1 Structure of sorcin

Sorcin belongs to the newly found family of penta E-F hand proteins, which contains five E-F hand motifs that associate with membranes in a calcium dependent manner. Binding of Ca^{2+} to the high affinity sites E-F1 and E-F2 induces translocation of sorcin to membranes where it interacts with specific targets (Zamparelli et al., 1997). Sorcin is capable of binding two calcium ions per monomer and exist as dimers in the absence of calcium (Zamparelli et al., 2000). Calcium free human sorcin forms a homodimer, in which each monomer adapts the penta E-F hand motif. Sorcin molecule has a globular shape apart from the extended N-terminal portion. The C-terminal domain is predominantly α-helical containing eight α-helices and connecting loops incorporating five E-F hands. The E-F hands associate into pairs in a way that E-F 1 pairs with E-F2 and E-F3 pairs with E-F4, The left E-F 5 motif is unpaired in the monomer but pairs with the E-F5 of the second monomer forming a dimer. Dimeric sorcin exhibits an asymmetrical structure (Xie et al., 2001).

1.4.2 Expression and subcellular localization of sorcin

Sorcin is widely expressed in most tissues including heart and skeletal muscle (Van der Bleik, et al., 1986). Sorcin also associates with presenilin-2 in brain and annexin-7 in adrenal medulla (Pack-Chung et al., 2000, Salzer et al., 2002). At subcellular level sorcin localizes to T-tubule junctions of cardiac SR (Meyers et al., 1995) and co-localizes with RYR at the Z-lines in the normal heart whereas the degree of co-localization is noticeably disrupted in myopathic heart (Pickel et al., 1997).
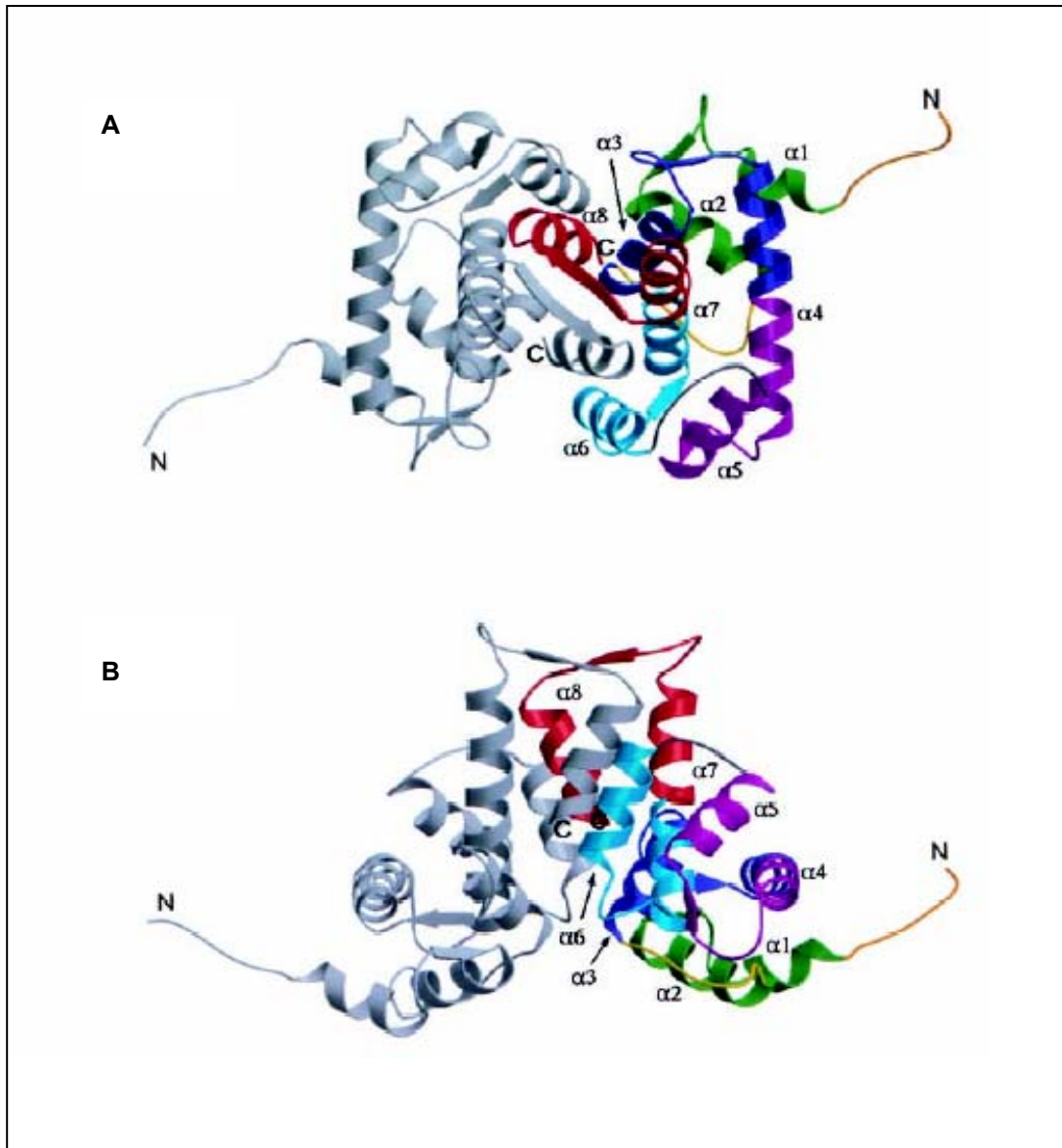
Fig. 1.3 Ribbon structure presentation of dimeric sorcin.

(A) Ribbon structure as viewed along the symmetry axis of the dimmer. Each monomer contains helices and loops that form five E-F hands. These E-F hands associate into pairs; E-F1 pairs with E-F2 whereas E-F3 pairs with EF4, and EF5 pairs with its counterpart from the other monomer to form part of the dimer interface. One of the monomers is shown in monochrome (gray) whereas the other is color-coded to show the sub-domain structures: E-F1 (green); E-F2 (blue); E-F3 (magenta); E-F4 (cyan); E-F5 (red); LE-F12, the linker connecting the adjacent E-F-hands within the first pair E-F1–E-F2 (yellow); LE-F34, the linker connecting the adjacent E-F hands within the second pair E-F3–EF-4 (gray); and the short N-terminal fragment (dark orange). For each E-F hand, the individual helices are denoted as E (N-terminal helix) and F (C-terminal helix) with an appropriate number indicating to which E-F hand it belongs, whereas the loops flanked by the E and F helices are denoted as L with the same corresponding number. A sorcin monomer contains eight helices that are numbered from _1 to _8. **(B)** Ribbon structure of sorcin as viewed perpendicular to the symmetry axis. Xie et al. (2001).

1.4.3 Interaction of sorcin with other calcium binding proteins

Sorcin associates with the cytoplasmic side of RYR in skeletal and cardiac muscle and participates in channel gating (Meyers et al., 1995). Co-immunoprecipitation of metabolically labelled cardiac myocyte proteins and several other *in vitro* binding studies indicated that sorcin inhibits open cardiac RYR2 from being incorporated into planar lipid bilayers with high affinity. This inhibitory effect of sorcin on ryanodine receptor was relieved by phosphorylation of sorcin with the catalytic subunit of PKA (Farell et al., 2003).

In cardiac myocytes, sorcin significantly inhibits both the spontaneous activity of RYR in quiescent cells (visualized as calcium sparks) and the inward calcium current triggered activity that gives rise to intracellular transients. Sorcin decreases spark efficiency and amplitude, and the dynamic interaction with RYR2 occurs at a rate that would allow for modulation of the channel by sorcin on a beat-to-beat basis (Farell et al., 2003). The rapid and reversible effect of sorcin on RYR2 closure is kinetically capable of playing a role in terminating the positive feedback loop of calcium induced calcium release (Seidler et al., 2003). Calcium bound sorcin binds to the cytoplasmically oriented C-terminal domain of the cardiac L-type calcium channel's pore-forming alpha 1-C subunit, either at or near the I-Q calmodulin binding region, thus participating in channel inactivation. The functional effects of sorcin on RyR2 and the L-type calcium channel suggest that sorcin plays a role in interchannel communication (Meyers et al., 1998).

Sorcin interacts with SERCA in sorcin overexpressing adult rat cardiac myocytes (Matsumoto et al., 2005) and increases NCX activity in sorcin overexpressing rabbit cardiac myocytes (Seidler et al., 2003). Other binding partners for sorcin include presenilin-2, which in complex with sorcin, may be involved in intracellular calcium modulation in neuronal cells (Pack-Chung et al., 2000) and annexin-7, as sorcin has been shown to inhibit annexin-7 mediated aggregation of chromaffin granules isolated from adrenal medullary tissue (Verzili et al., 2000).

1.4.4 Adenoviral mediated gene transfer and transgenic mouse model

A transgenic mice model overexpressing sorcin by mouse α-myosin heavy chain (α-MHC) promoter was developed. The transgenic mice developed normally with no change in expression of other calcium regulatory proteins. However, contractile abnormalities were observed in isolated adult transgenic myocytes along with significant depression of Ca^{2+} transient amplitudes. The rate of inactivation of transgenic myocyte L-type Ca^{2+} channels was accelerated by 15%, as compared to wildtype, while the whole cell calcium density and time course of channel activation were found to be normal (Meyers et al., 2003).

On contrary, the adenoviral mediated overexpression of sorcin in either normal or diabetic mice and in adult rat cardiomyocytes using an adenoviral gene transfer approach showed an increase in cardiac contractility of the normal heart and dramatically rescued the abnormal contractile function of the diabetic heart. This study advocated that viral vector mediated delivery of sorcin to cardiac myocytes is beneficial resulting in improved contractile function in diabetic cardiomyopathy (Suarez et al., 2004).

One study proclaimed that a point missense mutation in sorcin gene resulting in phenylalanine to leucine (F112L) was associated with an uncommon apical form of familial hypertrophic cardiomyopathy and hypertension. The prevalence of this mutation was 2 out of 200 patients with hypertrophic cardiomyopathy. The study reported that sorcin F112L lacks the inhibitory action of sorcin in RYR mediated Ca^{2+} release

(Mohiddin et al., 2002).

Another study indicated that a mild over expression of sorcin (1.7 fold) exhibits a significantly higher peak force of contraction. Echocardiography of *in vivo* transfected rat hearts with the adenoviral based overexpression showed enhanced fractional shortening and decreased end-systolic diameters indicating increased cardiac contractility though the gross morphology did not show any remarkable difference in the sorcin over expressed hearts (Frank et al., 2005).

1.5 Aims of the thesis

Despite the growing literature, advocating the role of sorcin in calcium cycling and intracellular calcium homeostasis, the role of sorcin in heart remains controversial. The present study was aimed at apprehending the role of sorcin in Ca^{2+} signalling pathway by using antisense RNA strategy directed against *de novo* synthesis of sorcin. The adenoviral antisense sorcin vector was utilized to transfect isolated adult rat cardiomyocytes to investigate functional, biochemical and molecular consequences of adenoviral mediated downregulation of sorcin. In addition, the antisense sorcin vector was used for the adenoviral mediated *in vivo* sorcin gene delivery in rat hearts to study the functional consequences of depleted sorcin in the whole heart.

The aims of the thesis were to specifically address the following questions:

1. Does the downregulation of sorcin affects the cardiac Ca^{2+} handling and excitation- contraction coupling?
2. Does the downregulation or ablation of sorcin induce any compensatory mechanism in the expression or activity of the Ca^{2+} binding proteins and alters the contractility in the E-C coupling?
3. Does lowered expression of sorcin affect the SR Ca^{2+} storage and SR Ca^{2+} release?
4. Does reduced expression of sorcin result in functional remodelling of the heart *in vivo*?
5. Does the ablation of sorcin affect the transcriptional regulation in the heart?

2. Materials and Methods

2.1 Materials

2.1.1 Animals

Male wistar rats, 220–250 g were used for the isolation of adult rat cardiomyocytes (ARC). For the catheter based *in vivo* gene transfer in hearts, male wistar rats 240-350 g were used. All the animals used were obtained from Charles River, Germany. The rats were housed in plastic cages in a room with a controlled humidity of 40 % and temperature of 22 °C. A controlled environmental 12 hour light-dark cycle was maintained. The experimental design was carried out according to German animal care legislation.

2.1.2 Materials (reagents, buffers, cell culture medium, enzymes and antibodies)

(a) Antisense adenoviral expression vector

AdEasy^{TM} adenoviral vector system, Stratagene

Shuttle vector pAdTrack-CMV, Stratagene

PCR 2.1 cloning vector, Invitrogen

Restriction endonucleases, New England Biolabs

Alkaline phosphatase, New England Biolabs

Polyfect transfection kit, Stratagene

PCR purification kit, Qiagen

Electroporation cuvettes, Biorad

Cell electroporator, Biorad

AD293 cells, Stratagene

Growth medium for AD293 cells: DMEM (4.5 g/L glucose, 110 mg/L sodium pyruvate and 2 mM L-glutamine) supplemented with 10% v/v heat inactivated foetal bovine serum.

Sea plaque$^{®}$ agarose, Stratagene

(b) Isolation of rat cardiomyocytes

Cell culture medium: Medium M199 500 ml, Gibco, MEM-Vitamin   10 ml, Gibco, non essential amino acids 5 ml, Gibco; Penicillin/Streptomycin 100 IU/ml 5 ml, Sigma, Insulin H 40 IE/ml, Höchst.

Diethylether, Roth

Powell-Medium (in mM): NaCl 110, KCl 2.5, KH_2PO_4 1.17, $NaHCO_3$ 25, Glucose 2 g/l.

Carbogen (95% O_2 + 5% CO_2), Linde

Collagenase Typ II, Biochrom

Calcium chloride, Sigma

Laminin natural mouse, Sigma

Bovine serum albumin (BSA), Sigma

(c) Protein preparation from transfected rat cardiomyocytes

Cell-lysis buffer (in mM): Tris-HCl (pH 7.5) 5, EDTA (pH 8.0) 5

Complete mini EDTA free protease inhibitor cocktail tablet, Sigma

Freezing buffer (in mM): Saccharose 400, HEPES 5, TRIS 5, pH 7.2.

(d) Quantitative immunoblotting

Acrylamide-Bis 30%/0.8 % v/v, Roth

Coomassie brilliant blue, Serva

Dodecyl sodium sulphate (SDS), Serva

Enhanced Chemiluminiscence (ECL) Kit, Amersham Life Science

Acetic acid, Merck

Glycerine, Merck

Glycine, Merck

Kaleidoscope prestained protein standards ($\cong$ 7 –205 kDa), BioRad

2-βMercaptoethanol 98% v/v, Sigma

N, N, N´, N´-tetramethylendiamine (TEMED), Serva

TBS (in mM): NaCl 150, Tris-HCl 10; pH 7.5

TBST (in mM): NaCl 150, Tris-HCl 10, 0.05% v/v TWEEN 20, pH 7.5

TWEEN 20, Merck

Polyvinyldienfluoride (PVDF) membrane, BioRad

Ponceau S, Serva

Loading buffer (2x): 100 mM TRIS/HCl (pH 6.8), 2% v/v

2-βMercaptoethanol, 4% SDS w/v, 0.2% Bromphenolblue 20% v/v

X-ray film, Amersham

(e) Antibodies for western blot

Monoclonal (Mouse) Anti-sorcin antibody, (1:1000), Zymed,

Polyclonal (Rabbit) Anti-sorcin antibody, (1:1000), self produced

Monoclonal (Mouse) Anti-ryanodine receptor isoform 2 antibody, (1:1000), Affinity BioReagents

Monoclonal (Mouse) Anti-calsequestrin antibody, (1:1000), Biomol

Polyclonal (Rabbit) Anti-calcineurin-A antibody, (1:1000), Santa Cruz Biotechnology

Polyclonal (Rabbit) Anti-FKBP12.6 antibody, (1:1000), Biomol

Monoclonal (Mouse) Anti-SERCA2 ATPase antibody, (1:1000), Affinity Bioreagents

Monoclonal (Mouse) Anti-triadin antibody, (1:1000), Affinity Bioreagents

Monoclonal (Mouse) Anti-phospholamban antibody, (1:1000), Upstate Biotechnology

Ployclonal (Rabbit) Anti-GATA-4(H112) antibody, (1:1000), SantaCruz Biotechnology

Polyclonal (Goat) Anti-NF-AT$_{C3}$ antibody, (1:1000), Santa Cruz Biotechnology

Peroxidase-conjugated Anti goat IgG antibody, (1:2000), Sigma

Peroxidase-conjugated Anti-mouse IgG antibody, (1:2000), Sigma

Peroxidase-conjugated Anti-rabbit IgG antibody, (1:2000), Sigma

(f) Immunofluoroscence measurement in transfected cardiomyocytes

Triton X-100, Sigma,

Polyclonal (Rabbit) Anti-sorcin antibody (1:500), self produced

Alexa fluor^{TM} 546 Anti-rabbit IgG, Molecular probes

DAKO mounting medium, Molecular probes

PBS (in mM): NaCl 137, KCl 2.6, K_2HPO_4 1.8, Na_2HPO_4 10 (pH 7.4)

Paraformaldehyde (4% w/v in PBS), Sigma

(g) Contractility measurement of the transfected cardiomyocytes

Tyrode buffer (in mM): NaCl 132, KCl 4.8, $MgCl_2$ 1.2, $CaCl_2$ 1.8, Glucose 10, HEPES 10, pH 7.3, Sigma

Forskolin, Calbiochem

(h) RNA isolation and reverse transcription

RNase free water, Invitrogen

Ethanol, Merck

Ist strand buffer, Gibco

0.1M dithiothreitol (DTT), Gibco

Random primer, RNase inhibitor, Promega

M-MLV reverse transcriptase, Gibco

Deoxynucleotide triphosphate set, PCR grade, Roche Diagnostics

Chloroform, Merck

2-Propanol, Roth

Table 2.1 List of primers

GAPDH	Forward	ACC ACA GTC CAT GCC ATC AC
	Reverse	TCC ACC ACC CTG TTG CTG TA
Sorcin	Forward	TGC TGT AGC TGG ACA GGA TG
	Reverse	AGC ATT GAA ACC ATA AGC CG
Phospholamban	Forward	CGG GAT CCA TGG GCG TGG AGA TCG
	Reverse	GCA GCA GAC ATA TCA AGA TGA A
FKBP 12.6	Forward	CCC CAG ACT ATG CCT ATG GA
	Reverse	AAG AGT GGT GGG ACA TCAGG
SERCA2a	Forward	CTG CGA GCT CTT GCT CGA GTT GAA CC
	Reverse	CGG GAT CCT GCA CAC ACT CTT TAC
Calcineurin-A	Forward	TCA CCG GTT GAC ATC TGA AG
	Reverse	ATG GTT TTC TCC CGC CTA AG
NF-AT$_{C3}$	***Forward***	TTG GCT TAC CAC ATC ATG GA
		TGG GCA TTC AAA GGG TTT AG
	Reverse	
GATA-4	Forward	CAG TTT CTG GAG CAA CCA CA
	Reverse	ACC AAA GCG ACA AGA ATT GG
BNP	Forward	CAG CTC TTG AAG GAC CAA GG
	Reverse	AGA CCC AGG CAG AGT CAG AA
β-MHC	Forward	ACG GAT GCC ATA CAG AGG AC
	Reverse	CCT CAT AGG CGT TCT TGA GC
ANP	Forward	GGA ATG AGT CCA CTT TAA ATC CTT T
	Reverse	GAG CTT TTT AAC TGC AGC AAC TTT A

For each primer pair the annealing temperature (T_A) was calculated according to the following formula:

$T_A = 2(A + T) + 4(G + C) – 5$

(i) Calcineurin activity measurement in transfected cardiomyocytes

Tris, Roth

Acetylated BSA (Bovine serum albumin), Promega

Nickel chloride, Sigma

Calmodulin (phosphodiesterase $3^{'}$-$5^{'}$–cyclic nucleotide activator), Sigma

PNPP (p-Nitrophenyl phosphate), Sigma

ELISA reader MRX Revealation , DYNEX Technologies

(j) Measurement of calcium transient in transfected cardiomyocytes

X- rhod-1 AM, Molecular Probes

Tyrode sloution (in mM): NaCl 132, KCl 4.8, MgCl$_2$ 1.2, CaCl$_2$ 1.8, Glucose 10, HEPES 10, pH 7.3 aCl$_2$ 1.8

Stimulator

Confocal laser scanning microscope LSM 510 Meta, Zeiss

(k) Expression and purification of recombinant sorcin

Luria Bertani (LB) medium (1l) Bacto-trypton 10 g, Yeast extract 5 g, NaCl 5 g, ddH$_2$O to 1l (pH 7.3)

Ampicillin 100 mg/ml, Sigma

IPTG, Sigma

Elution buffer: Reduced glutathione 50 mM Tris-HCl (pH 8.0), Sigma

PBS (in mM): NaCl 137, KCl 2.6, K$_2$HPO$_4$ 1.8, Na$_2$HPO$_4$ 10 (pH 7.4).

Lysozyme, Sigma

EDTA, Roth

TritonX-100, Sigma

Glutathione agarose beads, Amersham

(l) Sarcoplasmic reticulum Ca^{2+} uptake

Potassium dihydrogen phosphate, Merck

Sodium fluoride, Merck

Sucrose, Roth

Phenylmethanesulfonylfluoride (PMSF), Sigma

Dithiothreitol, Merck

Imidazole, Merck

Potassium chloride, Merck

Sodium azide, Merck

Magnesium chloride hexahydrate, Merck

Ethylene glycol bis (β-Aminoethyl ether)-N, N, N$^{'}$, N$^{'}$, tetra acetic acid, Sigma

Potassium oxalate monohydrate, Merck

Calcium chloride dihydrate, Merck

Ruthenium red, Sigma

Tris, Roth

Adenosine-5$^{'}$-triphosphate, Roche

Whatman glass microfibre filters 2.5 cm, poresize 0.45 μm

ACS II scintillation cocktail, Amersham

Liquid scintillation analyzer TR-1600, Packard

(m) Catheter based adenoviral injection in rat hearts and Echocardiography

Acetylcholine, Sigma

Isoflurane, Sigma

Ketamine, Sigma

Diazepam, Sigma

Epinephrine, Hoechst

Heparin 100 IU, Sigma

Sodium bicarbonate, Braun

3F balloon catheter, 2 F lumen balloon catheter, Edwards life science

Pressure transducer, Stratham P23 XL

Four chamber power lab system, AD instruments

2.2 Methods

2.2.1 Generation of adenoviral antisense sorcin GFP (Ad.as.Sor.GFP)

Adenovirus serotype 5 with antisense sorcin GFP (Ad.as.SOR.GFP) was generated using the AdEasy[TM] Adenoviral vector system from stratagene (Hajjar et al., 1997).

(a) Cloning sorcin cDNA and insertion in transfer vector

Sorcin human cDNA fragment was cloned in PCR 2.1 vector and confirmed by restriction digestions and sequencing. The cloned cDNA fragment was subsequently inserted in the multiple cloning site of shuttle vector pAD-TrackCMV (9.2kb) in reverse orientation using the endonuclease restriction enzyme sites Hind III and Xho I. The ligation was performed by using T4 DNA ligase (Molar ratio from Insert: Vector = 5:1) The orientation of the fragment was confirmed by restriction digestion and sequence analysis.

(b) Production of recombinant Ad plasmid by homologous recombination

The shuttle plasmid was linearized by Pme I, confirmed the complete digestion by agarose gel electrophoresis and purified by Qiagen purification kit to remove any salts, which can interfere in the subsequent electroporation. The purified linearized plasmid was dephosphorylated with alkaline phosphatase for 1 h at 37 $^\circ$C. The BJ5183 cells were cotransformed with the linearized shuttle vector containing sorcin cDNA and the pAdEasy vector as per the manufacturer's instructions, which resulted in the recombination event inside the BJ5183 cells. In short 1 μg of linearized, dephosphorylated shuttle vector and 1 μl of pAdEasy supercoiled vector (100 ng/ μl) were mixed with BJ5183 gently and transferred to prechilled electroporation cuvettes. A pulse of 200 Ω, 2.5 kV, 25 μF was used for electroporation. The cuvette was removed immediately; 1 ml of sterile LB broth was added and gently mixed by pipetting up and down to resuspend the cells. The transformants were incubated at 37 $^\circ$C for 1 h while shaking at 225-250 rpm. The recombinant reaction mixture was plated on kanamycin plates and incubated overnight at 37 $^\circ$C. The recombinant Ad plasmid was purified from the clone and confirmed by restriction digestion with Pac I enzyme.

(c) Production of recombinant Ad virus

The positive recombinant Ad plasmid was used to transform XL10-GOLD ultracompetent cells to amplify the recombinant adenovirus plasmid DNA by using the heat shock method following the manufacturer's protocol. Briefly 50 ng of plasmid DNA was added to the pre aliquoted 100μl XL10-Gold ultra competent cells and incubated for 30 min on ice followed by heat pulsing the reaction mixture at 42 $^\circ$C for 30 s. The reaction tube was incubated on

ice for 2 min, 0.9 ml of pre warmed (42 $^{\circ}$C) NZY^{+} broth was added and incubated at 37 $^{\circ}$C for 1 hour at 225-250 rpm. The transformant reaction was plated on kanamycin plates and incubated overnight at 37 $^{\circ}$C. Positive colonies were checked by restriction digestion with Pac I. A maxiprep was done and purified by standard caesium chloride density gradient centrifugation to get highly pure DNA. The plasmid DNA was subjected to Pac I digestion, purified the reaction mixture with Qiagen PCR purification kit and resuspended in PCR grade water. AD293 cells produce the adenovirus E1 gene in *trans* allowing the production of infectious virus particles when the cells are transfected with E1 deleted pAdEasy vector. 7-8 x 10^{5} AD293 cells were plated in 60 mm tissue culture dish containing growth medium. After 24 hours the transfection was done by using Polyfect^{TM} transfection kit following the manufacturer's instructions. The progress of the transfection was monitored by the fluorescence microscopy (by detecting GFP expression). Adenovirus producing AD293 cells were washed with PBS and harvested by scraping the cells in 0.5 ml of PBS. The cell suspension was subjected to four rounds of freeze/thaw by alternating the tubes between dry ice-methanol bath and 37 $^{\circ}$C water bath. The cellular debris were collected by microcentrifugation at 12000 g for 10 min at room temperature. The supernatant obtained was used as the primary virus stock. The titer (pfu/ml) was determined by plaque assay using agarose overlay. Similarly a control expressing GFP (Ad.GFP) was generated with the shuttle vector. Fig. 2.1 represents the schematic presentation of the generation of the adenoviral vectors.
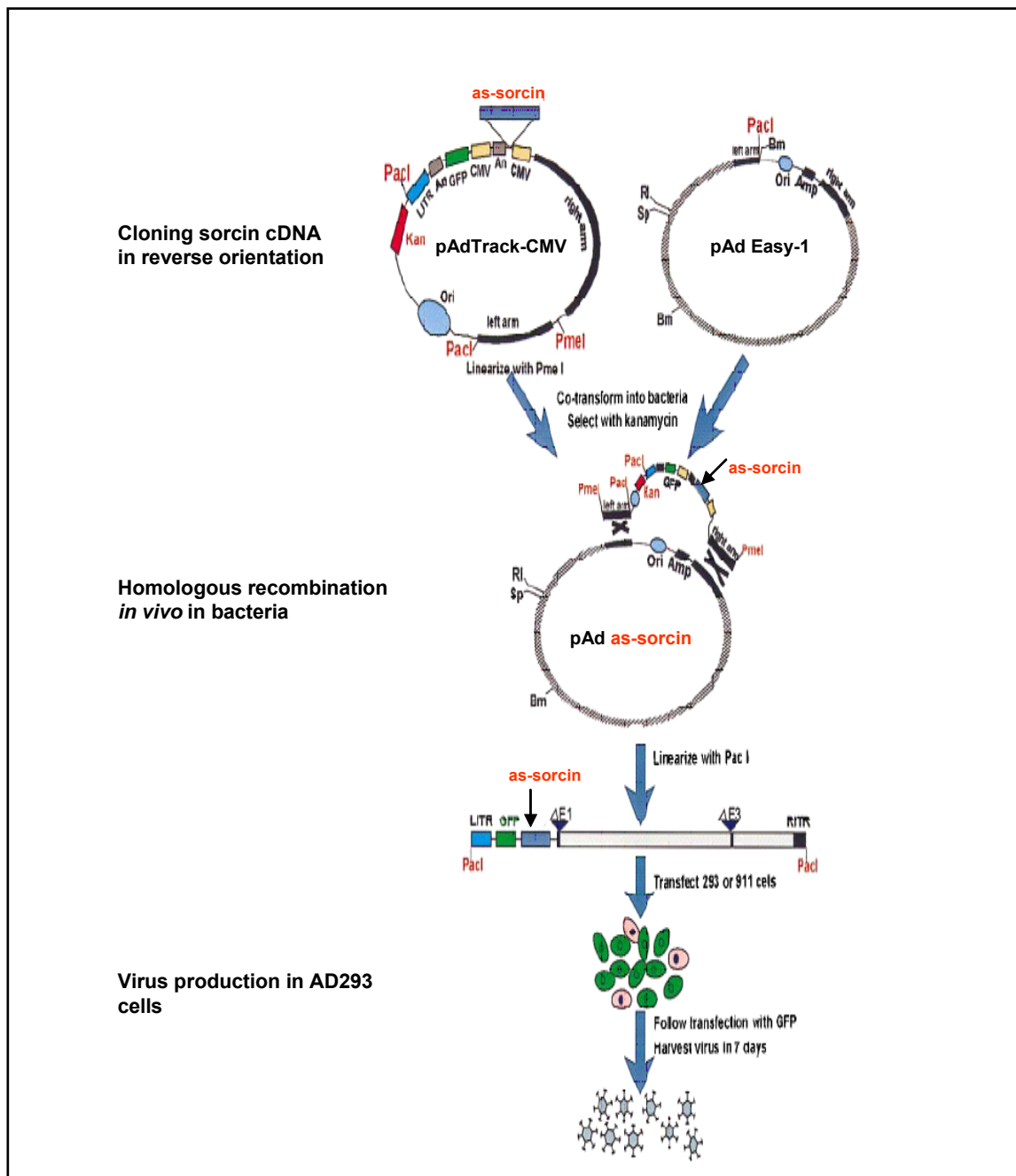
Fig. 2.1 Schematic outline of the generation of adenoviral vector using AdEasy system

The gene of interest (sorcin) was first cloned in reverse direction into shuttle vector pAdTrack-CMV. The resultant plasmid was linearized by digesting with Pme I and subsequently cotransformed into E.coli BJ5183 cells with an adenoviral backbone plasmid pAdEasy-1. Recombinants were selected for kanamycin resistance and recombination was confirmed by multiple restriction endonuclease analyses. Finally the linearized recombinant plasmid was transfected into adenovirus packaging cell line (AD293 cells). The "left arm" and "right arm" represents the regions mediating homologous recombination between the shuttle vector and adenoviral backbone vector. Modified from Tong-Chuan He et al. (1997).
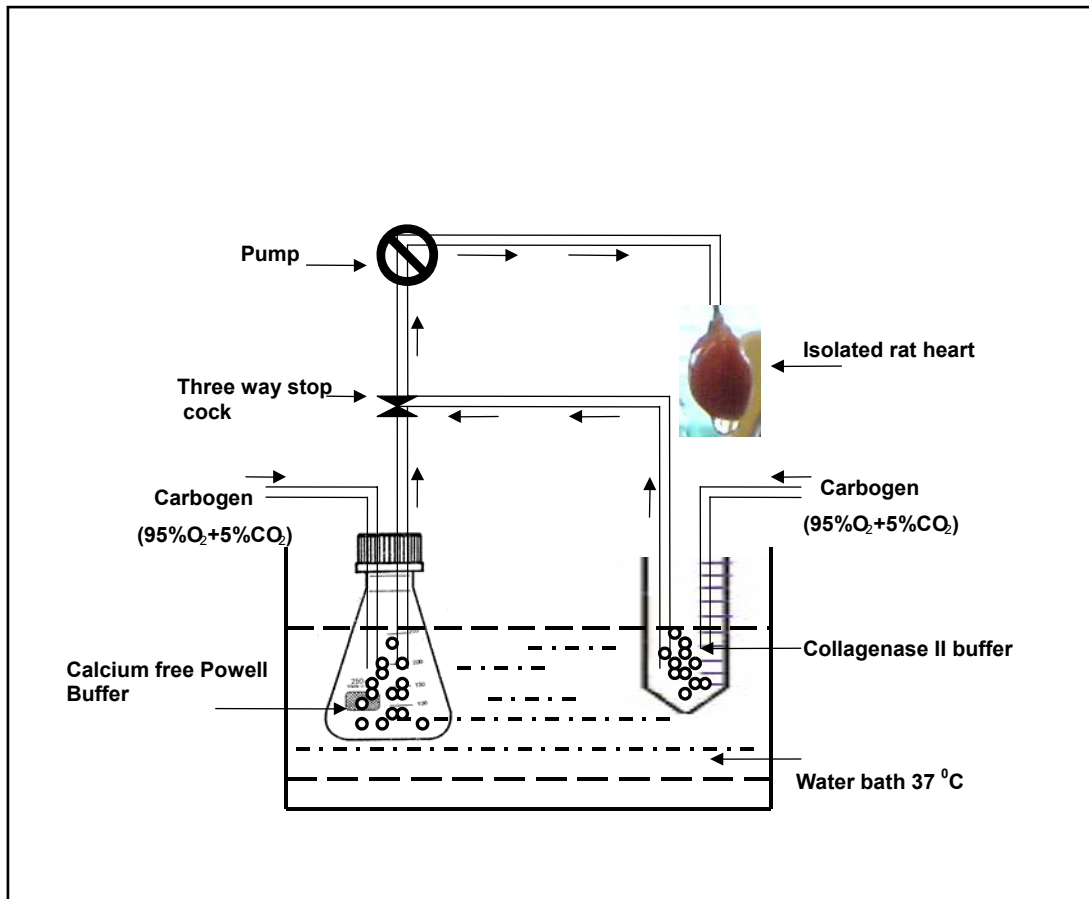
2.2.2 Isolation of adult rat cardiomyocytes (ARC)

The isolation of cardiomyocytes was done by the enzymatic digestion technique. Male wistar rats (age 10-12 weeks, 220 – 250 g) were anaesthetised by diethyl ether followed by cervical dislocation. Hearts were quickly excised, aorta cannulated and perfused with the calcium free oxygenated (95% O2 + 5% CO2) powell buffer on the Langendorff perfusion apparatus for 5 minutes at 37 $^{\circ}$C at a constant flow rate of 8 ml/min. The heart was retroperfused with collagenase buffer (collagenase II, Biochrome), 26-30 mg (210 U/mg) in 40 ml oxygenated powell buffer with 31.25 μM $CaCl_2$ at a constant temperature of 37° C for 15 to 20 min taking care that the buffer was oxygenated constantly. The heart was taken from the cannula and gently pipetted up and down in collagenase buffer with a blunt ended 10 ml pipette till all the cardiomyocytes were loosened, followed by centrifugation at 300 g for 3 min at room temperature, the supernatant was aspirated and the pellet (cardiomyocytes) was filtered through a nylon filter (200 μm) and adjusted to a volume of 10 ml with 4% BSA. The cardiomyocytes were subjected to increasing Ca^{2+} concentration in order to get calcium stable cardiomyocytes. Pre calculated volume of 100 mM $CaCl_2$ was added in four gradual steps at an interval of 3 min each to achieve the final Ca^{2+} concentration 1.8 μM, followed by final centrifugation step 300 g for 3 min at room temperature. Supernatant was aspirated and the cardiomyocyte pellet was resuspended in 10 ml of culture medium. Cardiomyocyte count was calculated with neubaeur chamber. The cardiomyoctes were plated on 10.5 cm laminin precoated culture plates for protein preparation and on the laminin precoated 18 mm and 12 mm glass coverslips for contractility measurement and immunocytochemistry, respectively. Fig. 2.2 depicts the scheme of isolation of the cardiomyocytes .

2.2.3 Transfection of cardiomyocytes

The isolated cardiomyocytes were transfected with the Ad.as.SOR.GFP with 100 moieties of infection (MOI) and Ad.GFP as control (MOI 100) after three hours of isolation and allowing the cells to adhere to the laminin coated plates. After incubation with the virus for 12-20 h the media was changed. Successful transfection of cardiomyocytes was determined by monitoring the culture plates for green fluorescence using Axiovert microscope (Zeiss) with an excitation wavelength 473 nm by a fluorescence filter. Expression of green fluorescence protein marker by the cardiomyocytes verified the successful transfection. The cardiomyocytes were cultured for 48 h before protein preparation and other functional studies.

Fig. 2.2 Schematic presentation of the isolation of adult rat cardiomyotes.

The aorta from the excised rat heart was cannulated and perfused with the Ca^{2+} free Powell buffer for 5 min followed by retroperfusion of collagenase II buffer for 15 to 20 min. All the buffers and solutions were constantly oxygenated (95% O2 + 5% CO2) and kept at 37 $^\circ$C in the water bath.

2.2.4 Protein preparation from the transfected cardiomyocytes

Cardiomyocytes were cultured on laminin coated plates for 48 h post transfection with Ad.as.SOR.GFP or Ad.GFP. Culture medium was changed and the cells were washed with PBS, 1 ml of lysis buffer (with complete mini EDTA free tablet / 10 ml of lysis buffer) was added to the culture plate and allowed to stand at room temperature for 5 min, the cells were scraped with the cell scraper and homogenised by using the ultrasonic homogeniser with two pulses for the whole cell homogenates. The cardiomyocyte homogenates were pooled from different preparations to scale up the amount of protein. The amount of protein was quantified by Bradford assay and stored in aliquots at −80 $^\circ$C.

2.2.5 Extraction of transcription factors from transfected cardiomyocytes

Isolation of nuclear extract and transcription factor was performed based on the protocol described earlier (Andrews et al., 1991). The procedure utilizes the hypotonic lysis followed by high salt extraction of nuclei. Briefly, 48 h post transfection, cardiomyocytes were scraped into 1.5 ml of cold PBS. Cells were pelleted and resuspended in 400 µl cold buffer A (10 mM HEPES-KOH pH 7.9 at 4 ^{0}C, 1.5 mM MgCl$_2$, 10 mM KCl, 0.5 mM dithithreitol, 0.2 mM PMSF). Cells were allowed to swell on ice for 10 min and then vortexed for 10 seconds. Samples were centrifuged and the supernatant discarded, the pellet was resuspended in 20-100 µl (according to starting number of cells) of cold buffer B (20 mM HEPES-KOH pH 7.9 at 4 ^{0}C, 25% v/v glycerol, 420 mM NaCl, 1.5 mM MgCl$_2$, 0.2 mM EDTA, 0.5 mM dithiothreitol, 0.2 mM PMSF) and incubated on ice for 20 min for high-salt extraction. Cellular debris were removed by centrifugation for 2 min at 4 $^\circ$C and the supernatant fraction (containing the DNA binding proteins) was stored at –70 $^\circ$C for later use.

2.2.6 Quantitative immunoblotting

(a) SDS PAGE

SDS-polyacrylamide gel electrophoresis (SDS-PAGE) was performed using the discontinuous buffer system (Laemmli, 1970). Discontinuous polyacrylamide gel was prepared using glass plates of 10 cm x 7.5 cm dimensions and spacers of 0.5 mm thickness. The composition of resolving and stacking gels is given in the table 2.2.

Table 2.2 Composition of stacking and separating gels for SDS PAGE

component	stacking gel 4%	separating gel 8%
AA/Bis (30 %/0.8 %)	4.1 ml	7.2 ml
1.5 M Tris pH 8.8	-	10.2 ml
0.5 M Tris pH 6.8	3.7 ml	-
H$_2$O	22.3 ml	9.2 ml
10% SDS	300 µl	300 µl
10% APS	300 µl	95 µl
TEMED	41 µl	24 µl

Samples were mixed with suitable volumes of loading buffer, denatured by heating at 95 ºC for 5 min and loaded into the wells of the stacking gel. A prestained molecular weight marker (kaleidoscope) was run simultaneously on adjacent lane as a standard to establish the apparent molecular weights of proteins resolved on SDS-PAGE. Electrophoresis was performed in 1x gel-running buffer at a constant voltage of 100-150 V until the bromophenol blue dye front had reached the bottom edge of the gel or had just run out of the gel.

(b) Transfer of protein to PVDF membrane

Proteins resolved on the gel were transferred electrophoretically to the PVDF membrane in Biorad blotting chamber in transfer buffer at constant current of 100 mA overnight at 4 °C. Membranes were checked by Ponceau S staining for complete transfer of protein.

(c) Ponceau-S staining of PVDF membrane

To check the transfer of proteins into the PVDF membrane, the membrane was stained in 10-15 ml of Ponceau S solution for 2-5 min at room temperature. After staining, the membrane was removed from the Ponceau S solution and rinsed with water to destain until bands of proteins were visible and the background was clear. The membrane was scanned for the documentation and washed with TBS to completely remove the stain.

(d) Immunodetection of the membrane bound protein

PVDF membranes with bound proteins were blocked with 5% low fat milk powder in TBST for two hours followed by washing in TBST three times, 10 min each. The membrane was incubated overnight at 4 °C with primary antibody diluted appropriately in TBST followed by washing three times of 10 min each in TBST buffer. The membrane were further blocked with 5% low fat milk in TBST for 20 min followed by washing in TBS. Appropriately diluted secondary antibody conjugated with horseradish peroxidase was added to the membrane and incubated at room temperature for one hour. Unbound antibody was rinsed in TBST buffer two times for 10 min and subsequently rinsed in TBS for 10 min. The reaction was detected using an enhanced chemiluminescence detection system (ECL kit, Amsersham).

(e) Developing the films

Signal from bound antibody was detected using an enhanced chemiluminescence assay by capturing the signal on X-ray film. Intensity of the bands was quantified by densitometric measurement with biorad XL-10 densitometer. Calsequestrin was used as the loading standard.

2.2.7 Immunofluorescence of transfected cardiomyocytes

Cardiomyocytes transfected with Ad.as.SOR.GFP or Ad.GFP were cultured for 48 hours on 12 mm laminin precoated coverslips. Cardiomyocytes were fixed with a freshly prepared 4% paraformaldehyde solution in PBS for 15 min and subsequently permeabilised with 1% Triton-X 100 in PBS for 4 min. Permeabilized cardiomyocytes were washed three times with PBS followed by blocking with 1% normal goat serum (NGS) for 30 min to avoid nonspecific binding. The blocked cardiomyocytes were incubated with the primary antibody diluted in PBS (1:500) for 60 min and washed four times with PBS before applying the fluorochrome conjugated secondary antibody in PBS 1:2000) for 60 min. Cells were washed three times with PBS to remove unbound secondary antibodies and incubated with bisbenzimide (0.1 μg/ml) for 5 min to stain the nuclei, washed twice to remove unbound bisbenzimide. Cover slips containing stained cells were carefully lifted from wells and mounted on histoslides with DAKO mounting medium. The steps after adding secondary antibody were performed in dark.

Image analysis

The immunofluorecence was observed with an inverted fluorescence microscope (Axiophot, Zeiss).

Digital images obtained were acquired with metamorph software and processed using Adobe Photoshop software.

2.2.8 Contractility measurement in the transfected cardiomyocytes

Contractility measurement was done by using the single cell investigation system based on the edge detection technique. A high speed video camera was attached to the objective to acquire the picture on the monitor, the cardiomyocytes were aligned on the longitudinal axis by turning the stage manually. The laminin coated glass plate with transfected cardiomyocytes were fixed on the perfusion chamber.

The perfusion chamber was maintained at a constant temperature of 30 $^\circ$C, the chamber was connected to a perfusion tube for the continuous flow of the buffer and a peristaltic pump was used to drain the excess fluid. The observation was done using the inverted microscope (Diaphot 200, Nikon, Japan). The microscope was attached to a computer which utilized the contraction transient software program to analyse the contractility in transfected cardiomocytes. Cardiomyocytes were field stimulated by using two platinum electrodes connected to a modulator. Tyrode solution perfused the cuvette at the rate of 0.5 ml /min at a constant temperature 30 $^\circ$C maintained in the cuvette. The cells were stimulated for an acclimatisation phase for 5 min at 50 V at a frequency of 0.5 Hz.

For the force frequency measurements, the frequency was increased from 0.25 Hz, 0.5 Hz, 1 Hz, 2 Hz, 3 Hz and 5 Hz gradually.For studying the effect of β-adrenergic stimulation, transfected cardiomyocytes were stimulated at 0.5Hz and measurements were taken over increasing concentration of forskolin ranging from 0.1μM to 1 μM. Fig. 2.3 depicts the schematic diagram of the single cell investigation system used for the contractility measurements.
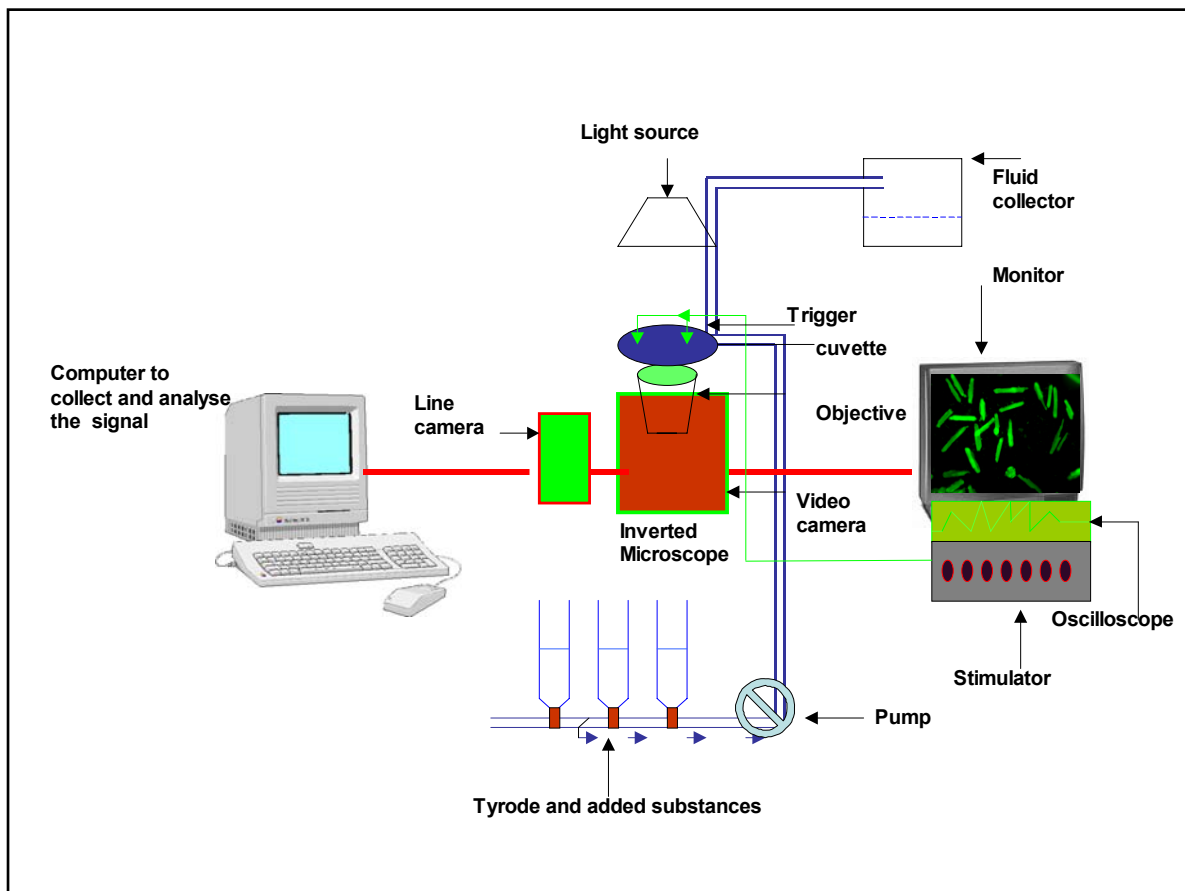
Fig. 2.3 Schematic presentation of the cardiomyocyte contractility measurement setup

The coverslips with transfected cardiomyocytes were fixed on the cuvette on stage of the inverted microscope Diaphot 200 (Zeiss) attached to the perfusion chamber driven by a peristaltic pump. The high-speed video camera acquired the picture on the monitor through which the cells can be aligned manually on edge detection system that records the contraction of the cardiomyocyte and sends the signal to the attached computer, which analyse and records the signal in terms of contractility using contraction transient software program.

2.2.9 Reverse transcriptase-PCR

(a) RNA isolation from the isolated cardiomyocytes

mRNA from the transfected cardiomyocytes was isolated with peqGOLD RNA pure[TM] according to manufacturer's instructions. Briefly, the cell suspension from isolated cardiomyocytes was mixed with peqGOLD RNA pure[TM]. The suspension was incubated at room temperature for 5 min in order to disassociate the nucleotide complex followed by adding 0.2 ml chloroform. The tubes were gently vortexed for 5 sec. The samples were incubated at room temperature for 3-10 min and centrifuged for 5 min at 12,000 g, which led to the separation in three different phases, yellow phase of the phenol- chloroform in bottom, aqueous phase on the top and an interphase. The RNA was present in the aqueous phase while the DNA and proteins were present in the interphase and phenol phase, respectively. The aqueous phase containing total RNA was transferred into a new microfuge tube, RNA precipitated with isopropanol, incubated at room temperature for 5 min and then centrifuged for 10 minutes at 20,000 g at 4 °C. The supernatant was discarded and the pellet

washed with 1 ml of 75% ethanol, vortexed and centrifuged at 12000 g (4 °C). The RNA pellet was dried at room temperature, resuspended in RNase free water, and stored at -80 °C for further use.

(b) RNA formaldehyde-agarose gel electrophoresis

Denaturing formaldehyde-agarose electrophoresis was used for separation and resolution of RNA to check the quality of isolated RNA (Lehrach et al., 1977). 20 μg of purified total RNA was mixed with an equal volume of RNA-sample buffer and denatured by heating at 65 ºC for 10 min. After denaturation, the sample was immediately transferred to ice and RNA loading buffer was added. Thereafter, the RNA samples were loaded onto a denaturing formaldehyde-agarose gel.

(c) Preparation of formaldehyde-agarose gel

For a total gel volume of 150 ml, 1.8 g agarose (final concentration 1.2%) was initially boiled with 111 ml DEPC-H_2O in an Erlenmeyer flask, cooled to 60 ºC, 15 ml of the RNA gel casting buffer, pH 8.0 and 24 ml of a 36% formaldehyde solution were added. The agarose solution was mixed by swirling and poured into a sealed gel casting chamber of the desired size. After the gel was completely set, denatured RNA samples were loaded and the gel was run in 1x RNA gel running buffer, pH 7.0, at 100 V until the bromophenol blue dye had migrated the appropriate distance through the gel, the gel was examined under UV light at 302 nm and was documented using the gel-documentation system.

10 x RNA gel casting buffer	10 x RNA gel running buffer
200 mM MOPS	200 mM MOPS
50 mM sodium acetate	50 mM sodium acetate
10 mM EDTA	10 mM EDTA
pH 8.0	pH 7.0
RNA sample buffer	RNA loading buffer
50% v/v formamide	50% w/v sucrose, RNase free
6% v/v formaldehyde	0.25% w/v bromophenol blue
in 1x RNA-gel-casting buffer	in DEPC-H_2O

(d) Generation of cDNA from isolated RNA

cDNA was generated using the MLV revert aid according to the manufacturer's protocol. Briefly, 1 μl random primer, 1 μg RNA and RNase free water (to make a final volume of 20 μl) was mixed in the microfuge tube, incubated the reaction mixture at 65 ºC for 10 min followed by incubating the tube on ice for 5 minutes. 4 μl first strand buffer, 2 μl dNTP (each), 2 μl DTT (0.1 M), 1 μl RNase inhibitor (5 units /μl) and 1 μl MLV-reverse transcriptase were subsequently added in the reaction tube. Reaction mixture was mixed well, incubated at 37 ºC for 1 h and the reaction stopped by heating the reaction mix to 95 ºC for 10 min to inactivate the reverse transcriptase.

(e) Polymerase chain reaction (PCR)

PCR was done by using specific primers for sorcin, phospholamban, FKBP12.6, calcineurin, SERCA2a, ANF, BNP, β-MHC, NF-AT$_{C3}$, and GATA-4. A standard PCR programme is shown in Table 2.3. The PCR products were analysed on 2% agarose gel electrophoresis. GAPDH was used as the loading standard.

Table 2.3 A standard PCR programme

Step	Cycles	Temperature	Time
Initial denaturing	1	95 ^{o}C	1min
Denaturing	25-35	95 ^{o}C	30 s
Annealing	25-35	*calculated	60 s
Elongation	25-35	68 ^{o}C	1- 5 min
Final elongation	1	68 ^{o}C	10 min
Cooling	1	4 ^{o}C	

* as described in section 2.1.8

2.2.10 Calcineurin activity measurement in transfected cardiomyocytes

Calcineurin activity was measured by using Promega's non-radioactive Ser/Thr phosphatase assay system. The difference in absorbance arising due to the phophatase activity between the test (Ad.as.SOR.GFP transfected cardiomyocytes) and control group (Ad.GFP transfected cardiomyocytes) was used as the parameter of calcineurin activity. Calmodulin and NiCl$_2$ were used to ensure that phosphatase activity was attributed specifically to calcineurin. Assay was performed on the homogenized, transfected cardiomyocytes. Freshly prepared solution-A (20 mM PNPP, 0.5 mg/ml acetylated BSA, 50 mM Tris pH 7.4) and solution-B (20 mM PNPP, 0.5 mg/ml acetylated BSA, 50 mM Tris pH 7.4, 1 mM NiCl$_2$, 10 μg/ml calmodulin were dispensed (95 μl/well) in 96 well micro-titre plates and incubated at 30 ^{o}C for 10 min. 5 μl suspension of properly diluted homogenzed samples were added in triplicates to the wells, enzyme dilution buffer was used as the control. The plates were incubated for 15 min at 30 ^{o}C and the absorbance was measured at 410 nm with ELISA reader.

Activity of calcineurin was calculated according to the equation given below

Calcineurin activity (nmolp$_i$/min/μl) =

$$\frac{(\text{assay volume})(\text{dilution factor})(\text{sample absorbance 410 nm–control absorbance 410 nm})}{(\text{Sample volume })(\text{reaction time})(\text{extinct coefficient})(\text{path length})}$$

Assay volume = 100 μl for 96 well plates

Dilution factor = fold dilution of sample

Sample volume = 5 μl for 96 well plates

Reaction time = 15 min

Extinction coefficient of p–nitrophenolate (pH 7.4) = 1.75 x 10^4 $M^{-1}cm^{-1}$)

Path length = 0.32 cm for 96 well plate

2.2.11 Isolation and purification of recombinant sorcin protein from pGEX 2TK vector

Isolation and purification of recombinant sorcin protein was performed utilizing sorcin human cDNA, cloned in pGEX2TK expression vector. Overnight culture of pGEX2TK containing sorcin cDNA transformed E.coli. was diluted to 1:10 and was incubated on a shaker (200 rpm) for 60 min at 37 $^{\circ}$C. Sorcin expression was induced by adding 100 mM IPTG to a final concentration of 0.1 mM and incubating the culture for another 4-6 h. The cells containing sorcin was harvested by centrifugation at 5500 g for 15 min. The cell pellet was lysed by freshly prepared lysozyme solution (20 mg/ml). 0.5 M EDTA, 100 mM PMSF and 10% Triton X-100 were added as proteinase inhibitors and detergent respectively. Sorcin was purified by affinity chromatography by using 1 ml of 50% slurry of glutathione agarose beads. Sorcin bound to the glutathione agarose beads was eluted by elution buffer (50 mM Tris pH 8.0, 5 mM reduced glutathione). The elute was run on 10% SDS gel and bands were visualized by coomassie staining. The purity of the obtained protein was confirmed by silver staining and western blot. Concentration of the purified sorcin was determined colorimetrically by Bradford protein estimation assay.

2.2.12 Sarcoplasmic reticulum Ca^{2+} uptake

The rate of Ca^{2+} uptake into cardiomyocyte homogenates was measured over the range 0.02-5 μM free Ca^{2+}, similar to the intracellular Ca^{2+} changes occurring between systole and diastole (Frank et al., 2000). The cell lysate from transfected cardiomyocytes was incubated at 37 $^{\circ}$C for 2 min in 40 mM EGTA, 11 mM ruthenium red and appropriate concentrations of $^{45}CaCl_2$ to yield 0.02 to 5 μM free Ca^{2+}. The reaction was started by adding 5 mM ATP. Ca^{2+} uptake was measured at 30, 60 and 90 s by adding an aliquot of the reaction mixture to the pre-soaked (in wash buffer) filter discs (pore size: 0.45 μm) and 60 μl reaction mixture to the standard vial. The filter discs were washed twice with 2 ml of wash buffer. The excess wash buffer was filtered and the dried filters discs were kept in the scintillation vials containing 9.5 ml of aqueous scintillation fluid (Amersham). The scintillation count was measured by liquid scintillation analyzer 1600 TR Packard. The uptake rates were determined by using the least square linear regression analysis over the time range measured and the obtained initial uptake rates were plotted as a function of each Ca^{2+} concentration.

2.2.13 Calcium transient measurement in transfected cardiomyocytes

To investigate whether the reduced expression of sorcin alters the cytosolic Ca^{2+} cycling, intracellular

Ca^{2+} transients were measured. Cardiomyocytes were cultured on self made culture dishes with glass cover slip bottom. After 48 h of transfection cardiomyocytes were incubated with X- rhod-1 AM (acetomethoxy) dye for 10 min at room temperature. Media was changed and the cells were incubated at 37 $^\circ$C for 30 min in a humified atmosphere with 5% CO_2. The dishes were fixed manually on the stage of Laser scanning microscope, LSM 510 META and the cardiomyocytes were stimulated at 40 V, 50 Hz. The line scans along the longitudinal axis of the cardiomyocytes were recorded using a time series of 1.5 ms for 1500 times. Only the healthy, rod shaped, beating cardiomyocytes were included in the study. Rhodamine fluorescence was normalized, Ca^{2+} transient amplitude, time to peak and time to 80% decay was calculated.

2.2.14 Catheter based adenoviral gene delivery into rat hearts

The adenoviral injection was performed as described by Ding et al (2004). Briefly, 6 male wistar rats were used in each group, animals were intubated and anaesthetized with isoflurane (1.5% v/v), a 3F balloon was placed into the right atrium and a 2F lumen balloon catheter was placed into the aortic root. After baseline measurements of physiological variables a transient cardiac arrest was induced and 500 μl ($1.0\text{-}1.2 \times 10^{11}$) of adenoviral suspension was applied by gently filling the coronary vascular system. After 3 min the animals were resuscitated via injection of adrenaline. Using the above technique a transfection rate between 35-60% was achieved.

2.2.15 Echocardiography and morphological assessment

Echocardiography was performed on anaesthetized rats before adenoviral gene delivery to the hearts and after 7 and 12 days. Cardiac function was assessed using a 10 Mhz echocardiography head. M-Mode and 2-D echocardiography were digitalized. End-systolic diameter, end-diastolic diameter and fractional shortening were evaluated from both M-mode and 2-D mode echocardiography. After 14 days of adenoviral transfection, the rats were sacrificed and the body, heart, liver and lung weights were obtained. Mid cavities slices from the transfected rat hearts was used for histological assessment.

2.2.16 Statistical analysis

Data are expressed as means ± SEM, and statistical significance was determined with students's t-test for non-paired observations. For the pharmacological effects of forskolin and time dependent changes in fractional shortening in the echocardiographic studies 2-way ANOVA was used. A $p<0.05$ was considered significant

3. Results

3.1 Generation and amplification of adenoviral vectors

Adenovirus serotype 5 vectors for antisense sorcin with GFP expression and a control vector comprising only of GFP driven by cytomegalovirus promoter (CMV) was constructed. Human sorcin cDNA was cloned in the reverse orientation in multiple cloning site of pAdTrackCMV shuttle vector (9.2 kb) (Fig. 3.1-A). The pAdTrackCMV vector containing sorcin cDNA was linearized with Pme I. pAdEasy vector and linearized pAdTrackCMV vector containing sorcin cDNA were cotransformed in BJ5183 cells. Homologous recombination event in BJ5183 cells resulted in recombinant Ad.plasmid. Positive clones were confirmed by Pac I digestion (Fig. 3.1-B).
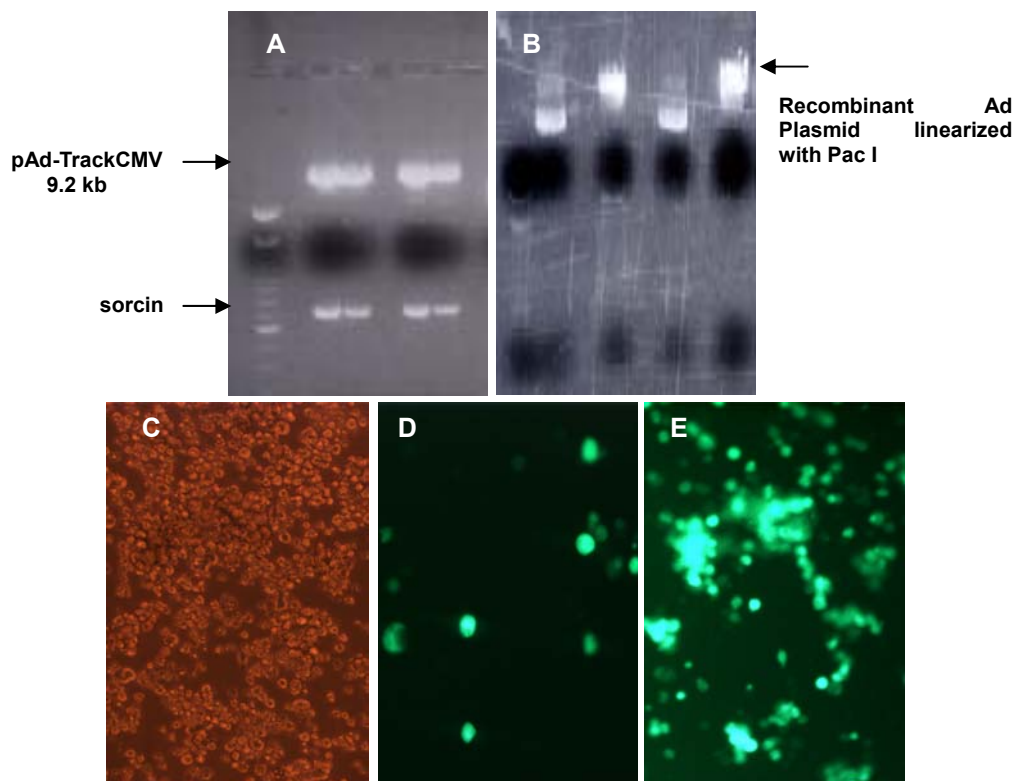
**Fig. 3.1 Generation of the Adenoviral vectors**

(**A**) Human sorcin cDNA (in reverse orientation) was cloned in multiple cloning site of the shuttle vector pAd-TrackCMV using Hind III and Xho I restriction sites. The orientation of the fragment was confirmed by restriction digestion. Upper band represent the 9.2 kb shuttle vector pAd-TrackCMV and lower band is 600bp sorcin cDNA. pAd-TrackCMV containing sorcin cDNA (pAd-TrackCMV-Sorcin) was linearized by using restriction endonuclease Pme I. The linearised pAd-TrackCMV-sorcin was cotransformed with pAdEasy vector into BJ5183 cells to produce recombinant adenoviral plasmid by homologous recombination. (**B**) Positive clones were checked with Pac I digestion. (**C**) Linearized recombinant Ad plasmid was transfected into adenovirus packaging cell line AD 293 cells. (**D**) GFP expression was visualized by fluorescence microscopy at 2 days. Only few cells were positive for GFP expression at day 2. (**E**) Comet like adenovirus producing foci was clearly visible at day 5.

The linearized plasmid was used to transfect AD293 cells (Fig. 3.2-C). Progress of the transfection was monitored by GFP expression (Fig. 3.1-D). After day 2 of transfection only few cells were positive for GFP expression and after day 5 the virus producing foci were visible as comet shaped (Fig. 3.1-E).

3.2 Optimization of transfection with adenoviral vectors

The generated adenoviral vectors were optimized for transfection efficiency in adult rat cardiomyocytes prior to the physiological and biochemical experiments.

Isolated cardiomyocytes were transfected at multiplicity of infection (MOI) of 1, 10, 50, 100 and 250 using Ad.GFP and Ad.as.SOR.GFP. Transfection efficiency of 95% or above was achieved at 100 MOI in both the vectors without any visible signs of toxicity (Fig. 3.2-A). Expression of GFP observed 48 h post transfection was used as a parameter of successful transfection (Fig. 3.2-B). 100 MOI was utilized for transfection throughout the study with isolated cardiomyocytes.
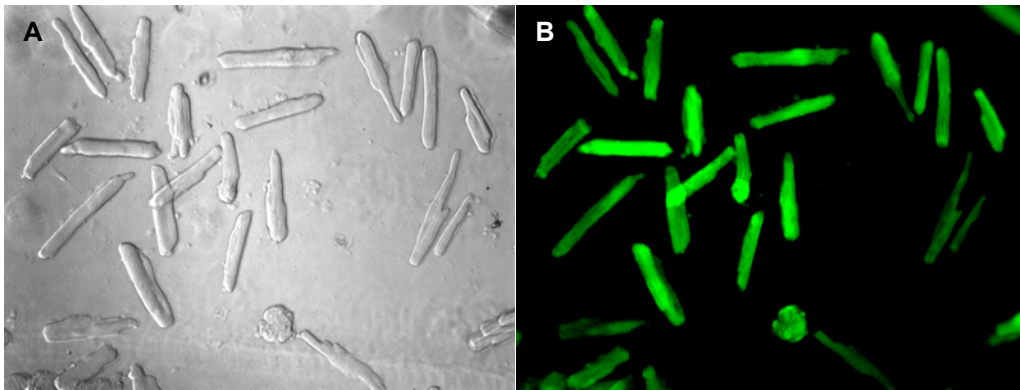
Fig. 3.2 Adult rat cardiomyocytes transfected with Ad.as.SOR.GFP

(**A**) Phase contrast image of cardiomyocytes transfected with 100 MOI of Ad.as.SOR.GFP 48 h post transfection. (**B**) Successful transfection was monitored by the expression of GFP visualized by fluorescent microscope at 473 nm. A transfection efficiency of higher than 95% was achieved without any visible signs of toxicity. All the experiments with isolated and cultured cardiomyocytes were carried out by using an MOI of 100.

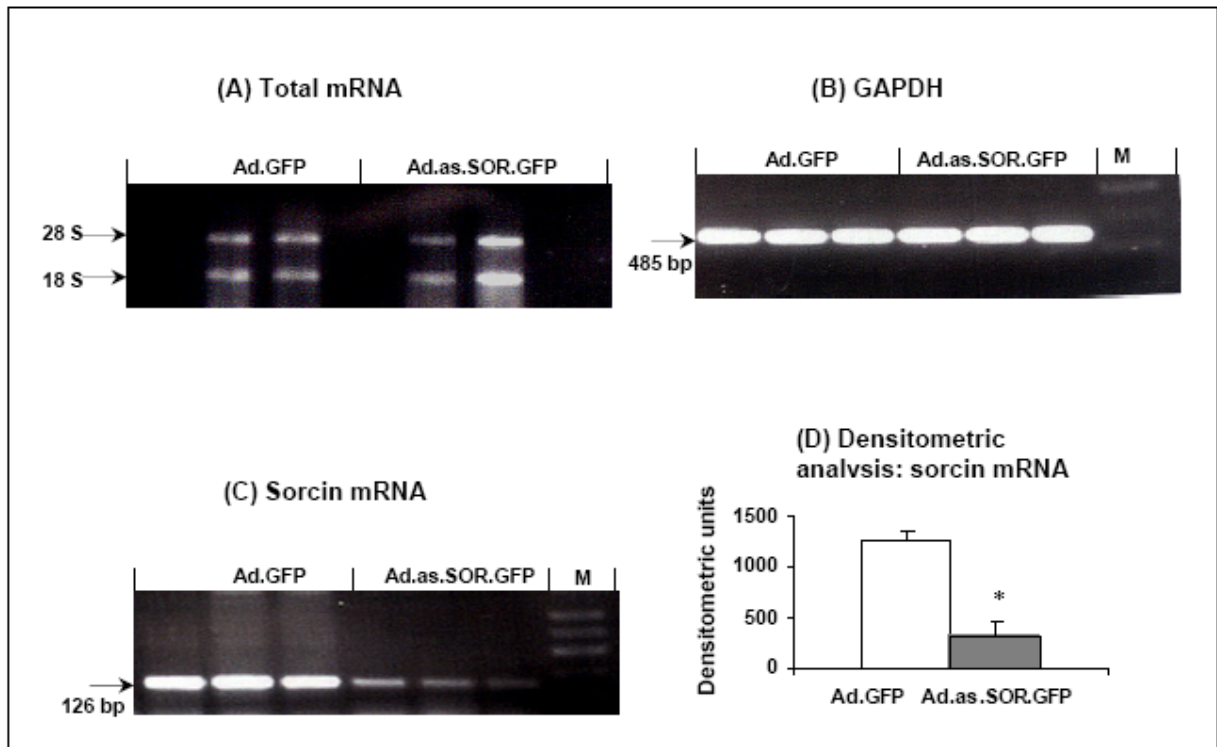## 3.3 Downregulation of sorcin by Ad.as.SOR.GFP

Isolated adult rat cardiomyocytes after 48 h of transfection with Ad.as.SOR.GFP were evaluated for downregulation of sorcin at mRNA and protein level. Ad.GFP was used as control.

3.3.1 Downregulation of sorcin mRNA

Transfected cardiomyocytes were cultured for 48 h and harvested for total RNA. Purity and integrity of RNA was determined spectrophotometrically by measuring the ratio of absorbance at 260/280 as well as electrophoretically by using (1.2%) agarose - formaldehyde gel (Fig 3.3-A). Expression of GAPDH was used as standard to ensure uniform loading (Fig 3.3-B). RT-PCR using specific primers for sorcin revealed 74.5 % decrease in the sorcin mRNA in the cardiomyocytes transfected with Ad.as.SOR.GFP as compared to the Ad.GFP transfected cardiomyocytes (Fig 3.3-C & D).

Fig 3.3 RT-PCR to evaluate downregulation of sorcin mRNA

Total RNA was isolated from transfected cardiomyocytes 48 h post transfection. **(A)** Integrity and purity of RNA

was verified with agarose-formaldehyde gel. **(B)** Expression of GAPDH was used as the loading control. **(C)** Downregulation of sorcin mRNA was revealed by RT-PCR at mRNA level in Ad.as.SOR.GFP transfected cardiomyocytes as compared to control Ad.GFP transfected cardiomyocytes **(D)** Densitometry analysis exhibited a significant ($p<0.05$) decrease in sorcin mRNA levels in Ad.as.SOR.GFP transfected cardiomyocytes (318.5 ± 147.9 densitometric units (DU)) as compared to control, Ad.GFP transfected cardiomyocytes (1250.7 ± 109.4 DU).

3.3.2 Downregulation of sorcin protein

To analyze whether the decrease in sorcin mRNA is followed by reduction of sorcin protein expression, transfected cardiomyocytes were evaluated by immunofluorescence staining and western blot.

3.3.2.1 Immunofluorescence staining of transfected cardiomyocytes

Transfected cardiomyocytes were fixed with 4% PFA after 24 and 48 h of transfection. Sorcin protein was detected by using commercially available monoclonal antibody (Zymed). DNA specific fluorochrome DAPI (blue) was used to visualize the nucleus. A significant decrease in the sorcin protein was observed after 24 h (visualized as red), which was further decreased after 48 h (Fig. 3.4).
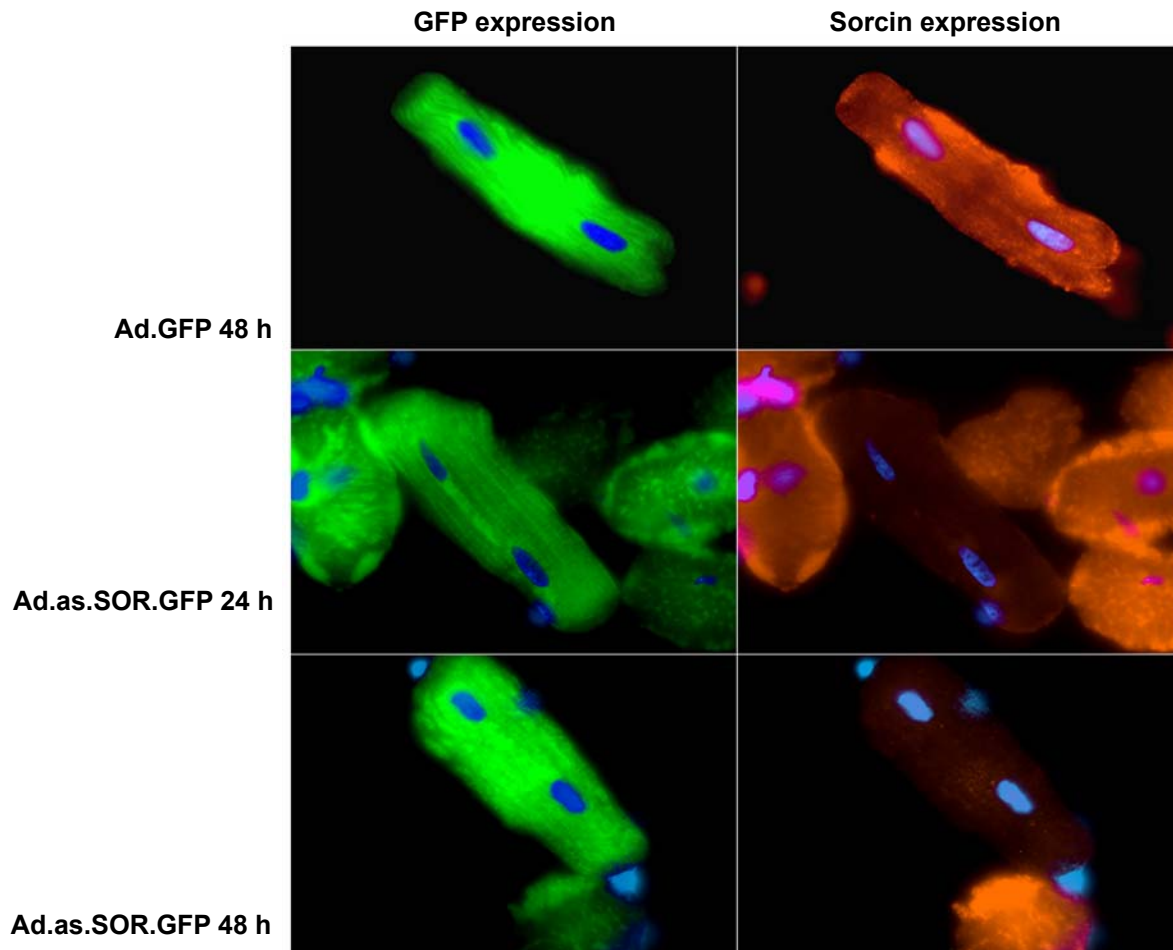

Fig 3.4 Immunofluorescence staining of the transfected cardiomyocytes

Cardiomyocytes were fixed with 4% PFA after 24 and 48 h of transfection. Immunofluorescence staining was performed using antibody directed against sorcin (red) and nucleus specific dye DAPI (blue). GFP (green) expression was monitored as the control for successful transfection. Ad.as.SOR.GFP transfected cardiomyocytes after 24 and 48 h showed significant decrease in protein as judged by decrease in the intensity of fluorescence in comparison to the control Ad.GFP transfected cardiomyocytes.

3.3.2.2 Immunoblotting of transfected cardiomyocytes

Transfected cardiomyocytes were lysed using lysis buffer containing protease inhibitors. Protein concentration was measured colorimetrically, using Bradford assay. Calsequestrin, a house keeping gene was used for the normalization of protein levels and to ensure uniform loading (Fig. 3.5-A). The cell lysate was analyzed by western blot using antibody raised against sorcin. Significant reduction in the amount of sorcin protein was observed in the cell lysate of Ad.as.SOR.GFP transfected cardiomyocytes as compared to the control (Fig. 3.5-

B). Densitometric analysis revealed 53.4% decrease in sorcin content in Ad.as.SOR.GFP transfected cardiomyocytes as compared to the control (Fig 3.5-C).
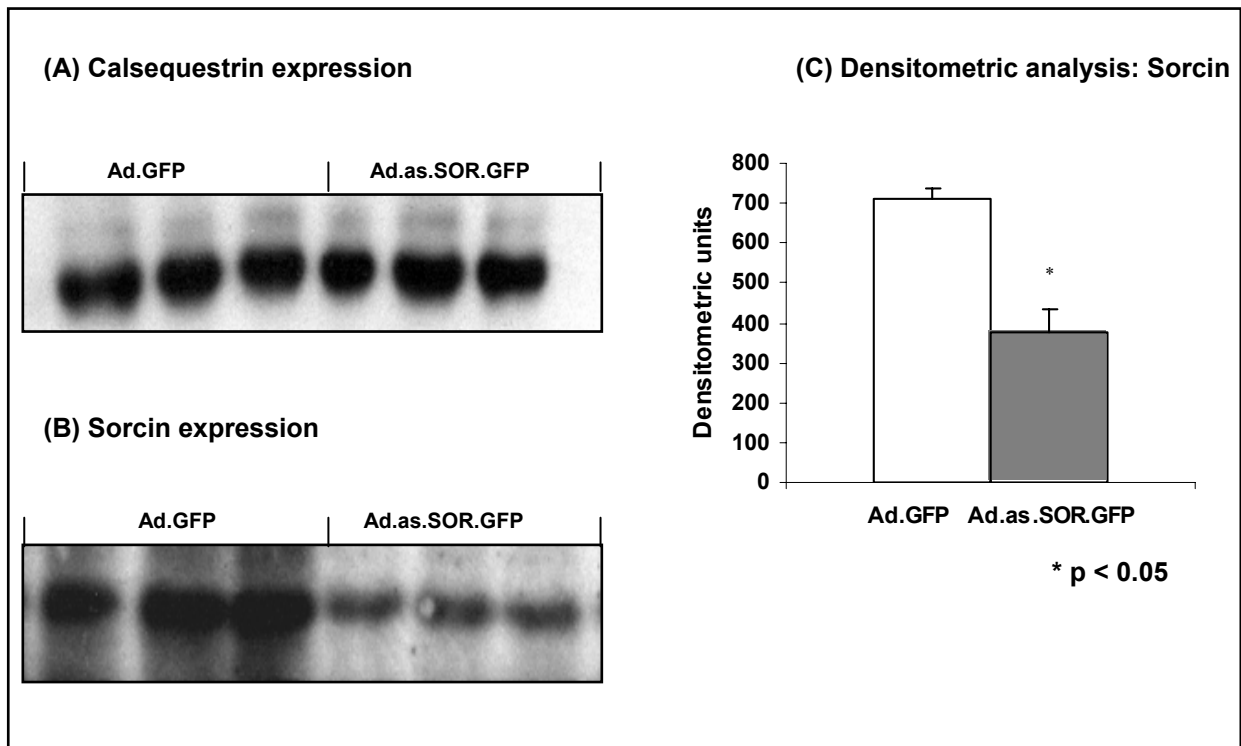

Fig 3.5 Evaluation of sorcin expression in Ad.as.SOR.GFP transfected cardiomyocytes by western blot

Cell lysate obtained from cardiomyocytes 48 h post transfection were analyzed for sorcin expression by western blot. (**A**) Protein levels were normalized by using calsequestrin expression. (**B**) Western blot using antibody directed against sorcin revealed significant reduction in the sorcin protein in Ad.as.SOR.GFP transfected cardiomyocytes as compared to control. (**C**) Densitometric analysis revealed a significant reduction in the sorcin protein levels (Ad.as.SOR.GFP: 379.0 ± 53.7 DU as compared to the Ad.GFP: 708.5 ± 29.8 DU; $*p < 0.05$) n = 6.

3.4.1 Measurement of contractility in transfected cardiomyocytes

To investigate the effect of downregulation of sorcin on contraction and relaxation properties single cell shortening of Ad.as.SOR.GFP and Ad.GFP transfected cardiomyocytes was measured using a video edge detection system, 48 h after transfection. Cardiomyocytes included in the study displayed characteristic rod shaped appearance, clear striations and unblebbed membranes.
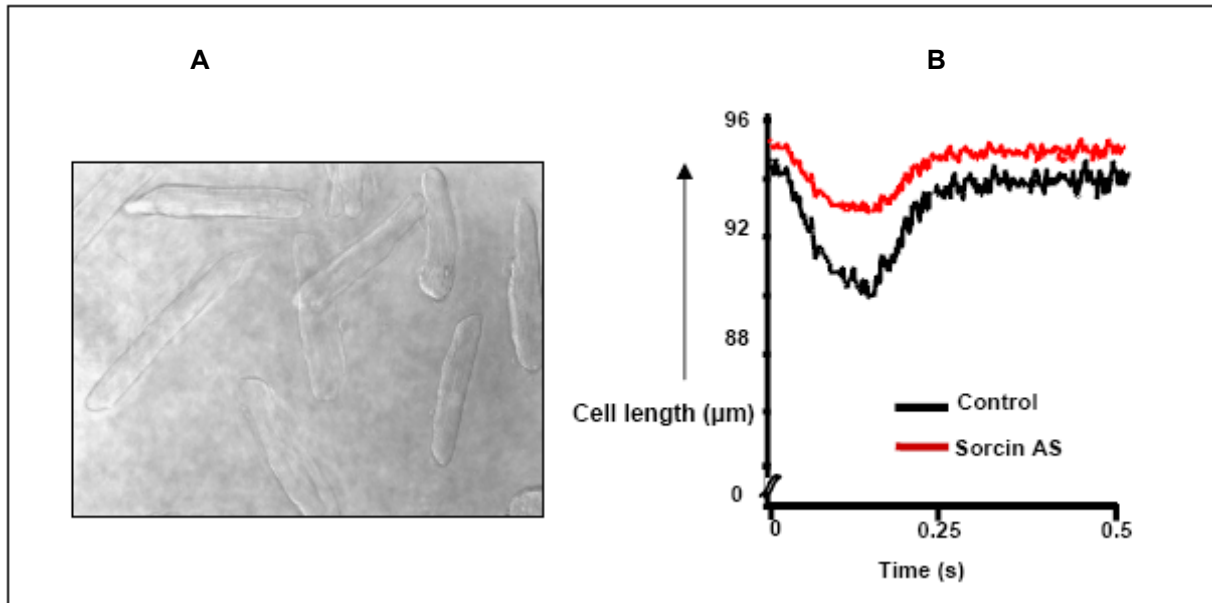
Fig 3.6 Measurement of fractional shortening in transfected cardiomyocytes

Transfected cardiomyocytes were investigated for fractional shortening on single cell edge detection system attached to a high speed video camera. (A) Cells were visualized on the screen attached to the inverted microscope to fix the edges of the cardiomyocytes to measure the fractional cell shortening at a stimulation frequency of 0.5 Hz. (B) Representative tracing of fractional shortening in Ad.as.SOR.GFP transfected (red) and Ad.GFP transfected (black) cardiomyocytes. Significant difference in the amplitude of cell contractility was observed in Ad.as.SOR.GFP transfected cardiomyocytes as compare to the Ad.GFP transfected cardiomyocytes.
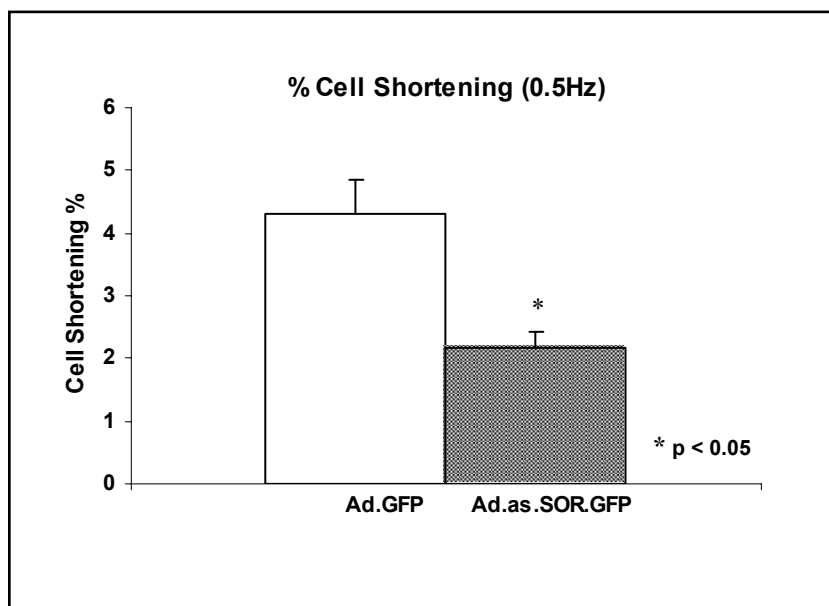
**Fig 3.7 Statistical analysis of fractional cell shortening in transfected cardiomyocytes**

Cell shortening (fractional shortening %) was analyzed in the transfected cardiomyocytes. The Ad.as.SOR.GFP transfected cardiomyocytes showed statistically significant decrease in the cell shortening (%). Ad.as.SOR.GFP (2.1 ± 0.25 %) exhibited a decrease of 43% in fractional cell shortening as compared to Ad.GFP (4.3 ± 0.55 %). Values presented are the ± SEM of 4 different experiments (n = 24); *p < 0.05.

(Fig 3.6-A). Cardiomyocytes were field stimulated at the basal frequency of 0.5 Hz and cell shortening (%

fractional shortening) was measured. Fig 3.6-B depicts a typical cell shortening tracing from Ad.GFP (black) and Ad.as.SOR.GFP (red) transfected cardiomyocytes A significant depression in the cell shortening was observed in Ad.as.SOR.GFP transfected cardiomyocytes as compared to the Ad.GFP transfected cardiomyocytes. Ad.as.SOR.GFP (4.3 ± 0.5 %), antisense sorcin transfected cardiomyocytes showed statistically significant 48.3% depressed amplitude of the cell shortening as compared to Ad.GFP (2.1± 0.25%); *p<0.05, n = 24 (Fig 3.7).

3.4.2 Intracellular Ca^{2+} transient measurement in cardiomyocytes

To determine whether depletion of sorcin protein affects the calcium transients in intact cardiomyocytes intracellular Ca^{2+} transients were measured. Transfected cardiomyocytes were cultured on laminin coated glass bottomed culture dishes (Fig 3.8-A), loaded with rhodamine dye X-rhod 1 (Fig 3.8-B), stimulated at basal frequency of 1 Hz and recorded the line scans along the longitudinal axis of cardiomyocyte (Fig 3.8-C) with a time series of 1500 for 1.5 ms using laser scanning microscope (Zeiss).
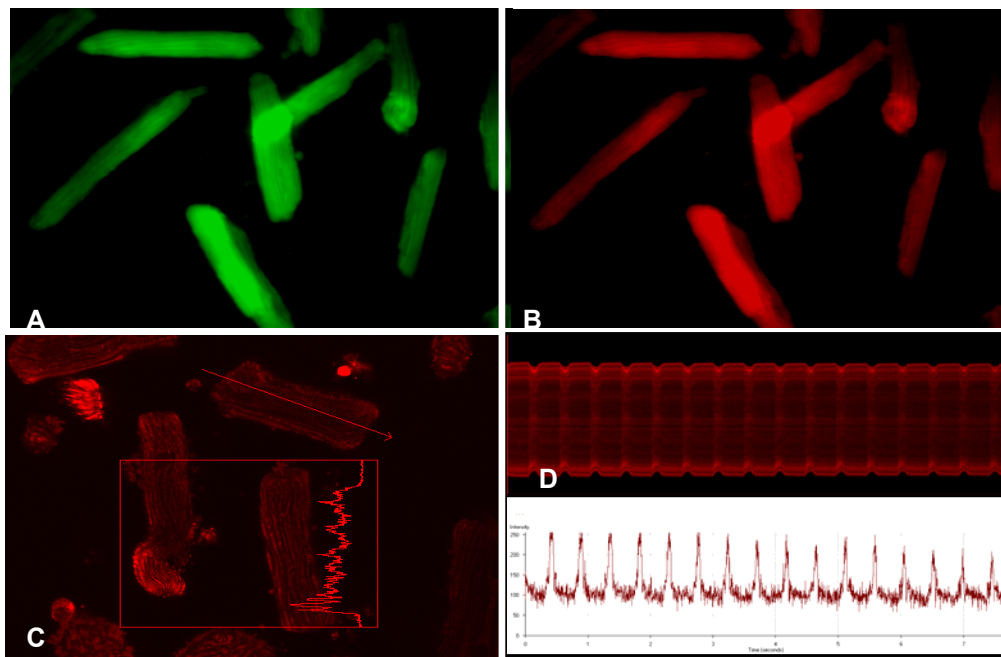

Fig 3.8 Intracellular Ca^{2+}-transient measurement in transfected cardiomyocytes

Transfected cardiomyocytes were cultured on laminin coated glass bottomed dishes. (A) Expression of GFP was monitored for the successful transfection. (B) Cardiomyocytes were incubated with X-rhod-1 (rhodamine based dye) and proper loading was confirmed. (C) Cardiomyocytes were field stimulated at a stimulation frequency of 1 Hz and line scans were recorded along the longitudinal axis. (D) Representative line scans of a stimulated Ad.GFP transfected cardiomyocyte and corresponding calcium transient recording.

Fig 3.8-D presents a typical line scan and recorded calcium transients in an Ad.GFP transfected cardiomyocyte. Recorded calcium transients were collected by using software LSM510 META. Fig 3.9-A depicts a filled spectrum image of calcium transients recorded in Ad.GFP transfect cardiomyocyte. The data obtained was analyzed; the amplitude of the [Ca^{2+}]$_I$ transients in Ad.as.SOR.GFP transfected cardiomyocytes

was 33.1 % lesser as compared to the control (Fig 3.9-B).

(A) Original tracing of Ca^{2+} transient

(B) Peak Ca^{2+}

*p < 0.05

(C) Time to peak

(D) T to 80%
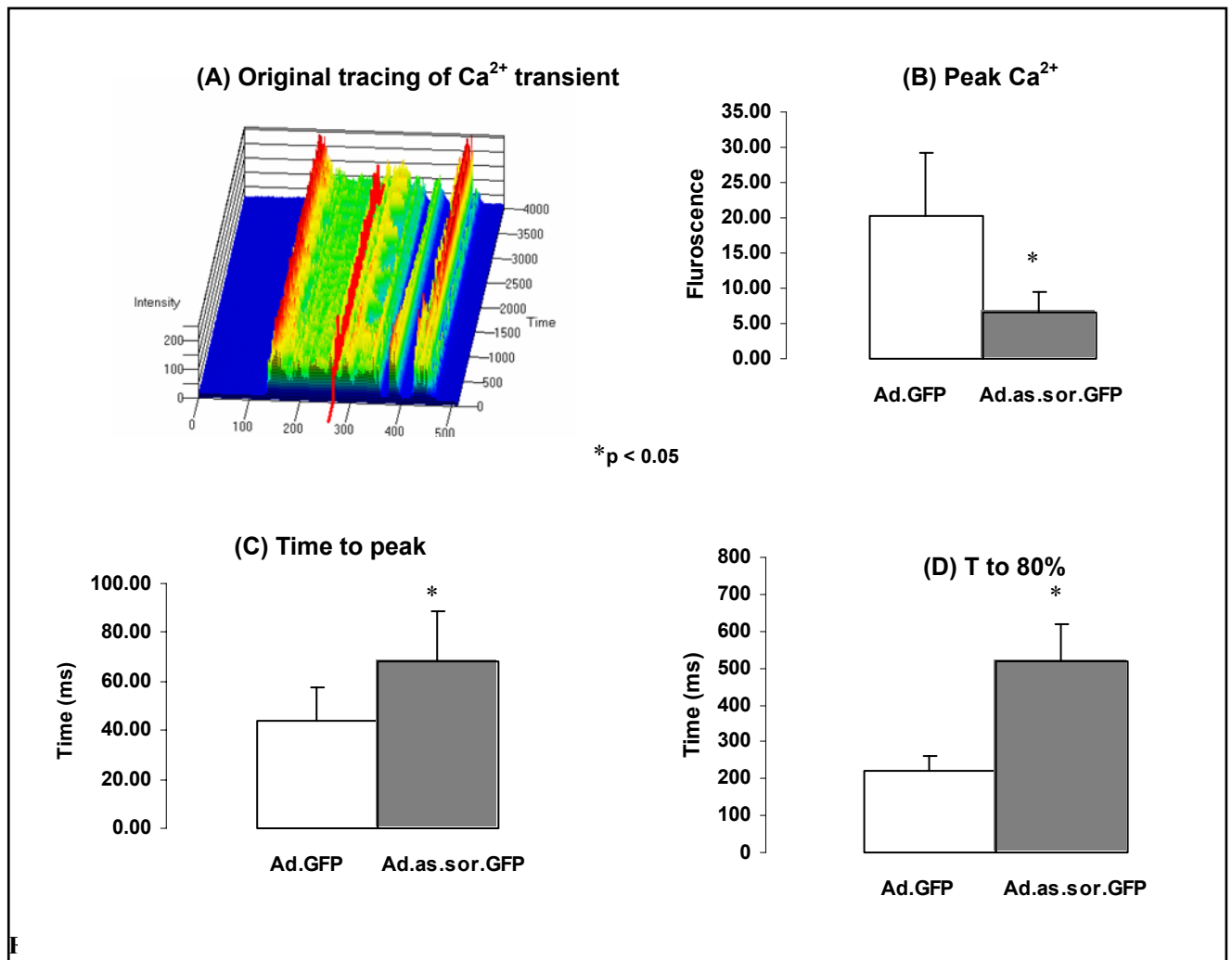
The line scans of the transfected cardiomyocytes were recorded and data was collected using software LSM 510 META® **(A)**. Representation of a filled spectrum transient recorded in an Ad.GFP transfected cardiomyocyte. **(B)** Ad.as.SOR.GFP transfected cardiomyocytes exhibited significantly lowered amplitude of whole cell transient (6.70 ± 2.8 normalized fluorescent units, NFU; *p< 0.05) as compared to Ad.GFP (20.2 ± 9.0 NFU; *p< 0.05) transfected cardiomyocytes. **(C)** Time to reach maximum amplitude (T to Peak) was significantly increased in antisense SOR transfected cardiomyocytes as compared to control (68.0 ± 20.4 ms vs. 44.2 ± 13.1 ms; *p< 0.05) **(D)** Along with the decreased amplitude and increased time to peak , the relaxation was also significantly prolonged as evident by the significant increase in T 80% in antisense SOR transfected cardiomyocytes (515.8 ± 104.9 ms) as compared to Ad.GFP transfected cardiomyocytes (220.9 ± 40.4 ms) The cardiomyocytes included in the study were from four different myocyte isolations , n = 25; *p < 0.05.

Time taken to reach the maximum amplitude, Time to peak was significantly increased in the Ad.as.SOR.GFP transfected cardiomyocytes showing an increase of 53.8 % as compared to the Ad.GFP transfected cardiomyocytes (Fig 3.9-C), Decreased amplitude of transient and increased time to peak (T to peak) was accompanied by significantly prolonged transients in the Ad.as.SOR.GFP transfected cardiomyocytes, evident from 133.4% increase in the relaxation time calculated as T-80% (Fig 3.9-D). All the above three parameters described were statistically significant (*p<0.05) n =25.

3.4.3   Force-frequency   relationship   in   transfected cardiomyocytes

To analyze the effect of increasing stimulation frequency on the Ad.as.SOR.GFP transfected cardiomyocytes, the changes in contraction amplitude corresponding to the increasing frequency of stimulation (0.25 Hz to 5 Hz) were recorded in field stimulated cardiomyocytes using a single cell edge detecting system. The increase in frequency of stimulation was associated with a negative force-frequency relationship in Ad.as.SOR.GFP transfected cardiomyocytes in contrast to control Ad.GFP transfected cardiomyocytes, which exhibited positive force frequency relationship. The force of contraction (FOC), judged by the cell shortening (% cell shortening) was significantly lower at stimulation frequencies ranging from 0.25 Hz to 5 Hz in Ad.as.SOR.GFP transfected cardiomyocytes as compared to control.
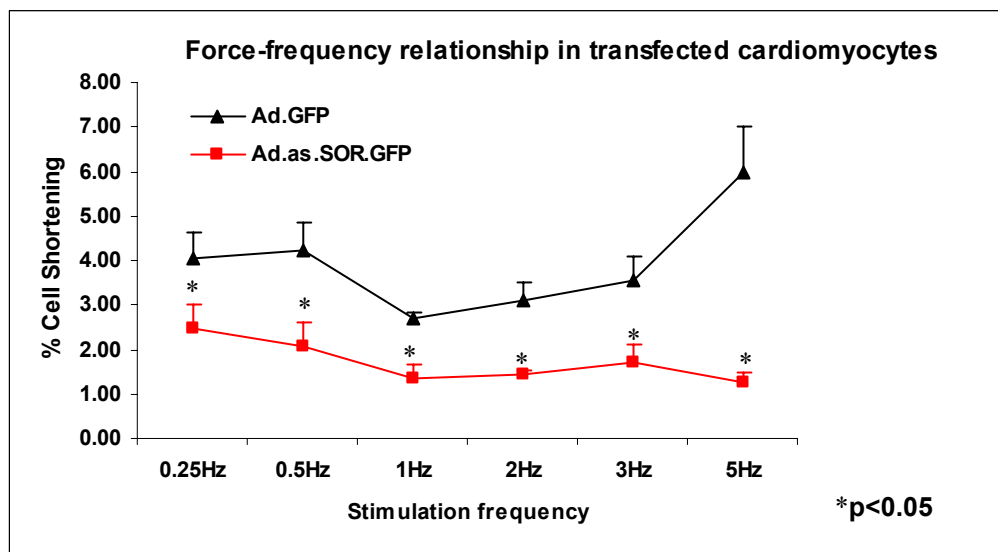
**Fig 3.10 Force-frequency relationship in transfected cardiomyocytes.**

Transfected cardiomyocytes were cultured on 18 mm glass coverslips coated with laminin for 48 h, fixed the coverslips on the stage of Axiophot inverted microscope (Nikon) and field stimulated with increasing frequency rising from 0.25 Hz up to 5 Hz. Antisense SOR transfected cardiomyocytes showed a negative force-frequency relationship unlike the control Ad.GFP transfected cardiomyocytes, which exhibited a steady state force-frequency relationship with an increase in stimulation frequency, statistically significant difference in the cell shortening (%) at frequencies ranging from 0.25 Hz to 5 Hz was recorded.; *p<0.05.

Significantly depressed cell shortening (in %) was observed in the Ad.as.SOR.GFP transfected cardiomyocytes at the baseline levels (0.25 Hz, *p<0.05) as compared to Ad.GFP transfected cardiomyocytes and was not augmented while increasing stimulation frequency (Fig. 3.10). The difference in cell shortening remained

unchanged between Ad.GFP and the Ad.as.SOR.GFP transfected cardiomyocytes throughout all the frequencies measured (0.25 Hz to 5 Hz).

3.4.4 Pharmacological interventions in transfected cardiomyocytes

Binding of sorcin to the ryanodine receptor is influenced by beta-adrenergic stimulation upon protein kinase A dependent phosphorylation (Lokuta el al., 1997). To study the effect of beta- adrenergic stimulation on cardiomyocytes with decreased levels of sorcin expression, cardiomyocytes were subjected to stimulation with the adenylate cyclase stimulating agent forskolin. Ad.as.SOR.GFP transfected cardiomyocytes exhibited significantly lower fractional shortening as compared to the Ad.GFP transfected cardiomyocytes in the absence of forskolin at baseline contractility (0.5 Hz). However, a dose dependent increase in the fractional shortening (in %) was observed in both the groups after adding forskolin ranging from 0.1 μm to 1 μm (Fig. 3.11). This indicated that the β-adrenergic responsiveness remained intact in the Ad.as.sor.GFP transfected cardiomyocytes.
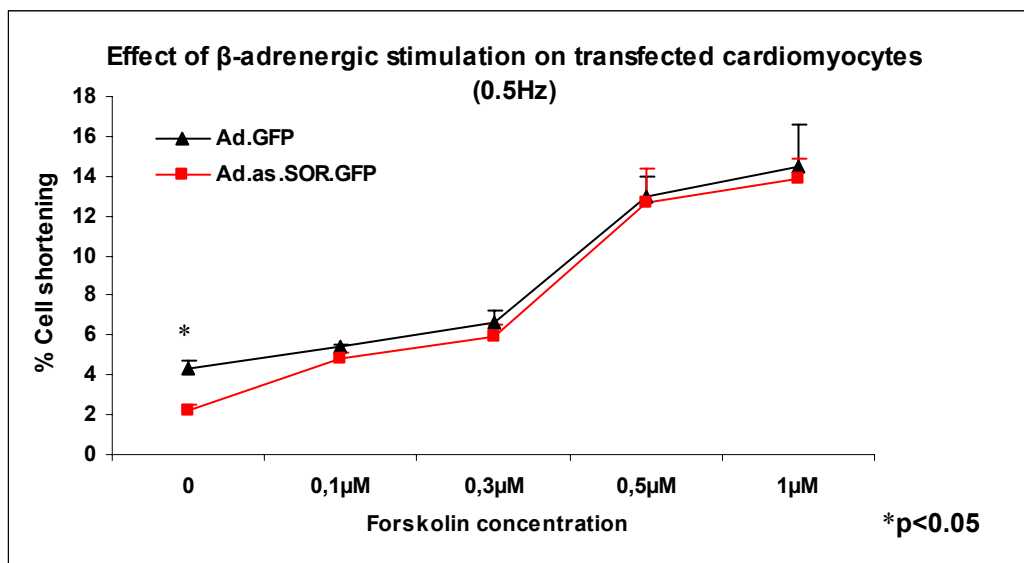

Fig 3.11 Effect of forskolin on transfected cardiomyocytes

To study the effect of beta-adrenergic stimulation on transfected cardiomocytes, cardiomyocytes were subjected to increasing concentration of forskolin at stimulation frequency of 0.5 Hz (each group n=13). Increased cell shortening was observed at all concentrations of forskolin in Ad.as.SOR.GFP as well as Ad.GFP transfected cardiomyocytes. However, significantly decreased baseline levels in cell shortening were observed in Ad.as.sor.GFP as compared to Ad.GFP transfected cardiomyocytes.

3.5 Expression and purification of recombinant GST-sorcin

Recombinant GST-sorcin was expressed in E.coli. BL21 using pGEX2TK expression vector by induction with 100 mM IPTG as described in the method section. Maximum yield was obtained 4 to 6 h post IPTG induction. Expressed sorcin was purified by affinity chromatography by using glutathione agarose beads to the lysed pellet and eluting the bound protein by four successive elutions. Fig. 3.12-A shows the analysis of the elutes

obtained on SDS-PAGE (10% gel) as visualised by coomassie staining, the purity of expressed sorcin was confirmed by silver staining. Maximum yield was obtained from the first elute (Fig. 3.12-B). Concentration of the purified sorcin was determined colorimetrically by Bradford protein estimation assay, the yield of the protein obtained was 500 to 600 μg per preparation. The purified sorcin was used in the sarcoplasmic reticulum Ca^{2+} uptake assays.
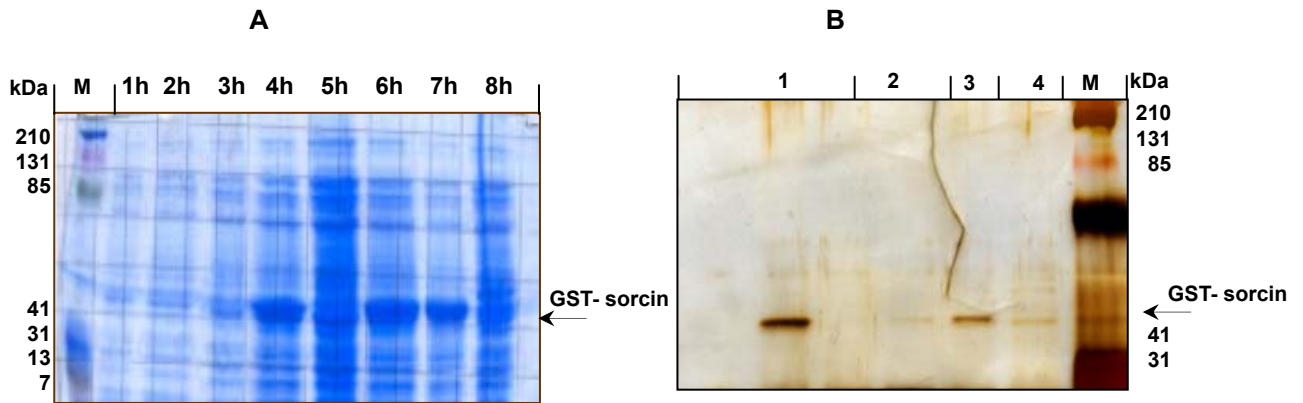

Fig. 3.12 Expression and purification of recombinant GST-sorcin

(**A**) 10 μl aliquots obtained at time points ranging from 1 to 8 h post IPTG induction were loaded on 10% SDS gel to analyze the expression of sorcin. Gel was stained with coomassie blue to visualize the expressed protein. Maximum yield was obtained at 4 to 6 h post IPTG induction. The band representing sorcin expression was shifted up to 47kDa due to the 26 kDa GST tag bound to 21.6 kDa sorcin. (**B**) Expressed sorcin was purified by affinity chromatography by using glutathione agarose beads, silver staining was performed to verify the purity of the expressed protein. Highly pure sorcin was obtained with this method, maximum yield was obtained from the first elute. Lanes 1-4: elutes, M: Protein standard.

3.6 Sarcoplasmic reticulum Ca^{2+} uptake

To examine the effect of sorcin on Ca^{2+} uptake function in the sarcoplasmic reticulum, oxalate-facilitated Ca^{2+} uptake assays were performed. As shown in Fig, 3.13, decreased expression of sorcin resulted in decreased Ca^{2+} uptake rate. Furthermore, addition of 1 μM of sorcin increased the maximal rate of SR Ca^{2+} uptake indicating a shift towards the normal levels in the SR Ca^{2+} uptake. This implies that decreases expression of sorcin leads to diminished SR Ca^{2+} uptake rates.
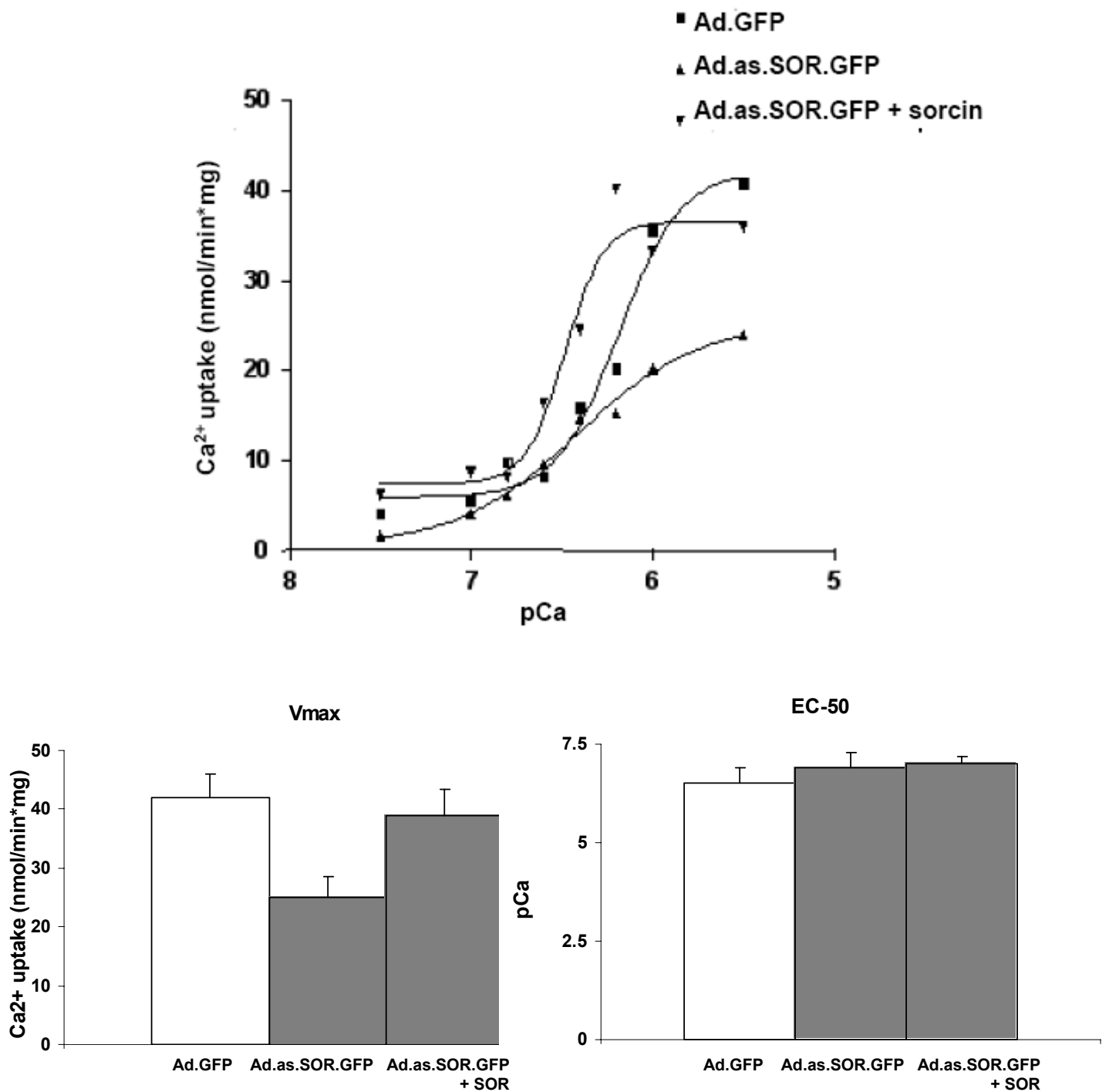
Fig. 3.13. Sorcin regulates sarcoplasmic reticulum Ca^{2+} content

The rate of Ca^{2+}-uptake into cardiomyocyte homogenates was measured by oxalate-facilitated Ca^{2+} uptake assay over the range 0.02-5 uM free Ca^{2+} (pCa = 8-5). The uptake rates were determined by using the least square linear regression analysis over the time range measured and obtained initial uptake rates were plotted as a function of each Ca^{2+} concentration. Decreased expression of sorcin resulted in decreased oxalate facilitated Ca^{2+}-uptake rate. Addition of 1 μM of sorcin increased the maximal rate of SR Ca^{2+} uptake

3.7 Effect of down regulation of sorcin on expression of calcium handling proteins

Excitation-contraction coupling is a coordinated sequence between intracellular calcium handling proteins. To

investigate the effect of downregulation of sorcin on intracellular calcium handling proteins, expression of ryanodine receptors (RYR2), sarcoplasmic reticulum (SR) Ca^{2+}-ATPase (SERCA2a), phospholamban (PLB), FK binding protein 12.6 (FKBP12.6) and triadin was evaluated in Ad.as.SOR.GFP transfected cardiomyocytes and compared to the control Ad.GFP transfected cardiomyocytes. GAPDH was used as the control in the RT-PCR to ensure uniform loading and calsequestrin as the standard for uniform loading in western blot in all the experiments.

3.7.1 Ryanodine Receptor

The SR calcium release channel or ryanodine receptor (RYR2) is a key component in cardiac excitation-contraction coupling. It facilitates the systolic release of Ca^{2+} to initiate force of contraction at the myofilaments. To analyze whether depletion of sorcin in Ad.as.SOR.GFP transfected cardiomyocytes affects the expression of RYR2, cell lysate from the transfected cardiomyocytes were subjected to immunoblotting utilizing anti-RYR2 antibody (Fig. 3.14-A). No significant alteration in the expression of RYR2 was observed. Signals obtained were analyzed densitometrically. Statistical evaluation revealed no significant difference in the expression of RYR2 in Ad.as.SOR.GFP transfected cardiomyocytes as compared to the control. (Ad.GFP 3922.6 ± 788.6 DU vs. Ad.as.SOR.GFP 3484.4 ± 503.2 DU); n = 6, (Fig. 3.14-B).

3.7.2 Sarcoplasmic reticulum Ca^{2+} ATPase

Sarcoplasmic reticulum Ca^{2+} ATPase (SERCA) is the key channel protein for the diastolic calcium transport into the sarcoplasmic reticulum (SR). During diastole the majority of released Ca^{2+} is pumped back into the SR to prepare the subsequent contraction cycle. The expression of SERCA2a, the main isoform expressed in cardiac muscle was evaluated by RT-PCR and western blot in Ad.as.SOR.GFP transfected cardiomyocytes. The mRNA expression of SERCA2a was significantly downregulated in the adenoviral transfected cardiomyocytes (Fig. 3.15-A).

Ryanodine receptors expression
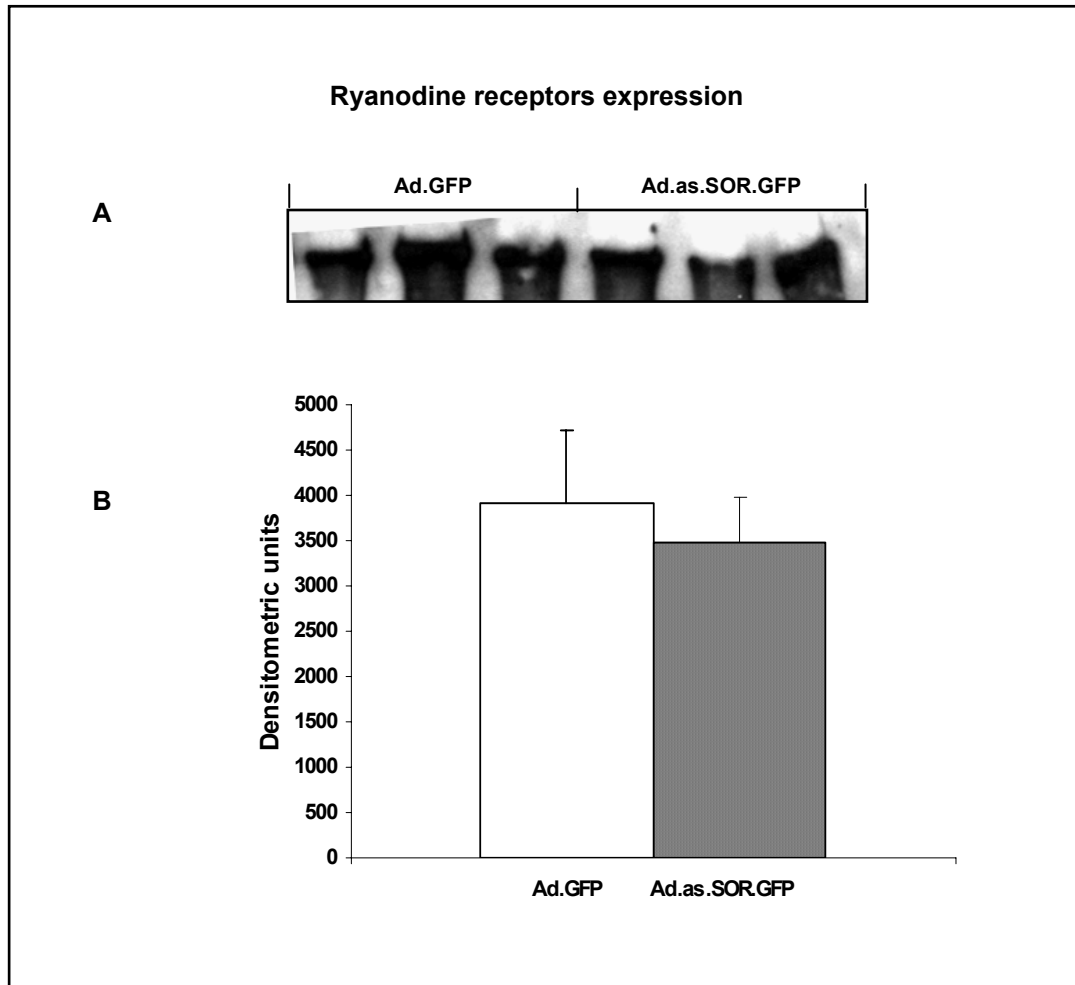
Fig 3.14 Expression of Ryanodine Receptors (RYR2) in the transfected cardiomyocytes

(A) Expression of Ryanodine Receptor (RYR2) was investigated in cell the lysates of Ad.as.SOR.GFP transfected cardiomyocytes by western blot, using antibody directed against RYR2. No significant difference was observed in the expression of RYR2 in Ad.as.SOR.GFP transfected cardiomyocytes as compared to the control (Ad.GFP). **(B)** Signals obtained were analyzed by densitometry followed by statistical analysis. No significant alteration in the expression of RYR2 in the Ad.as.SOR.GFP transfected cardiomyocytes as compared to the Ad.GFP transfected control cardiomyocytes (Ad.GFP 3922.6 ± 788.6 DU vs. Ad.as.SOR.GFP 3484.4 ± 503.2 DU; n = 6, was detected.
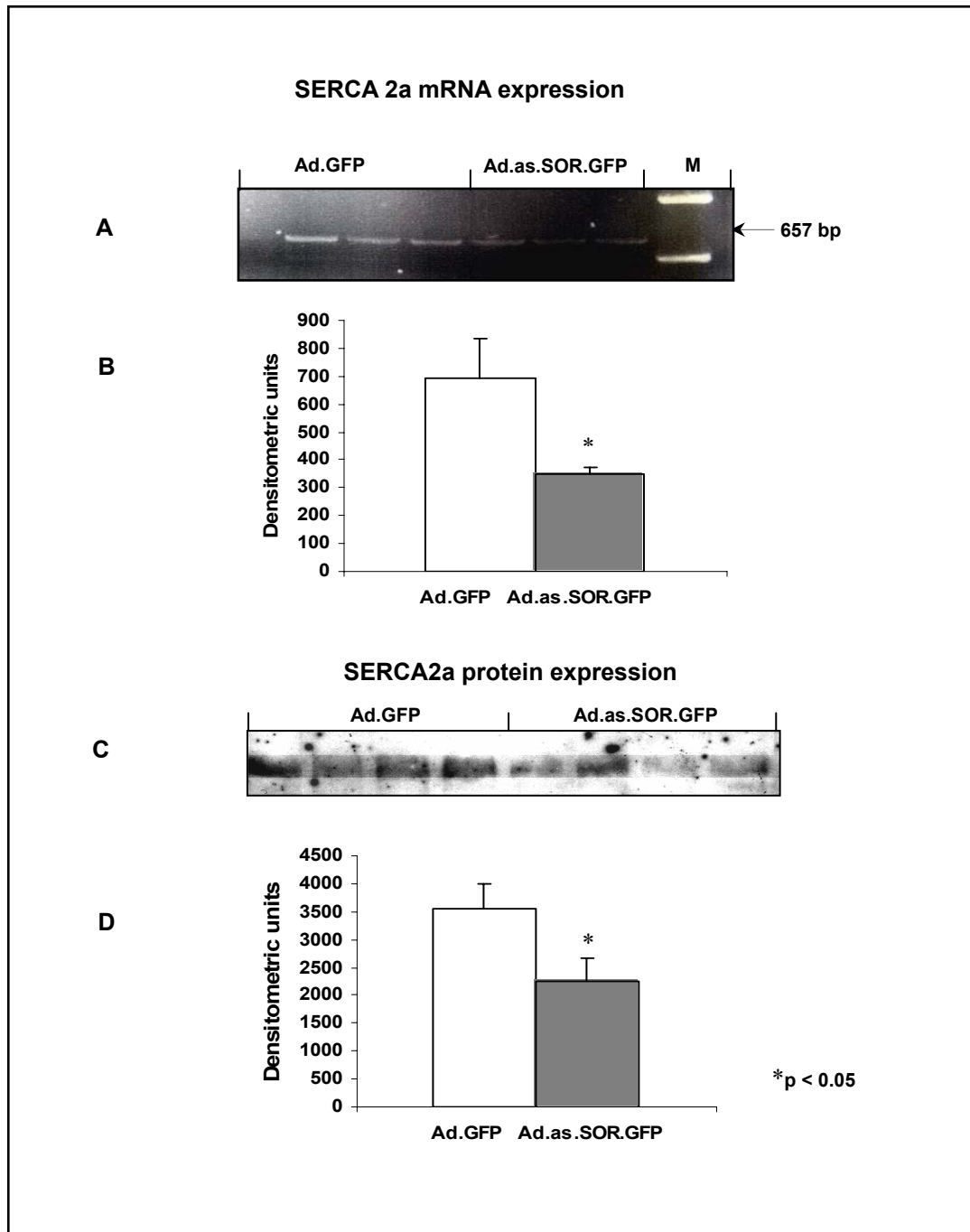
Densitometric analysis revealed a significant decrease in SERCA2a mRNA expression in Ad.as.SOR.GFP transfected cardiomyocytes as compared to the control (Ad.GFP 692.9 ± 142.5 vs. Ad.as.SOR.GFP 349.2 ± 25.0); n = 6, *p<0.05 (Fig. 3.15-B). Western blot using the cell lysate from the transfected cardiomyocytes,

utilizing antibody directed against SERCA2a ndicated significant downregulation in the SERCA2a protein expression (Fig. 3.15-C). Densitometric analysis revealed a statistically significant decrease in the SERCA2a protein levels in the Ad.as.SOR.GFP transfected cardiomyocytes as compared to the control (Ad.GFP 3539.5 ± 459.0 vs. Ad.as.SOR.GFP 2239.8 ± 429.4); n = 6, *p< 0.05 (Fig. 3.15-D).
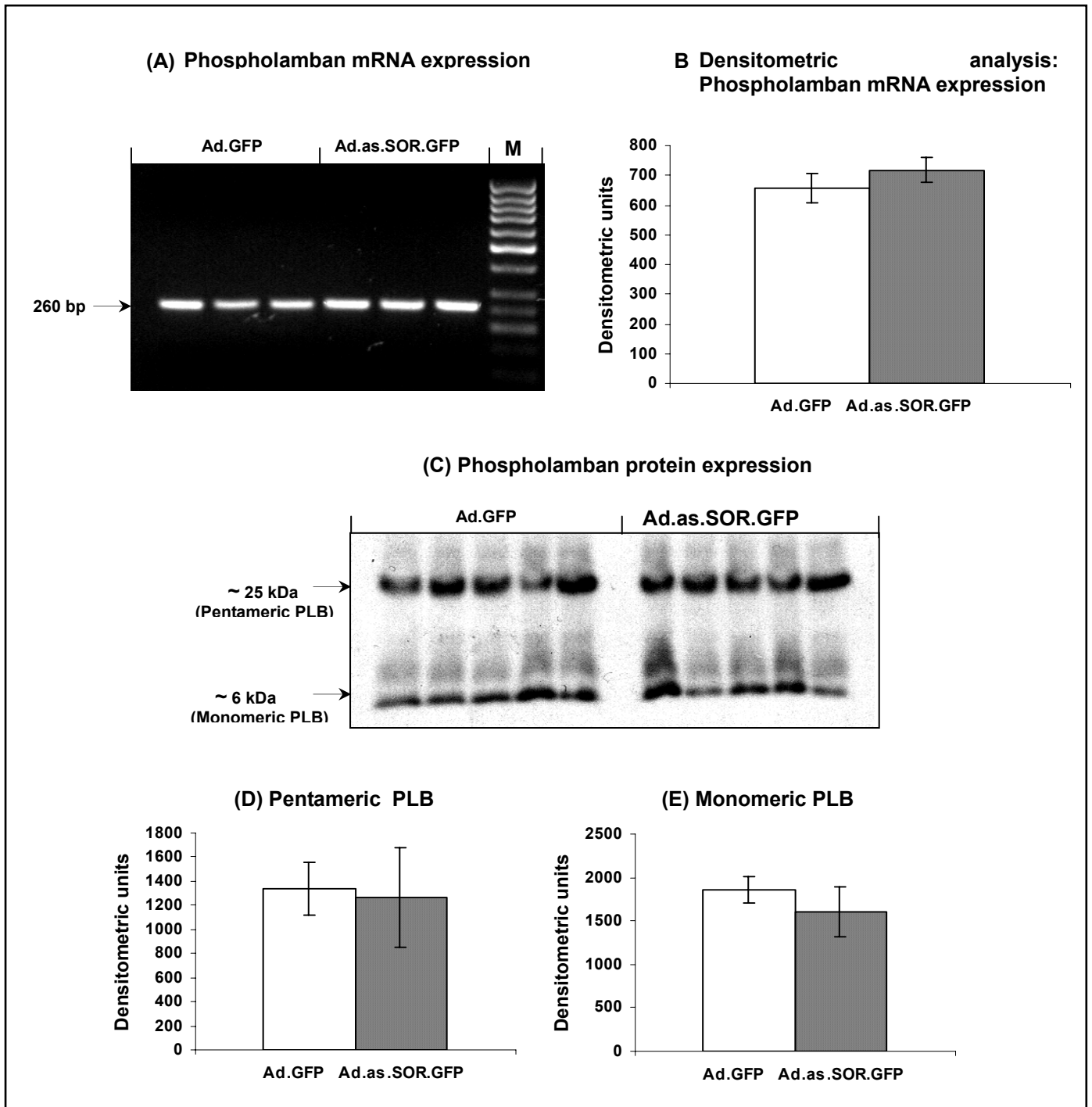
3.7.3 Phospholamban

Phospholamban (PLN), a 52 amino acid sarcoplasmic reticulum protein regulates sarcoplasmic reticulum Ca^{2+}ATPase activity by inhibiting SERCA2a in its unphosphorylated state. Phosphorylation through protein kinase A relieves this inhibition and activates the SR Ca^{2+}-transport during stress response. The effect of depletion of sorcin on mRNA, protein and monomeric/pentameric assembly of PLB was investigated in Ad.as.SOR.GFP transfected cardiomyocytes. RT-PCR performed by using specific primers for PLB, followed by densitometric analysis, revealed no significant alteration in the mRNA level of PLB (Ad.GFP 656.6 ± 48.0 DU vs. Ad.as.SOR.GFP 717.4 ± 42.2 DU); n = 6, (Fig. 3.16-A&B). Immunoblotting was performed on the cell lysate of the transfected cardiomyocytes utilizing anti-phospholamban antibody. Two distinct signals were obtained, one at ~ 6 kDa representing the monomeric and other at ~25 kDa yielding the pentameric or phosphorylated state of PLB (3.16-C). Densitometric analysis performed on the western blot signals indicated no significant difference in the monomeric (Ad.GFP 1340.9 ± 218.5 DU vs. Ad.as.SOR.GFP 1266.5 ± 413.1 DU; n = 6, p< 0.05) or pentameric assembly of PLB (Ad.GFP 1854.1 ± 147.6 DU vs. Ad.as.SOR.GFP 1604.0 ± 289.7 DU); p< 0.05(Fig. 3.16-D&E).

Fig. 3.15 Expression of sarcoplasmic reticulum Ca^{2+} ATPase (SERCA2a) in transfected cardiomyocytes

(A) The transfected cardiomyocytes were harvested for the total RNA preparation. RT-PCR was performed using specific primers for SERCA2a. A significant downregulation of SERCA2a mRNA was observed in the adenoviral antisense sorcin transfected cardiomyocytes as compared to the control. **(B)** Densitometric analysis revealed significant decrease in the SERCA2a mRNA levels in Ad.as.SOR.GFP transfected cardiomyocytes as compared to the Ad.GFP transfected cardiomyocytes (Ad.GFP 692.9 ± 142.5 vs. Ad.as.SOR.GFP 349.2 ± 25.0); n = 6, *p< 0.05. **(C)** Protein expression of SERCA2a was investigated in the cell lysate of the transfected cardiomyocytes by western blot utilizing an anti-SERCA2a antibody. Significant downregulation of SERCA2a protein was observed in the adenoviral antisense sorcin transfected cardiomyocytes as compared to the control. **(D)** Densitometric analysis of the western blot indicated a significant reduction in the SERCA2a protein level in Ad.as.SOR.GFP transfected cardiomyocytes as compared to the Ad.GFP transfected cardiomyocytes (Ad.GFP 3539.5 ± 459.0 vs. Ad.as.SOR.GFP 2239.8 ± 429.4); n = 6, *p< 0.05.

(A) Pholpholamban mRNA expression

B Densitometric analysis: Phospholamban mRNA expression

(C) Phospholamban protein expression

(D) Pentameric PLB

(E) Monomeric PLB

Fig. 3.16 Expression of Phospholamban (PLB) in transfected cardiomyocytes

(A) Cardiomyocytes after 48 h of transfection were harvested for the isolation of total RNA. RT-PCR using specific primers was performed. First three lanes present the PLB mRNA expression in Ad.GFP transfected cardiomyocytes and the next three lanes in Ad.as.SOR.GFP transfected cardiomyocytes. "M" represents the DNA marker. **(B)** Densitometric analysis of the obtained signals from the RT-PCR revealed no significant alteration in the PLB mRNA expression in Ad.as.SOR.GFP transfected cardiomyocytes as compared to the control Ad.GFP transfected cardiomyocytes (Ad.GFP 656.6 ± 48.0 DU vs. Ad.as.SOR.GFP 717.4 ± 42.2 DU); n = 6. **(C)** Immunoblotting from cell lysate of the transfected cardiomyocytes was performed by using anti-phospholamban antibody. Two distinct signals at ~ 6 kDa and ~25 kDa were obtained representing the native (or monomeric) and the pentameric (phosphorylated) state of PLB respectively. **(D)** Densitometric analysis revealed no significant difference in either the monomeric (Ad.GFP 1340.9 ± 218.5 DU vs. Ad.as.SOR.GFP 1266.5 ± 413.1 DU; n = 6. **(E)** or phosphorylated (Ad.GFP 1854.1 ± 147.6 DU vs. Ad.as.SOR.GFP 1604.0 ± 289.7 DU; n = 6, state of PLB in Ad.as.SOR.GFP transfected cardiomyocytes as compared to the Ad.GFP transfected cardiomyocytes.

3.7.4 FK binding protein 12.6

FK506 binding protein (FKBP 12.6) is one of the main accessory proteins of ryanodine receptors and is implicated in the modulation of SR calcium release (Prestle et al., 2001). To examine whether the depletion of sorcin in Ad.as.SOR.GFP transfected cardiomyocytes affects the expression of FKBP12.6, the mRNA and protein expression were investigated.
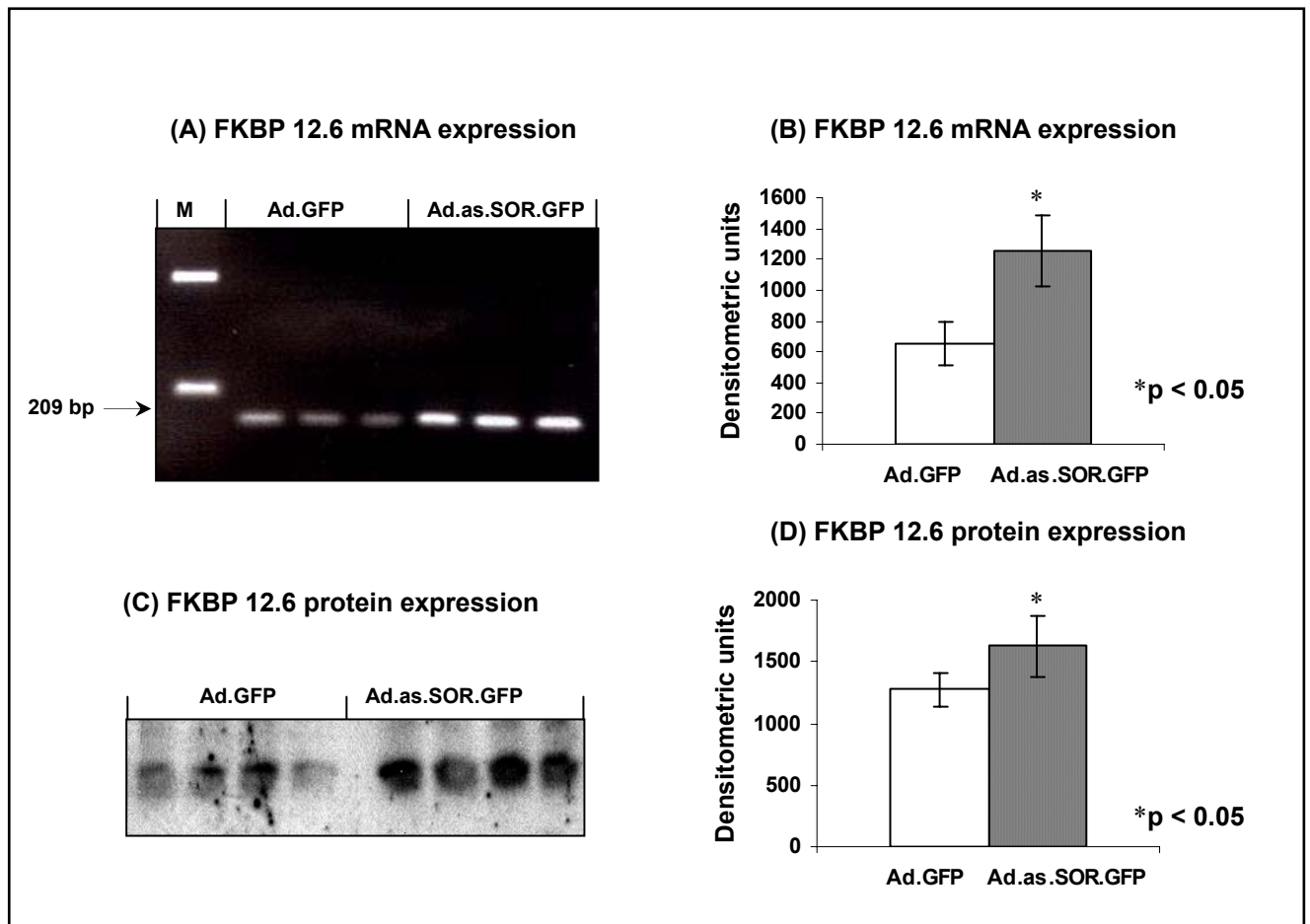
Fig. 3.17 mRNA and protein expression of FKBP 12.6 in the transfected cardiomyocytes

The effect of the reduced sorcin levels on the expression of FKBP12.6 in the transfected cardiomyocytes was investigated by RT-PCR and western blot. **(A)** RT-PCR was preformed on the total RNA preparation from the transfected cardiomyocytes. First three lanes, next to the DNA marker "M" represent the Ad.GFP transfected cardiomyocytes and the next three lanes present the Ad.as.SOR.GFP transfected cardiomyocytes. A significant upregulation of the mRNA level was observed. **(B)** Densitometric analysis revealed a statistically significant increase in the mRNA level of FKBP 12.6 in Ad.as.SOR.GFP transfected cardiomyocytes as compared to the Ad.GFP transfected cardiomyocytes (Ad.GFP 652.6 ± 139.0 DU vs. Ad.as.SOR.GFP 1253.1 ± 226.3 DU); n = 6, *p< 0.05. **(C)** Western blot using the cell lysate from the transfected cardiomyocytes was performed by utilizing the anti-FKBP 12.6 antibody. First four lanes present the FKBP12.6 protein expression in Ad.GFP transfected cardiomyocytes and the next four lanes in Ad.as.SOR.GFP transfected cardiomyocytes. A significant increase in the protein levels of FKBP 12.6 in Ad.as.SOR.GFP as compared to the control Ad.GFP transfected cardiomyocytes was observed. **(D)** Densitometric analysis revealed a statistically significant increase in the FKBP 12.6 protein level in Ad.as.SOR.GFP transfected cardiomyocytes as compared to the control (Ad.GFP 1273.7 ± 142.2 DU vs. Ad.as.SOR.GFP 1626.0 ± 242.6 DU); n = 6, *p< 0.05.

RT-PCR using specific primers for FKBP 12.6 followed by densitometric analysis revealed a significant

increase in mRNA level of FKBP 12.6 in Ad.as.SOR.GFP transfected cardiomyocytes as compared to Ad.GFP transfected cardiomyocytes (Ad.GFP 652.6 ± 139.0 DU vs. Ad.as.SOR.GFP 1253.1 ± 226.3 DU); n = 6, *p<0.05 (Fig. 3.17-A&B).

Upregulation of the mRNA level was accompanied by statistically significant upregulated protein level of FKBP12.6 in Ad.as.SOR.GFP transfected cardiomyocytes as compared to Ad.GFP transfected cardiomyocytes as judged by the immunoblot of cell lysate from the transfected cells using anti-FKBP12.6 antibody and analyzing the obtained signals by densitometry (Ad.GFP 1273.7 ± 142.2 DU vs. Ad.as.SOR.GFP 1626.0 ± 242.6 DU); n = 6, *p<0.05 (Fig. 3.17-C&D).

3.7.5 Triadin

Triadin, an integral sarcoplasmic reticulum protein binds to the high capacity calcium binding protein calsequestrin and anchors calsequestrin to the ryanodine receptors.
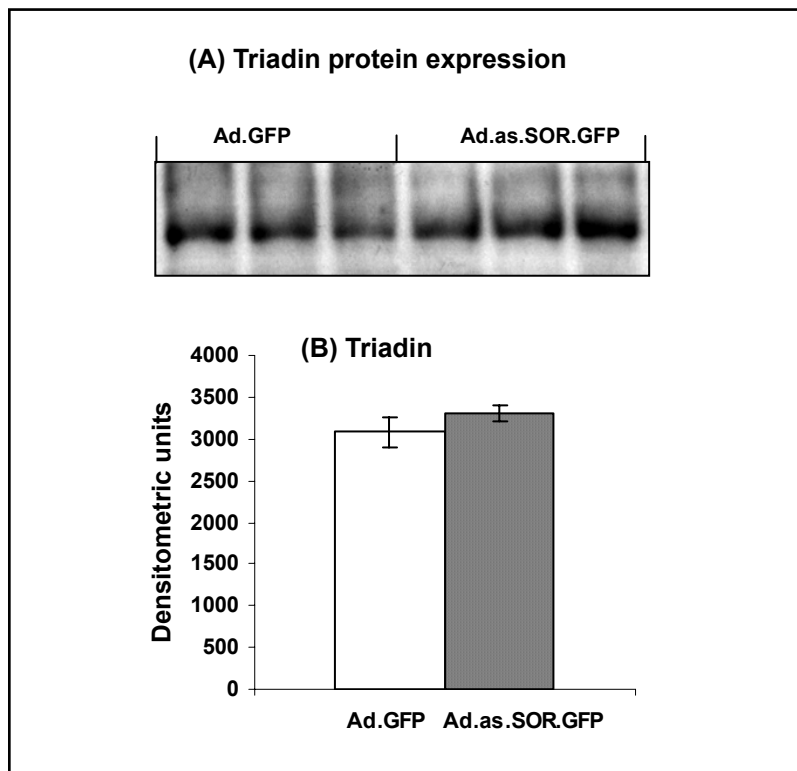
**Fig. 3.18 Triadin expression in the transfected cardiomyocytes**

(A) Cell lysate obtained from the transfected cardiomyocytes were subjected to western blot by utilizing the anti-triadin antibody. First three lanes represent the protein expression of triadin in Ad.GFP transfected cardiomyocytes and the next three lanes in Ad.as.SOR.GFP transfected cardiomyocytes. No significant difference was observed in between the two groups. **(B)** Densitometry on the obtained signals revealed no significant difference in triadin expression in Ad.as.SOR.GFP transfected cardiomyocytes as compared to the Ad.GFP transfected cardiomyocytes (Ad.GFP 3084.3 ± 180.8 DU vs. Ad.as.SOR.GFP 3294.5 ± 95.3 DU); n = 6, *p< 0.05.

The triadin-calsequestrin-ryanodine receptor interaction is calcium sensitive and is indicated to modulate the intracellular calcium handling. To analyze whether downregulation of sorcin affects the expression of triadin, western blot utilizing the anti-triadin antibody was performed in cell lysate obtained from the transfected

cardiomyocytes (Fig. 3.18-A). Densitometric analysis of the signals obtained revealed no significant alteration in the protein expression of triadin in Ad.as.SOR.GFP transfected cardiomyocytes as compared to the control Ad.GFP transfected cardiomyocytes. (Ad.GFP 3084.3 ± 180.8 DU vs. Ad.as.SOR.GFP 3294.5 ± 95.3 DU); n = 6, *p< 0.05 (Fig. 3.18-B).

3.8 *In vivo* adenoviral based sorcin gene delivery in adult rat hearts

The physiological and biochemical experiments performed on Ad.as.SOR.GFP transfected cardiomyocytes clearly indicated the role of sorcin in intracellular calcium handling. To examine whether the effect of downregulation of sorcin on the cellular level is reproducible *in vivo*, a catheter based intracoronary adenoviral sorcin gene delivery was conducted.
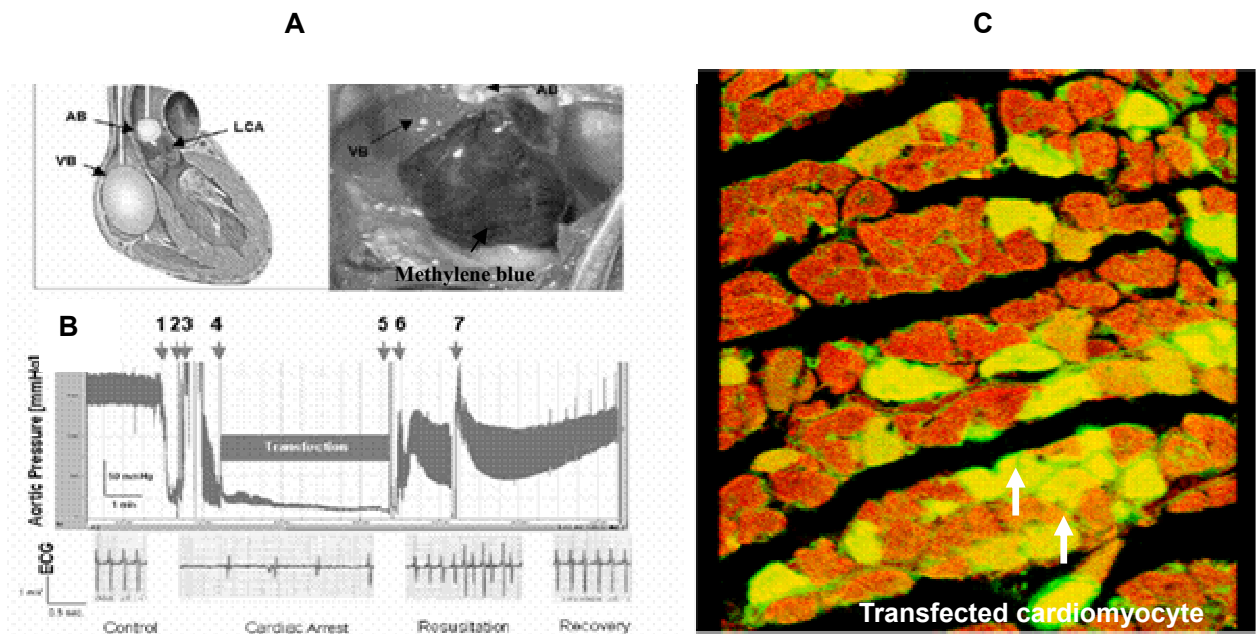

Fig. 3.19 *In vivo* transfection of adult rat hearts using a catheter based approach
(**A**) The adenoviral based sorcin gene delivery was achieved by catheter based intracoronary injections. Coronary circulation was isolated by aortic occlusion created by arterial balloon (AB) and right atrial occlusion was created by venous balloon catheter (VB). The technique resulted in cardiac specific delivery as illustrated by injection of methylene blue via the aterial balloon catheter. (**B**) Different phases of *in vivo* gene delivery: phase 1-2 represents the inflation of AB and VB respectively, phase 3 represents the cardiac arrest, phase 4 represents the injection of adenoviral suspension, phase 5 reprents the deflation of AB and VB. Phase 6 represnts the cardiopulmonary resuscitation and phase 7 represents the recovery phase (Modified from Ding et al., 2004). (**C**) Transverse slices of *in vivo* transfected hearts were used for immunofluorescence staining. Expression of GFP was used as the parameter of successful transfection. A transfection rate of 30-60% was achieved.

Male wistar rats (240-350 grams) were subjected to transfection of Ad.as.SOR.GFP (n=6) and Ad.GFP (n=6) using the injection method of Ding et al. (2004). The adenovirus was injected through a balloon catheter into right and left ventricular coronary arteries. During the injection, the balloon was inflated in the ascending aorta. To minimize reflow through coronary veins a second venous balloon catheter was placed and inflated in

the right atria (Fig. 3.19-A). The heart stopped beating under inflating conditions for approximately 3 min. Exposure of the adenovirus and transfection of the myocardium was optimal under no flow condition. After 3 min of adenoviral exposure, the animal was resuscitated using epinephrine (Fig. 3.19-B).
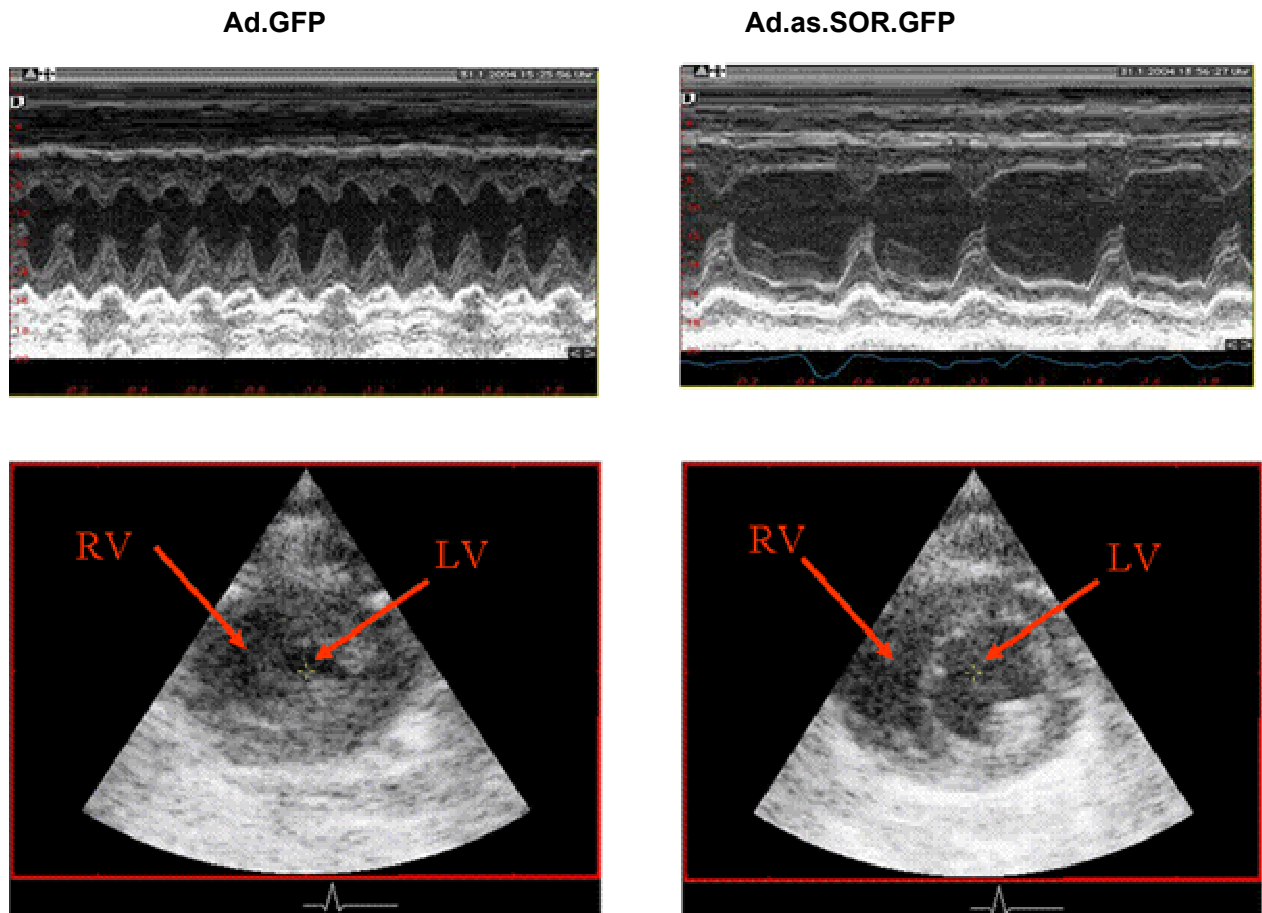
Ad.GFP   **Ad.as.SOR.GFP**

Fig 3.20 M-Mode echocardiography transversal two chamber view in antisense sorcin (Ad.asSOR.GFP) and control rat hearts (Ad.GFP)
Decreased expression of Sorcin resulted in severe dilatation of left ventricular (LV) chamber size after 12 days of transfection in comparison to control transfected hearts. Please note also the right ventricular chamber dimensions that were significantly enlarged in the Ad.ASSOR.GFP transfected hearts. Heart rate was significantly reduced in the Ad.as.Sor.GFP transfected hearts.

After hemodynamic stabilization, the animals were returned to the cages for post interventional recovery. Immunostaing was performed on the transversal slices of the *in vivo* transfected hearts. Successfully transfected cardiomyocytes exhibited green fluorescence when observed at 473 nm (Fig. 3.19-C). The rate of transfection between 30-65 % was achieved with this technique. To assess the effect of Ad.as.SOR.GFP on cardiac function *in vivo*, echocardiography was performed pre injection (day 0), at day 7 and day 12 to monitor contractile function, end-systolic and end-diastolic diameters. M-Mode as well as transversal two-chamber views of Ad.asSOR.GFP and Ad.GFP transfected hearts were used.
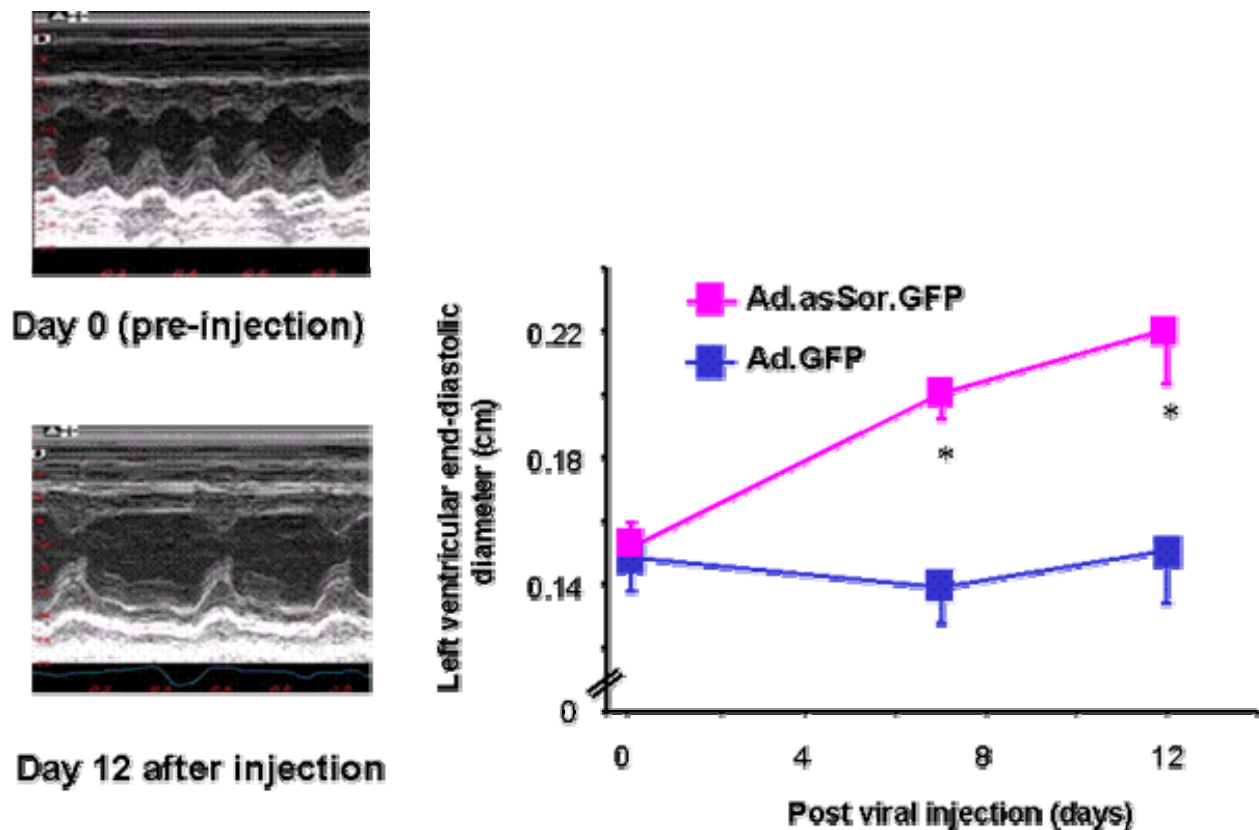
Fig 3.21 M-Mode echocardiography in antisense sorcin (Ad.as.SOR.GFP) and control rat hearts (Ad.GFP)
Decreased expression of sorcin resulted in severe dilatation of rat hearts after 12 days of transfection as judged by end-diastolic parameters (*$p < 0.05$). The control transfected hearts remained unchanged.

Fig 3.20 depicts M-mode echocardiography and transversal two chamber view in control (Ad.GFP) and sorcin downregulated (Ad.as.Sor.GFP) hearts at day 12 after adenoviral injection. Decreased expression of sorcin resulted in significant dilatation as well as right and left ventricular enlargement in Ad.asSOR.GFP.

As judged by the left ventricular end-diastolic diameters, Ad.as.SOR.GFP transfected hearts displayed significantly ($p < 0.05$) increased chamber dimensions. The dilatation of the left ventricular size increased with prolonged transfection time (Fig. 3.21). Fractional shortening was significantly reduced in Ad.as.SOR.GFP indicating diminished contractility in these hearts (Fig. 3.22-A). Thus, the Ad.as.SOR.GFP transfected hearts displayed functional features of dilated cardiomyopathy. In addition, Ad.as.SOR-GFP transfected hearts showed decreased heart rate in comparison to control transfected rat hearts (Ad.GFP). In both groups heart rates was decreased due to the anaesthesia with ketamine and diazepam (baseline: approximately 350 beats/min vs. anaesthesia: approximately 220 beats/min). However, transfection with Ad.as.SOR.GFP resulted in even more diminished rate as compared to Ad.GFP (Fig 3.22-B).
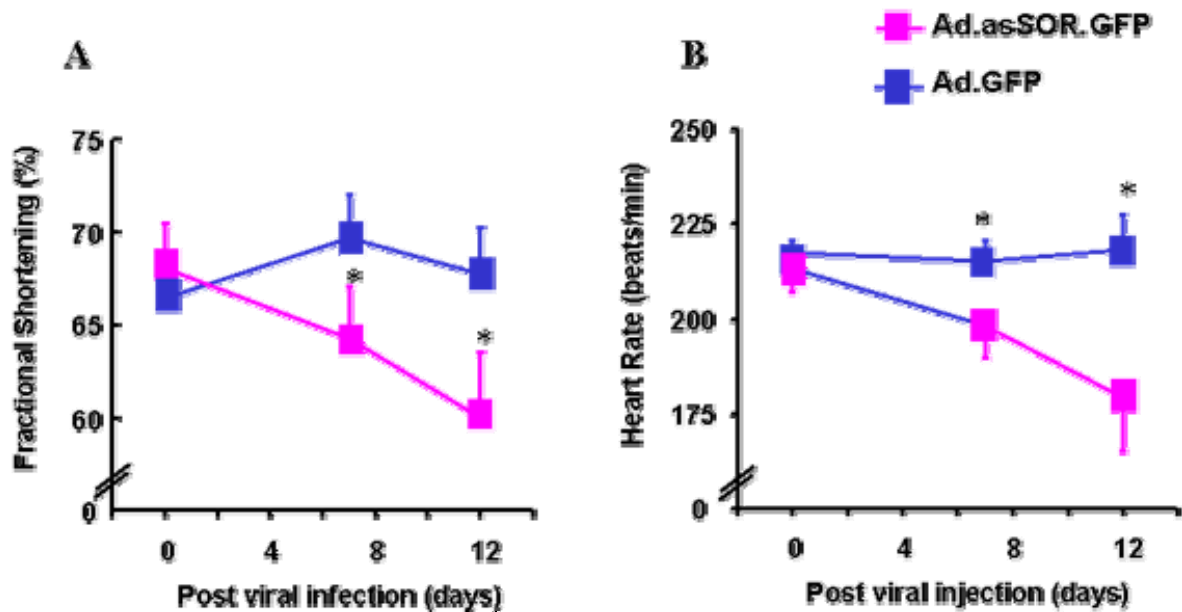
Fig 3.22 Fractional shortening and heart rate in antisense sorcin (Ad.as.SOR.GFP) and control (Ad.GFP) transfected rat hearts.
(A) Fractional shortening was significantly (*p<0.05) reduced in Ad.as.SOR.GFP (n=6) transfected rat hearts. In control transfected hearts (Ad.GFP) fractional shortening remained unchanged. **(B)** Heart rate was significantly reduced in Ad.as.SOR.GFP after 12 days of transfection, while heart rate stayed comparable in control Ad.GFP (n=6) at day 0, 7 and 12 after transfection.

After 14 days of transfection, the animals were sacrificed to study the morphological changes in the *in vivo* transfected hearts. Heart morphology and the weight was significantly (p<0.05) increased in Ad.as.SOR.GFP (n=6) in comparison to control (Ad.GFP; n=6) (Fig. 3.23-A&B). Total body weight remained similar in Ad.as.SOR.GFP and Ad.GFP (Fig. 3.23-C). This indicated hypertrophy and subsequent dilated cardiomyopathy in the anti-sense sorcin transfected heart. Liver weight was also assessed, since this may indicate heart failure. However, liver weight remained unchanged throughout the groups studied (Fig. 3.23-D).
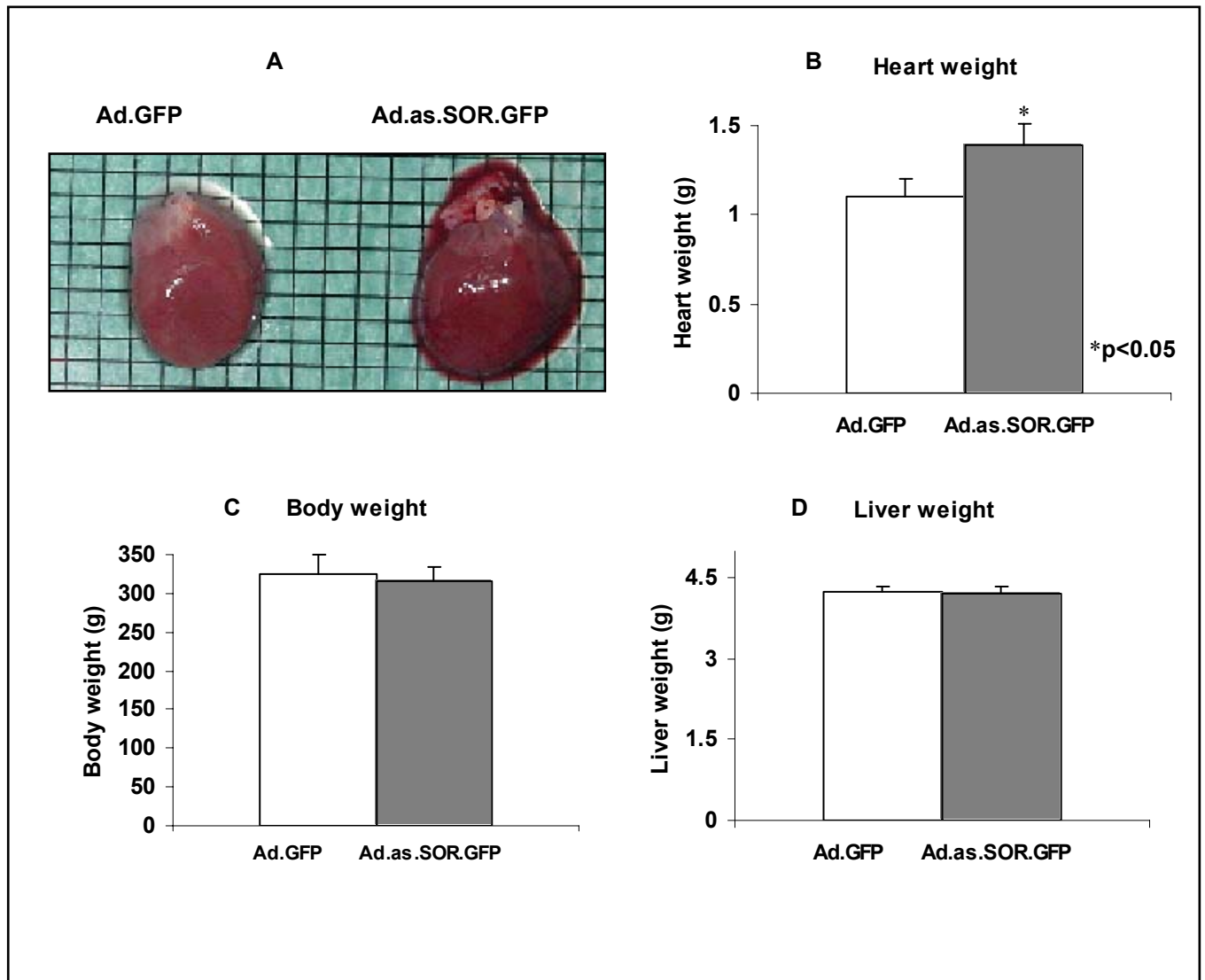
Fig 3.23 Gross morphological assessment of Ad.as.SOR.GFP (n=6) and control in vivo transfection rat hearts (Ad.GFP, n=6)
(A). Antisense transfected hearts exhibited increased gross morphology as compared to the control hearts. **(B)** Heart weight was singnificantly increased in the Ad.as.SOR.GFP transfected hearts (*p<0.05). **(C)** Body weight remained unchanged in Ad.as.SOR.GFP vs. Ad.GFP **(D)** To assess possible alteration in right heart function liver weight was evaluated. However, liver weight remained unchanged in Ad.asSOR.GFP in comparison to control.

3.9 Calcineurin signaling in the transfected cardiomyocytes

Alteration in intracellular calcium handling leads to compromised cardiac contractile performance resulting in the activation of molecular signaling pathways that regulate cardiac hypertrophy (Wilkins et al, 2004). Calcineurin, a calcium regulated Serine/Threonine protein phosphatase is activated by sustained elevation in intracellular calcium and functions as a positive regulator of cardiac hypertrophic growth through activation of nuclear factor of activated T-cells (NF-AT) transcription factors (Molkentin et al, 1998). To study whether the alteration in intracellular calcium level due to the depletion of sorcin in Ad.as.SOR.GFP transfected cardiomyocytes leads to the activation of calcineurin-NFAT signaling, calcineurin expression, calcineurin dependent phosphatase activity and nuclear translocation of NF-AT and GATA 4 expression in the transfected
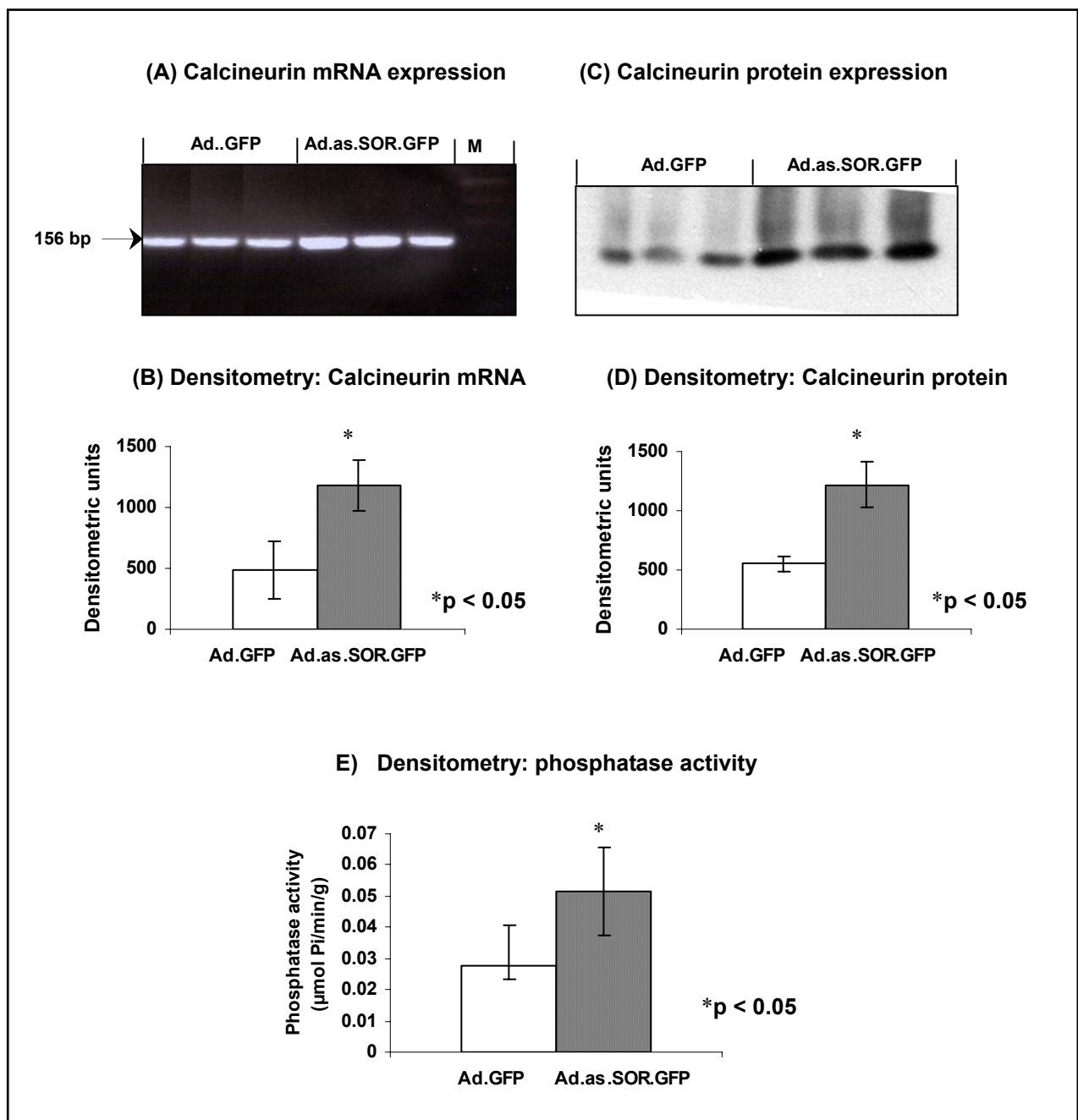
cardiomyocytes was studied.

3.9.1 Calcineurin expression

Calcineurin is comprised of a 59-63 kDa catalytic A (CN-A) subunit and a 19 kDa calcium binding (CN-B) subunit. Expression of CN-A (β) the main cardiac isoform of CN-A in mammalian cardiomyocytes was evaluated by RT-PCR and western blot followed by densitometric analysis of the obtained signals. The mRNA and protein expression of CN-A (β) was significantly increased in Ad.as.SOR.GFP transfected cardiomyocytes as compared to the Ad.GFP transfected cardiomyocytes (mRNA: Ad.GFP 482.1 ± 235.5 DU vs. Ad.as.SOR.GFP 1182.7 ± 206.6 DU, n = 6, (*p< 0.05) (Fig. 3.24-A&B); Protein: Ad.GFP 551.8 ± 65.5 DU vs. Ad.as.SOR.GFP 1217.8 ± 194.9 DU, n = 6; (*p< 0.05) (Fig. 3.24-C&D).

3.9.2 Calcineurin enzymatic activity

Calcineurin activation results in de-phosphorylation of the target protein NF-AT, which leads to nuclear translocation and activation of the hypertrophic gene program (Molkentin et al. 1998). Calcineurin phosphatase activity was measured by using non-radioactive serine/threonine phosphatase assay. A significant increase in calcineurin phosphatase activity was observed in Ad.as.SOR.GFP cardiomyocytes as compared to the Ad.GFP transfected cardiomyocytes (Ad.GFP 0.028 ± 0.013 µmol Pi/min/g vs. Ad.as.SOR.GFP 0.052 ± 0.014µmol Pi/min/g) n = 6; *p< 0.05 (Fig. 3.24-E).

(A) Calcineurin mRNA expression

(C) Calcineurin protein expression

(B) Densitometry: Calcineurin mRNA

(D) Densitometry: Calcineurin protein

E) Densitometry: phosphatase activity

Fig 3.24 Expression of CN-A (β) and calcineurin dependent phosphatase activity in the transfected cardiomyocytes

A) RT-PCR was performed on the total RNA isolated form the transfected cardiomyocytes by using CN-A (β) specific primers. The RT-PCR revealed increased mRNA expression of CN-A (β) in Ad.as.SOR.GFP transfected cardiomyocytes as compared to the control. **(B)** Densitometric analysis of the obtained signals revealed a significant increase in the mRNA expression of CN-A (β) in the Ad.as.SOR.GFP transfected cardiomyocytes as compared to the control (Ad.GFP 482.1 ± 235.5 DU vs. Ad.as.SOR.GFP 1182.7 ± 206.6 DU), n = 6; *p< 0.05. **(C)** Cell lysate from the transfected cardiomyocytes was used for the western blot utilizing anti-CN-A (β) antibody. Western blot indicated increased expression of CN-A (β) in the Ad.as.SOR.GFP transfected cardiomyocytes as compared to the control. **(D)** Densitometric analysis revealed significant increase in the Protein expression of CN-A (β) in Ad.as.SOR.GFP transfected cardiomyocytes as compared to the Ad.GFP transfected cardiomyocytes (Ad.GFP 551.8 ± 65.5 DU vs. Ad.as.SOR.GFP 1217.8 ± 194.9 DU), n = 6; *p< 0.05.**(E)** A significantly increased calcineurin phosphatase activity was observed in the Ad.as.SOR.GFP transfected cardiomyocytes as compared to the Ad.GFP transfected cardiomyocytes.

3.9.3 Expression and nuclear translocation of NF-AT in the transfected cardiomyocytes

Activated calcineurin dephosphorylates cytosolic NF-AT transcription factors resulting in their nuclear translocation (Molkentin et al., 1998, Ritter et al., 2002). To investigate whether increased calcineurin phosphatase activity in Ad.as.SOR.GFP transfected cardiomyocytes affects the expression and dephosphorylation of NF-ATc$_3$, one of the main NF-ATc isoform expressed in the cytosol of mammalian cardiomyocyte, the mRNA expression and nuclear translocation of NF-ATc$_3$ was evaluated in the transfected cardiomyocytes. RT-PCR using NF-ATc$_3$ specific primers exhibited significant increase in the NF-ATc$_3$ mRNA expression in the Ad.as.SOR.GFP transfected cardiomyocytes as compared to the Ad.GFP transfected cardiomyocytes (Ad.GFP 641.5 ± 77.0 DU vs. Ad.as.SOR.GFP 905.9 ± 21.2 DU); n = 6, *p<0.05 (Fig.3.25-A&B). To investigate the nuclear translocation of NF-ATc$_3$, western blots from cytosolic and nuclear fraction of the transfected cardiomyocytes were performed. Signals obtained from western blot were analyzed by densitometry. A significant decrease in the NF-ATc$_3$ level was observed in the cytosolic fraction (Ad.GFP 1800.0 ± 79.1 DU vs. Ad.as.SOR.GFP 1180.8 ± 270.5 DU); n = 6, *p<0.05 (Fig.3.25-C&D) in contrast to the increased NF-ATc$_3$ level in the nuclear fraction (Ad.GFP 717.0 ± 102.0 DU vs. 901.1 ± 35.9 Ad.as.SOR.GFP DU); n = 6, *p< 0.05 (Fig. 3.25-C&E) of the Ad.as.SOR.GFP transfected cardiomyocytes indicating an increased de-phosphorylation and nuclear translocation of NF-ATc$_3$ in the Ad.as.SOR.GFP transfected cardiomyocytes as compared to the control Ad.GFP transfected cardiomyocytes. The dephosphorylated fraction (nuclear fraction of NF-ATc$_3$ migrated faster on the gel as compared to the phosphorylated (cytosolic fraction) of NF-ATc$_3$.
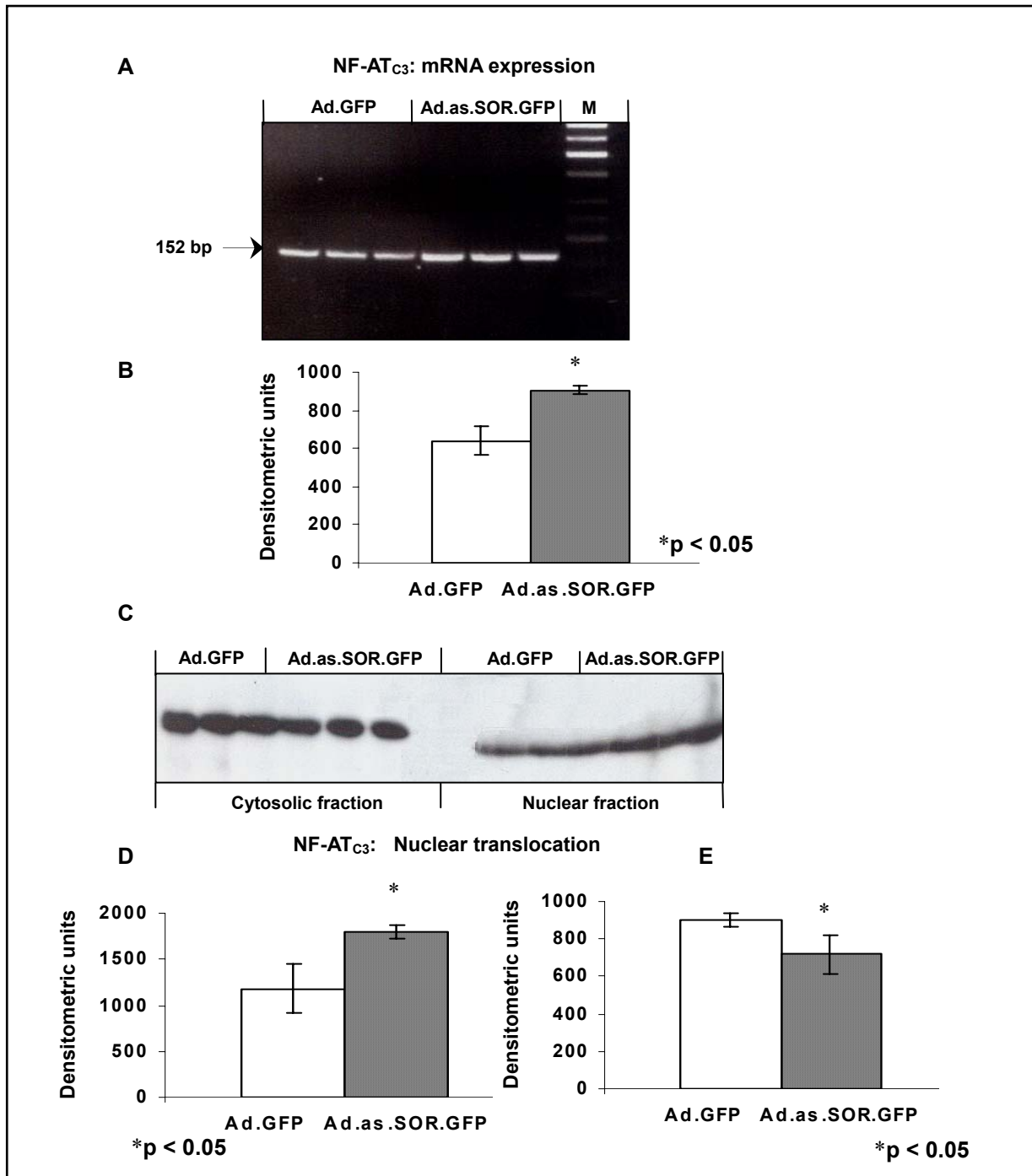
Fig. 3.25 mRNA expression and nuclear translocation of NF-ATc₃ in the transfected cardiomyocytes

(A) mRNA expression of NF-ATc$_3$ was investigated in the transfected cardiomyocytes. RT-PCR using primers specific for NF-ATc$_3$ was performed on the total RNA isolated from the transfected cardiomyocytes. (B) Densitometric analysis performed on the signals obtained from the RT-PCR revealed significant increase in the NF-ATc$_3$ mRNA expression in Ad.as.SOR.GFP transfected cardiomyocytes as compared to the Ad.GFP transfected cardiomyocytes (Ad.GFP 641.6 ± 77.1 DU vs. Ad.as.SOR.GFP 905.9 ± 21.3 DU); n = 6, *p< 0.05. (C) Western blot was performed on the cytosolic and nuclear fractions of the transfected cardiomyocytes using an anti- NF-ATc$_3$ antibody. In the cytosolic fraction depressed level of NF-ATc$_3$ protein was observed in the Ad.as.SOR.GFP transfected cardiomyocytes as compared to the Ad.GFP transfected cardiomyocytes, but in the nuclear fraction the NF-ATc$_3$ protein level was increased in the Ad.as.SOR.GFP transfected cardiomyocytes as compared to the Ad.GFP transfected cardiomyocytes. (D) Densitometric analysis revealed significant decrease of NF-ATc$_3$ in the cytosolic fraction and (E) significant increase in the dephosphorylated NF-ATc$_3$ in the nuclear fraction of the Ad.as.SOR.GFP transfected cardiomyocytes as compared to the Ad.GFP transfected cardiomyocytes (n = 6; *p< 0.05).

3.9.4 GATA-4 expression in the transfected cardiomyocytes

GATA-4 is one of the main nuclear transcription factors that interacts with and is activated by de-phosphorylated NF-ATc$_3$ resulting in the induction of genes typical of cardiac hypertrophy (Molkentin et al, 1998, Ritter, et al, 2002). Expression of GATA-4 was investigated in the transfected cardiomyocytes by RT-PCR and western blot. mRNA expression of GATA-4 was significantly upregulated in Ad.as.SOR.GFP transfected cardiomyocytes as compared to the control Ad.GFP transfected cardiomyocytes (Ad.GFP 564.0 ± 65.3 DU vs. Ad.as.SOR.GFP 762.3 ± 9.8 DU); n = 6, *p< 0.05 (Fig.3.26-A&B).
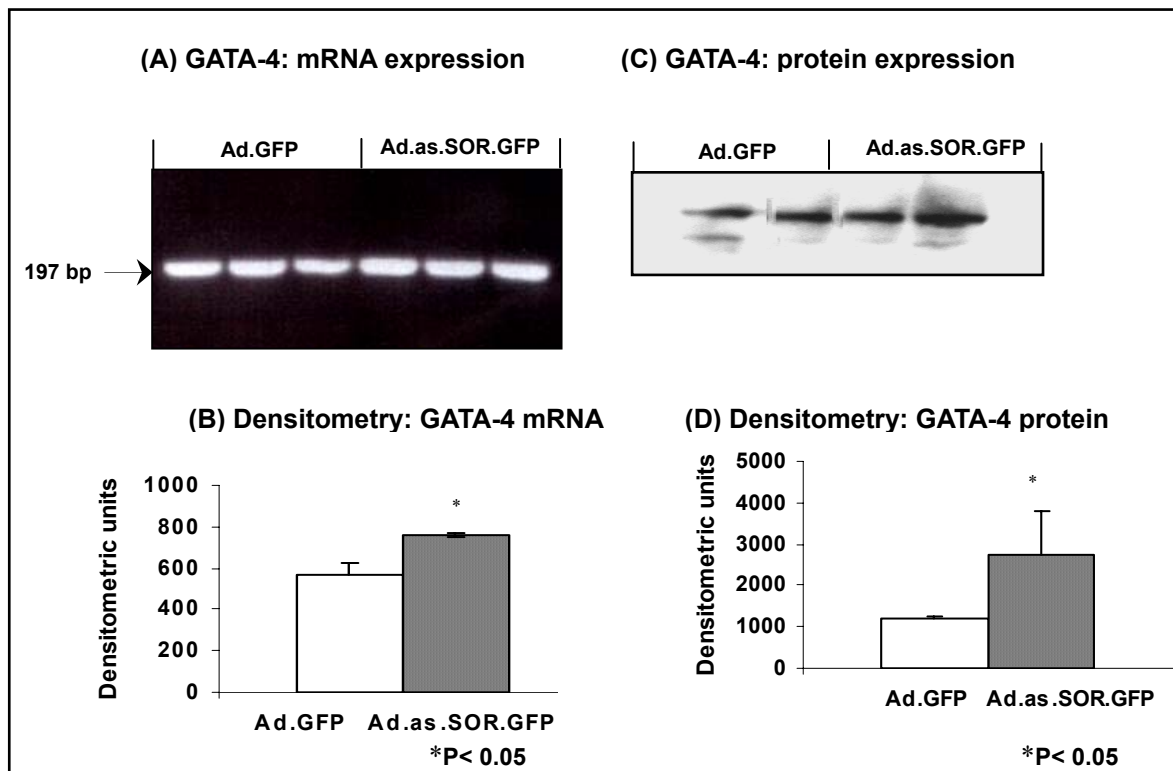
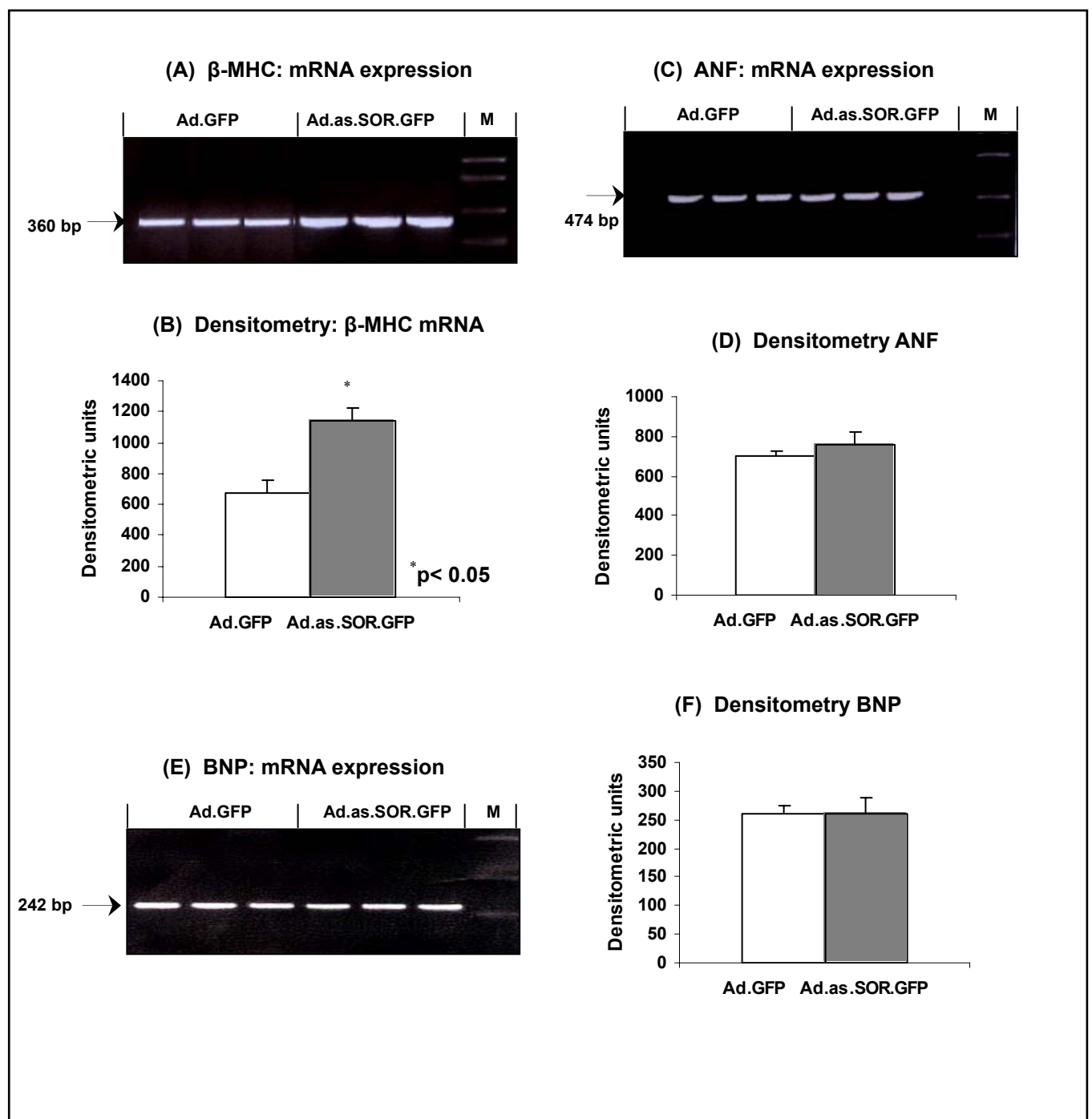**Fig. 3.26 Expression of GATA-4 in the transfected cardiomyocytes**

(A) Transfected cardiomyocytes were harvested for the total RNA preparation. RT-PCR was performed using GATA-4 specific primers. **(B)** Densitometric analysis revealed a significant increase in the mRNA expression of GATA-4 in the Ad.as.SOR.GFP transfected cardiomyocytes as compared to the Ad.GFP transfected cardiomyocytes (Ad.GFP 564.0 ± 65.3 DU vs. Ad.as.SOR.GFP 762.3± 9.8 DU); n = 6, *p< 0.05. **(C)** Protein expression of the GATA4 was investigated in the cell lysate of transfected cardiomyocytes with western blot utilizing anti-GATA-4 antibody. **(D)** Densitometric analysis of the western blot indicated significant increase in the GATA-4 protein expression in the Ad.as.SOR.GFP transfected cardiomyocytes as compared to the control Ad.GFP transfected cardiomyocytes (Ad.GFP 1202.8 ± 57.2 DU vs. Ad.as.SOR.GFP 2746.7 ± 506.5 DU); n = 6, *p< 0.05.

Morevever, significant increase in the protein expression of GATA-4 was also observed in the Ad.as.SOR.GFP transfected cardiomyocytes as compared to the control Ad.GFP transfected cardiomyocytes (Ad.GFP 1202.8 ± 57.2 DU vs. Ad.as.SOR.GFP 2746.7 ± 506.5 DU); n = 6, *p< 0.05 (Fig. 3.26-C&D).

3.9.5 Expression of cardiomyopathic marker genes in the

transfected cardiomyocytes

mRNA expression of β- myosin heavy chain (β-MHC), atrial natriuretic factor (ANF) and B-type natriuretic peptide (BNP) was investigated in Ad.as.SOR.GFP transfected cardiomyocytes followed by densitometric analysis to analyze whether the depletion of sorcin leads to the induction fetal cardiac genes as markers of cardiac hypertrophy. mRNA expression of β-MHC was significantly increased in Ad.as.SOR.GFP transfected cardiomyocytes as compared to the Ad.GFP transfected cardiomyocytes (Ad.GFP 674.0 ± 87.1 DU vs. Ad.as.SOR.GFP 144.4 ± 84.4 DU); n = 6, *p< 0.05 (Fig. 3.27-A&B). No significant alteration was observed in the mRNA expression of ANF (Ad.GFP 700.4 ± 24.3 DU vs. Ad.as.SOR.GFP 755.5 ± 66.1 DU); n = 6, (Fig. 3.27-C&D) and BNP (Ad.GFP 260.81 ± 12.76 DU vs. Ad.as.SOR.GFP 261.27 ± 28.49 DU); (Fig. 3.27-D&E) in the Ad.as.SOR.GFP transfected cardiomyocytes as compared to the control Ad.GFP transfected cardiomyocytes (Ad.GFP 564.0 ± 65.3 DU vs. Ad.as.SOR.GFP 762.3 ± 9.8 DU); n = 6.

(A) β-MHC: mRNA expression

(C) ANF: mRNA expression

(B) Densitometry: β-MHC mRNA

(D) Densitometry ANF

(E) BNP: mRNA expression

(F) Densitometry BNP

Fig.3.27 Expression of β-MHC, ANF and BNP in Ad.as.Sor.GFP transfected cardiomyocytes

Total RNA was isolated from the transfected cardiomyocytes, RT-PCR was performed using specific primers for β-myosin heavy chain (β-MHC), atrial natriuretic factor (ANF) and B-type natriuretic peptide (BNP). Products obtained from the RT-PCR were analyzed on 2% agarose gel. **A**, **C** and **E** represents the mRNA expression profile of β-MHC, ANF and BNP respectively. Densitometric analysis of obtained signals was performed. **B**, **D** and **F** present the densitometric analysis of β-MHC, ANF and BNP respectively. mRNA expression of β-MHC was significantly upregulated in Ad.as.SOR.GFP transfected cardiomyocytes as compared to the Ad.GFP transfected cardiomyocytes (Ad.GFP 674.0 ± 87.1 DU vs. Ad.as.SOR.GFP 144.4 ± 84.4 DU); n = 6, $p < 0.05$. mRNA expression of ANF and BNP appeared unaltered and no significant alteration was observed n = 6; $p < 0.05$.

4. Discussion

Myocardial Ca^{2+} cycling and Ca^{2+} dependent signaling pathways play a vital role in cardiac hypertrophy and heart failure. Thus, an adequate and efficient Ca^{2+} handling is the essential condition for effective functioning of the heart. Decreased peak systolic Ca^{2+} with prolongation of the duration of Ca^{2+} transient has been reported to be responsible for the systolic dysfunction, such as reduced force generation capacity and slower rates of force decay (Beuckelmann et al., 1992, Wehrens et al., 2003). Slower rates of SR Ca^{2+} uptake and various other changes in determinants of Ca^{2+} efflux produce rate dependent elevation in diastolic Ca^{2+}, which is responsible for diastolic defects in the failing heart (Schwinger et al., 1995). These key alterations in heart failure warrant further evaluation of proteins involved in regulatory mechanisms. In this respect, the Ca^{2+} binding protein, sorcin has been under investigation for its role in cardiac excitation contraction coupling.

Sorcin, a penta E-F hand family protein associates with cardiac ryanodine receptors (Meyers et al., 1995), L-type Ca^{2+} channel (Meyers et al., 1998) and modulates excitation contraction coupling in the heart. Interaction of sorcin with SR Ca^{2+} ATPase has also been implicated. All these interactions have projected sorcin as a potential regulator of intracellular Ca^{2+} homeostasis. Some studies reported a positive role of sorcin on the cardiomyocyte contractility (Frank et al., 2005, Matsumoto et al., 2005) and even indicated the capability of sorcin in rescuing the heart from the abnormal contractility in diabetic cardiomyopathy (Suarez et al., 2003). Other studies claimed decreased contractility and significantly depressed calcium transients in the sorcin overexpressing myocytes (Meyers et al., 2003, Farrell et al., 2003). Due to these discrepancies it remains unknown whether decreased expression or lack of sorcin results in phenotypical or contractility changes in the heart. The present thesis was aimed at understanding the role of sorcin in the cardiac modulation in isolated rat cardiomyocytes as well as in the whole rat hearts by using the adenoviral antisense RNA approach. Several studies have been reported with different overexpression models, for the first time this study used an adenoviral mediated sorcin downregulation approach to understand the role of sorcin in calcium handling, the effect of decreased level of sorcin on the remodeling of the heart and subsequent transcriptional regulation.

4.1 Depressed levels of sorcin and excitation contraction coupling

Adenoviral vectors have been used successfully to study the function and activity of various Ca^{2+} handling proteins (Hajjar et al., 1997, 1998, del Monte et al., 1999). A drastic decrease in the endogenous sorcin expression (74.5% on the mRNA level and 53% on the protein level) was obtained after 48 h by using the antisense adenoviral sorcin vector.

The downregulation of sorcin elicited adaptive and compensatory physiological alterations exhibited in terms of decreased cell contractility and significantly depressed Ca^{2+} transients amplitude accompanied with the decreased rate of relaxation. Frank et al. (2005) reported increased cell shortening without any alterations in the systolic kinetics of the contraction cycle (time to peak tension) as a result of a mild overexpression of sorcin (1.7 fold). Similar results were obtained in adenoviral studies displaying mild amounts of sorcin overexpression (Suarez et al., 2003, Matsumoto et al., 2005). However, other studies suggested that enhanced amounts of sorcin might diminish cardiac excitation contraction coupling resulting in a diminished Ca^{2+}

transients presumably via the binding of sorcin to RYR or LTCC (Farrel et al., 2003, Seidler et al., 2003, Meyers et al., 2003). Some disparities are attached to these findings. In a transgenic mouse model overexpressing sorcin driven by the cardiac α-MHC promoter diminished excitation contraction coupling was observed resulting in inhibited contraction and relaxation parameters. No phenotypical changes such as cardiac hypertrophy were reported. As a functional link depressed amplitudes of Ca^{2+} transients and whole cell $[Ca^{2+}]i$ were shown in transgenic isolated cardiomyocytes which suggested that diminished (I_{Ca}) was linked to a depressed activation of LTCC (Meyers et al., 2003). Seidler et al. (2003) reported no effects of overexpression of sorcin on LTCC in adenoviral transfected rabbit cardiomyocytes overexpressing sorcin. Siedler et al. (2003) reported that the diminished Ca^{2+} transients in myocytes overexpressing sorcin was due to an increased Na^{+}/Ca^{2+} exchanger activity which resulted in an outward movement of Ca^{2+} into the extracellular space accompanied by decrease in the SR Ca^{2+} content.

In contrast, a study by Suarez et al. (2004) reported that in adenoviral transfected cardiomyocytes of mouse hearts, sorcin overexpression resulted in enhanced cardiac contractility and even rescued the contractile dysfunction displayed in diabetic cardiomyopathy. These findings go in line with the present study as depleted levels of sorcin in the cardiomyocytes led to the decreased contractility, depressed amplitudes of peak systolic Ca^{2+} and prolonged Ca^{2+} transients. Similar results were obtained in the studies with adenoviral mediated mild overexpression of sorcin (Matsumoto et al., 2005). Since the overexpression studies reporting the positive effect of sorcin on contractility displayed mild over expression (1.7 fold and 3.5 fold) and the present study indicated the depressed contractility in the presence of decreased level of sorcin, it is suggested that sorcin indeed has a positive effect on the contractility and exhibits the contrasting results in terms of depressed contractility when expressed at pathologically higher levels indicating that pathologically higher concentration (> 10 fold) of sorcin might turn cardiotoxic.

4.2 Sorcin and SR Ca^{2+} content

Abnormal Ca^{2+} regulation in the myocytes is a central feature in the altered contractility of the failing heart (Hasenfuss et al., 1994, Schwinger et al., 1995, Frank et al., 2003). Decreased peak systolic Ca^{2+} with prolongation of the duration of Ca^{2+} transient has been described as the hallmarks of the failing heart (Beuckelmann et al., 1992). The central feature limiting Ca^{2+} transient amplitude is a decrease in sarcoplasmic reticulum Ca^{2+} content (Lindner et al., 1998). SR Ca^{2+} content reflects the balance between Ca^{2+} uptake (via SERCA), Ca^{2+} efflux via ryanodine receptor (RyR) and extracellular extrusion via the Na^{+}/Ca^{2+} exchanger. Thus, reduced SR content in heart failure can be attributed to diminished Ca^{2+} pumping by SERCA or increased SR Ca^{2+} leak via RYR2 (Schwinger et al., 1995, Marxs et al. ,2001). In addition, the diastolic decline of the Ca^{2+} transient is diminished due to the reduced activity of sarcoplasmic reticulum Ca^{2+} ATPase (SERCA2a) and reduced phosphorylation of phospholamban PLB (Schwinger et al., 1995, Bers et al., 1995, Schwinger et al., 1999).

The findings from the present study indicated decreased Ca^{2+} uptake by the SR in the cardiomyocytes with decreased expression of sorcin. However, incubating the SR preparations with 1 μM of recombinant sorcin enhanced the SR Ca^{2+} uptake indicating an active role of sorcin in the maintenance of SR Ca^{2+} content.

Furthermore, significantly depressed expression of sarcoplasmic reticulum ATPase was observed at mRNA as well as protein level. A recent study by Matsumoto et al. (2005) reported increased SR Ca^{2+} load in the rat cardiomyocytes with adenoviral mediated overexpression of sorcin. According to their study recombinant sorcin increased the Ca^{2+} uptake in a dose dependent manner, which goes in line with the present findings of depressed SR Ca^{2+} uptake upon transfection with adenoviral antisense sorcin inducing depressed expression of sorcin.

Suarez et al. (2004) reported an increase in SR Ca^{2+} content in the cardiomyocytes overexpressing sorcin. According to their report SR Ca^{2+} content was 49% higher in the cardiomyocytes overexpressing sorcin. They also reported enhanced peak of the systolic or upstroke phase of the Ca^{2+} transient.

In the present study the expression of phospholamban, the physiological regulator of SERCA2a was found to be unaltered. However, the SERCA2a/phospholamban ratio was decreased which resulted in the depressed activity of SERCA2a and the reduced Ca^{2+} content in SR. Decreased SERCA2a/phospholamban ratio resulting in depressed SERCA2a activity leading to reduced Ca^{2+} content in SR is well documented (Schwinger et al., 1995, Chu et al., 1998, Minamisawa et al., 1999). No alteration in the expression of RYR2 and triadin was observed which suggests that the release channel (RYR2) was in an unaltered state. The expression of FKBP12.6 was significantly increased which suggests a compensatory mechanism to restore the SR Ca^{2+} content. With respect to the SR Ca^{2+} release mechanism, RYR2 function has been shown to be significantly dependent on FKBP 12.6. RYR forms a complex with FKBP, the phosphatases PP1, PP2a and the Protein kinase A anchoring protein mAKAP (Marx et al., 2000). It has been proposed that phosphorylation of FKBP significantly modulates inactivation of RYR channels and favours a more leaky state of RYR in failing myocardium (Marx et al., 2002). The lack of FKBP 12.6 induces cardiac sudden death (Wehrens et al., 2003). Sorcin and FKBP 12.6 may act as counterparts in modulation of SR Ca^{2+} release through ryanodine channels (Lokuta et al., 1997). The mild increase in expression of FKBP 12.6 upon adenoviral downregualtion of sorcin can be seen as a compensation of sorcin effect on ryanodine receptors. Following the notion of inhibitory effects of sorcin in functional studies in cardiomyocytes *in vivo* (Meyers et al., 2003) and *in vitro* (Farrell et al., 2003, Seidler et al., 2003), depressed expression of sorcin indicate a decreased inhibition of the open probability of cardiac RYR leading to lesser released systolic Ca^{2+}. This mechanism is paired with decreased SR Ca^{2+} uptake rates that result in an insufficient storage of SR Ca^{2+}. The diminished SR Ca^{2+} uptake leads to an outward movement of Ca^{2+} outside of the myocyte via the Na^+,Ca^{2+} exchanger depleting the cardiac cell of Ca^{2+} that may be useable for subsequent contractions.

4.3 Decreased expression of sorcin: Effect on force-frequency relationship and β-adrenergic stimulation

The present study showed that the increase in frequency of stimulation was associated with a negative force-frequency relationship in cardiomyocytes with depressed sorcin, unlike the control-transfected cardiomyocytes, which exhibited flat and positive force frequency relationship. The force of contraction (FOC), judged by the cell shortening (% cell shortening) was significantly lower at stimulation frequencies ranging from 0.25 Hz to 5 Hz in cardiomyocytes with depressed sorcin expression. Significantly depressed cell

shortening (%) was observed at the baseline levels and was not augmented while increasing stimulation frequency. The difference in cell shortening remained unchanged throughout all frequencies measured (0.25 Hz to 5 Hz). Several studies demonstrated an altered force-frequency relationship in failing heart (Schwinger et al., 1992, Gwathmey et al., 1987). In these studies, force of contraction increased in nonfailing myocardium but not in diseased cardiac tissue. In this respect sorcin depleted cardiomyocytes exhibit similar force-frequency behavior as failing human myocardium. Thus, reduced sorcin levels accompanied with the alteration in SR Ca^{2+} uptake mechanism mimic the cellular and functional remodeling observed in dilated cardiomyopathy (Schwinger et al., 1993, Hasenfuss et al., 1994, Schwinger et al., 1995, Frank et al., 1998). A dose dependent increase in cell shortening in the cardiomyocytes with depressed level of sorcin as well as the control transfected cardiomyocytes upon forskolin stimulation was observed. The amount of increase in cell shortening was similar in both groups implying a preserved β-adrenergic stimulation even in the presence of lowered content of sorcin.

Frank et al., (2005) reported that adenoviral mediated mild overexpression of sorcin (1. 7 fold) in rat cardiomyocytes resulted in a dose dependent increase in cell shortening on β-adrenergic stimulation in sorcin overexpressing cardiomyocytes as well as in control group. According to this study time to peak tension remained unchanged upon β-adrenergic stimulation and no difference in the rate of relaxation between control and sorcin overexpressing cardiomyocytes was observed. This study suggested that the positive inotropic effect of sorcin was independent of β-adrenergic stimulation. Lokuta et al. (1997) showed a dissociation of sorcin following protein kinase A dependent phosphorylation under *in vitro* conditions. Following the notion that lesser binding of sorcin to the ryanodine receptor results in an increased open probability of the SR Ca^{2+} release channel, protein kinase A phosphorylation leads to an increase in force of contraction. This phenomenon was also observed in the present study in cell shortening experiments in antisense transfected cardiomyocytes. However, protein kinase A is responsible for phosphorylating several other targets in the cardiomyocytes, such as phospholamban (Frank et al., 2000), L-type Ca^{2+}-channels (Van der Hayden et al., 2005), FKBP (Marks et al., 2000) and myofibrillar Troponin I (Kentish et al., 2001). All these downstream phosphorylatable target proteins influence cardiac contractility and may compensate for the decreased expression of sorcin in case of β-adrenergic stimulation. Thus, no difference in cell shortening was observed upon higher β-adrenergic stimulation with forskolin. Moreover, β-adrenergic stimulation experiments were performed after 48 h of transfection in isolated cardiomyocytes which is not similar to the chronically reduced expression of sorcin in the heart. The longer duration of time with depressed sorcin levels in the *in vivo* hearts indicated overt heart failure and dilated cardiomyopathy, which is independent of β-adrenergic stimulation.

4.4 Decreased expression of sorcin and functional remodeling of the heart

Dilated cardiomyopathy has been clinically defined as a condition with depressed systolic and diastolic function accompanied by chamber dilatation and in later stages by heart failure (Packer et al., 1990). The most common cause of heart failure is coronary artery disease, followed by hypertension and valvular pathologies. The initial cardiac insult is accompanied by impaired contractility, ventricular remodeling (changes in wall thickness and/or volume) and activation of the sympathetic nervous system activity as compensatory response

to maintain cardiac output (Hunt, et al., 2001). Although these responses initially support cardiac output, they eventually lead to abnormalities like chamber dilation, fibrosis as well as functional abnormalities that ultimately restrict cardiac performance and result in cardiac failure. Along these lines, downregulation of sorcin *in vivo*, followed by adenoviral antisense RNA transfer through intracoronary injection resulted in severe chamber dilation. Echocardiography revealed dramatic remodeling of the heart with ventricular enlargement, decreased heart rate and increased chamber dimension. The fractional shortening was reduced and contractility was diminished indicating the presence of dilated cardiomyopathy in the heart with depleted level of sorcin. The dilation progressed with the duration of time. After 14 days the animals were sacrificed and an increase in the heart weight was observed, while body weight and liver weight remained unchanged at this time point. All these parameters indicated that with lowered expression of sorcin the heart undergoes ventricular remodeling emphasizing the role of sorcin in contractility as well as progressive pathogenesis of heart failure. Adenoviral mediated *in vivo* gene delivery of sorcin resulted in increased fractional shortening and decreased end diastolic diameters (Frank et al., 2005). In this study, the morphology remained unchanged after 14 days of adenoviral exposure, suggesting a positive inotropic effect of sorcin under *in vivo* conditions which possibly explains the decreased contractility, and reduced fractional shortening in the hearts with depleted levels of sorcin. In transgenic mice overexpressing sorcin no changes were observed in heart weight and dimensions (Meyers et al., 2003). However, function of whole heart hemodynamics and isolated mouse cardiac myocytes revealed decreased force, Ca^{2+} transients and calcium sparks, which were mainly due to the L-type Ca^{2+} channel function. This indicated that overexpression of sorcin did not exhibit cardiac remodeling. Moreover, another *in vivo* study depicted a significant enhancement of cardiac performance upon overexpressing of sorcin in cardiomyopathic hearts (Suarez et al., 2004), another study showed that sorcin expression is significantly reduced in the rabbit model of left ventricular dysfunction (Elliot et al., 2004). The difference in these overexpression studies might arise from variation in the experimental set up and exposure of overexpressed sorcin over longer durations in a transgenic model, while high protein levels of sorcin may induce adaptive changes and more complex phenotype which could also be a result of altered Ca^{2+} handling proteins upon aging. The result from the present study in whole hearts strengthens the hypothesis that depressed levels of sorcin results in depressed contractility accompanied by ventricular remodeling of the heart complying with the findings from Frank et al (2005) that short-term exposure to sorcin and relatively low expression levels may result in a beneficial alteration of cardiac performance. The crucial role may be a dose dependent effect of sorcin on intracellular Ca^{2+} handling, with improvement of Ca^{2+} availability at low levels of overexpression and detrimental effects at depressed as well as extremely higher levels of sorcin overexpression.

4.5 Calcineurin-NF-AT signaling

The hypertrophic growth of cardiomyocytes is initiated by endocrine, paracrine, and autocrine factors that stimulate a wide array of membrane-bound receptors. Their activation results in the triggering of multiple cytoplasmic signal transduction cascades, which ultimately affects nuclear factors and the regulation of gene expression. Calcineurin has been implicated as a regulator of the hypertrophic response in conjunction with the

nuclear factor of activated T cells (NF-AT) (Molkentin et al., 2001). Calcineurin is a Serine-Threonine phosphatase that is uniquely activated by calcium-calmodulin. The calcineurin enzyme consists of a 59 to 61 kDa catalytic subunit termed calcineurin-A and a 19 kDa calcium-binding E-F hand domain containing protein called calcineurin-B. Once activated, calcineurin dephosphorylates $NF\text{-}AT_{C3}$ in the cytoplasm, resulting in its nuclear translocation (Lim et al., 2000). In the present study the cardiomyocytes with the decreased expression of sorcin exhibited increased expression of Calcineurin-A protein along with the increased calcineurin phosphatase activity as measured by using a serine/threonine phosphatase assay. Increased calcineurin activity was also confirmed by the enhanced dephosphorylation of $NF\text{-}AT_{C3}$ resulting in increased translocation of $NF\text{-}AT_{C3}$ to the nucleus. For the first time, Molkentin et al. (1998) reported that overexpression of activated calcineurin in the heart of transgenic mice resulted in profound cardiac hypertrophy that underwent a transition to dilated cardiomyopathy within 2 months. Calcineurin was subsequently shown to operate through $NF\text{-}AT_{C3}$ in the heart because transgenic mice expressing a constitutively nuclear mutant of $NF\text{-}AT_{C3}$ also demonstrated cardiac hypertrophy. The specificity of the transgenes was demonstrated by the observation that cyclosporine-A inhibited cardiac hypertrophy in calcineurin-transgenic mice, but not in $NF\text{-}AT_{C3}$ -transgenic mice (Lim, et al., 2000). Pharmacologic calcineurin inhibition attenuated dilated and hypertrophic cardiomyopathy in three different mouse models of heart disease owing to alterations in sarcomeric proteins. However, two separate studies concluded that calcineurin inhibitors had no effect in blocking pressure overload hypertrophy in rodents (Zhang et al., 1999, Ding et al., 1999). The reason for these conflicting data is not yet resolved, but factors such as effective drug dosage, age, sex of animals and activation of other hypertrophic pathways may underlie the disparities.

Two separate studies reported no change in calcineurin activity in response to pressure overload hypertrophy in the heart (Zhang et al., 1999; Meguro et al., 1999). The assessment of calcineurin enzymatic activity in cardiac protein extracts is technically difficult given the relatively low calcineurin content in the heart. Calcineurin-A activity was suggested to be significantly elevated in failed human hearts through the use of a calmodulin co-immunoprecipitation assay (Lim et al.,1999). More recently, these results were extended by the observation that calcineurin-A protein levels and total calcineurin enzymatic activity are each significantly elevated in both hypertrophied and failed human hearts (Lim et al., 2000). In the context of downregulation of sorcin the calcineurin pathway was activated and at least partially explains the development of dilated cardiomyopathy. Calcineurin is activated by chronically elevated Ca^{2+} levels (Molkentin et al., 1998). Considering the activation of calcineurin phosphatase activity, increased expression of calcineurin-A, increased nuclear translocation of $NF\text{-}AT_{C3}$ along with the diminished Ca^{2+} transients and prolonged Ca^{2+} decay upon sorcin depletion it can be concluded that calcineurin and its downstream target $NF\text{-}AT_{C3}$ contributes to the development of impaired function and heart failure. The increased signaling of the calcineurin-NFAT3 pathway contributes at least partially to the development of heart failure in hearts with depressed sorcin levels.

GATA-4 transcription factor has been shown to play an important role in cardiac development and regulation of cardiac-specific gene expression (Orkin 1995, Charron et al., 1999). The six GATA members can be divided into two subfamilies; GATA-1, -2 and -3, which are expressed in hematopoietic cells, and GATA-4, -5 and -6, which are expressed in various tissues, including the heart. Binding motifs for GATA factors have been

identified within the promoters of most cardiac expressed genes. In the present study the expression of GATA-4 significantly increased at the mRNA as well as protein level upon 48 h of adenoviral transfection (Liang et al., 2001) reported that adenoviral overexpression of GATA-4 enhanced sarcomeric organization, induced an increase in cell surface area and increased total protein accumulation in cultured neonatal cardiac myocytes. Transgenic mice with 2.5-fold overexpression of GATA-4 in the adult heart demonstrated an increase in heart to body weight ratio, histological features of cardiomyopathy, and activation of hypertrophic genes, such as ANP and BNP (Liang et al., 2001). It has been recently shown that pressure overload and hypertrophic agonists regulate gene expression via GATA-4 dependent mechanism (Hautala et al., 2001) and those hypertrophic agonists activate GATA-4 dependent gene expression by increasing GATA-4 binding or transactivating activity (Liang and Molkentin, 2002). GATA-4 is calcineurin dependent and activates corresponding subset of genes responsible for hypertrophic response. In the present study, elevated GATA-4 expression leads to the remodeling of the heart and eventually to heart failure. Whether this is solely calcineurin dependent remains unclear since other pathway may activate GATA-4 signaling as well. Adenoviral overexpression of GATA-4 was shown to enhance sarcomeric organization and increase total protein accumulation leading to development of cardiac hypertrophy (Liang et al., 2001). This implies that GATA-4 participates in hypertrophic gene expression without direct binding to a gene promoter, probably by interacting with other transcription factors present in the nucleus, such as NFAT3 and MEF2.

The present study indicated increased mRNA expression of β-MHC isoform in cardiomyocytes with depressed expression of sorcin. It is reported that pathological remodeling of the heart in rodent models is accompanied by upregulation of β-MHC expression with consequent reduction in myofibrillar ATPase activity and reduced shortening velocity of cardiac myofibres, leading to contractile dysfunction (Braunwald et al., 2000) which goes in line with the present findings. The mRNA expression of ANF and BNP was found to be unaltered in the cardiomyocytes with decresed expression of sorcin. ANF and BNP are considered as the stress marker and are often activated in cardiomyopathic animal models (Feldman et al., 1991; 1993). However, Karen et al. (1998) and Bueno et al. (2002) suggested that the pathways for cardiac hypertrophy and induction of the fetal program can at least in part be dissociated since in some hypertrophic models ANP expression was unaltered inspite of the increased BNP and β-MHC expression.

In the present study the activation of well characterized calcineurin pathway is activated due to reduced levels of sorcin. The consequences of this activation are overt cardiac dysfunction and animal as well as human cardiomyopathies. However, no single intracellular transduction cascade regulates cardiac hypertrophy in isolation, but instead each pathway operates as an integrated component of an orchestrated response. The possible activation of other pathways responsible for the hypertrophy induced by decreased expression of sorcin needs to be studied.

4.6 Conclusion

In conclusion, this study demonstrates that sorcin downregulation diminishes the cardiac contractile performance. Decreased expression of sorcin results in depressed cardiac contractility, depressed amplitude of intracellular Ca^{2+} transients and decreased rate of relaxation due to the reduced SERCA2a activity and reduced Ca^{2+} content. This ultimately leads to the left and right ventricular remodeling of the heart expressed in terms of ventricular enlargement, increased chamber dimension and decreased heart rate. This process is at least partially due to the activation of calcineurin-NFAT signaling pathway. This study establishes the concept that sorcin is an *in vivo* and *in vitro* regulator of myocardial contractility. The mechanism of action of sorcin involves regulation of cytosolic Ca^{2+} fluxes and SR Ca^{2+} content. Depletion of sorcin results in overt heart failure underlining the importance of this protein in excitation contraction coupling. The present study emphasizes the importance of antisense RNA approach as a valuable tool to identify targets that potentially improve cardiac contractility and cardiac performance especially in states of diminished cardiac output, such as heart failure. This will further increase the understanding of excitation contraction coupling and may provide new avenues to beneficially enhance cardiac performance in the therapy of myocardial diseases and heart failure.

5 References

1.   Andrews NC, Faller DV. A rapid micropreparation technique for extraction of DNA-binding proteins from limiting numbers of mammalian cells. Nucleic Acids Res 1991;19(9):2499.

2.   Arai M, Alpert NR, MacLennan DH, Barton P, Periasamy M. Alterations in sarcoplasmic reticulum gene expression in human heart failure. A possible mechanism for alterations in systolic and diastolic properties of the failing myocardium. Circ Res 1993;72(2):463-9.

3.   Baker DL, Hashimoto K, Grupp IL, Ji Y, Reed T, Loukianov E, Grupp G, Bhagwhat A, Hoit B, Walsh R, Marban E, Periasamy M. Targeted overexpression of the sarcoplasmic reticulum Ca2+-ATPase increases cardiac contractility in transgenic mouse hearts. Circ Res 1998;83(12):1205-14.

4.   Bers DM, Berlin JR. Kinetics of [Ca]i decline in cardiac myocytes depend on peak [Ca]i. Am J Physiol 1995;268(1 Pt 1):C271-7.

5.   Bers DM. Cardiac excitation-contraction coupling. Nature 2002;415(6868):198-205.

6.   Bers DM, Eisner DA, Valdivia HH. Sarcoplasmic reticulum Ca2+ and heart failure: roles of diastolic leak and Ca2+ transport. Circ Res 2003;93(6):487-90.

7.   Bers DM. Macromolecular complexes regulating cardiac ryanodine receptor function. J Mol Cell Cardiol 2004;37(2):417-29.

8.   Bers DM, Guo T. Calcium signaling in cardiac ventricular myocytes. Ann N Y Acad Sci 2005;1047:86-98.

9.   Beuckelmann DJ, Nabauer M, Erdmann E. Intracellular calcium handling in isolated ventricular myocytes from patients with terminal heart failure. Circulation 1992;85(3):1046-55.

10.   Braunwald E, Bristow MR. Congestive heart failure: fifty years of progress. Circulation 2000;102(20 Suppl 4):IV14-23.

11.   Bristow MR. The adrenergic nervous system in heart failure. N Engl J Med 1984;311(13):850-1.

12.   Brixius K, Hoischen S, Reuter H, Lasek K, Schwinger RH. Force/shortening-frequency relationship in multicellular muscle strips and single cardiomyocytes of human failing and nonfailing hearts. J Card Fail 2001;7(4):335-41.

13.   Brixius K, Savvidou-Zaroti P, Mehlhorn U, Bloch W, Kranias EG, Schwinger RH. Increased Ca2+-sensitivity of myofibrillar tension in heart failure and its functional implication. Basic Res Cardiol 2002;97 Suppl 1:I111-7.

14.   Charron F, Paradis P, Bronchain O, Nemer G, Nemer M. Cooperative interaction between GATA-4 and GATA-6 regulates myocardial gene expression. Mol Cell Biol 1999;19(6):4355-65.

15.   Chen X, Piacentino V, 3rd, Furukawa S, Goldman B, Margulies KB, Houser SR. L-type Ca2+ channel density and regulation are altered in failing human ventricular myocytes and recover after support with mechanical assist devices. Circ Res 2002;91(6):517-24.

16.   Chidsey CA, Harrison DC, Braunwald E. Augmentation of the plasma nor-epinephrine response to exercise in patients with congestive heart failure. Nord Hyg Tidskr 1962;267:650-4.

17.   Chien KR. Genotype, phenotype: upstairs, downstairs in the family of cardiomyopathies. J Clin Invest 2003;111(2):175-8.

18.   Chu G, Luo W, Slack JP, Tilgmann C, Sweet WE, Spindler M, Saupe KW, Boivin GP, Moravec CS, Matlib MA, Grupp IL, Ingwall JS, Kranias. Compensatory mechanisms associated with the hyperdynamic function of phospholamban-deficient mouse hearts. Circ Res 1996;79(6):1064-76.

19.   Chu G, Ferguson DG, Edes I, Kiss E, Sato Y, Kranias EG. Phospholamban ablation and compensatory responses in the mammalian heart. Ann N Y Acad Sci 1998;853:49-62.

20.   Daaka Y, Luttrell LM, Lefkowitz RJ. Switching of the coupling of the beta2-adrenergic receptor to different G proteins by protein kinase A. Nature 1997;390(6655):88-91.

21.   Dash R, Frank KF, Carr AN, Moravec CS, Kranias EG. Gender influences on sarcoplasmic reticulum Ca2+-handling in failing human myocardium. J Mol Cell Cardiol 2001;33(7):1345-53.

22.   Ding B, Price RL, Borg TK, Weinberg EO, Halloran PF, Lorell BH. Pressure overload induces severe hypertrophy in mice treated with cyclosporine, an inhibitor of calcineurin. Circ Res 1999;84(6):729-34.

23.   Ding Z, Fach C, Sasse A, Godecke A, Schrader J. A minimally invasive approach for efficient gene delivery to rodent hearts. Gene Ther 2004;11(3):260-5.

24.   Elliott EB, Currie S, Smith GL. Decreased sorcin expression in a rabbit model of left ventricular dysfunction. In: Proceedings of the physiological society (communications); The Journal of Physiology; 2004.

25.   Fabiato A. Time and calcium dependence of activation and inactivation of calcium-induced release of calcium from the sarcoplasmic reticulum of a skinned canine cardiac Purkinje cell. J Gen Physiol 1985;85(2):247-89.

26.   Fan GC, Gregory KN, Zhao W, Park WJ, Kranias EG. Regulation of myocardial function by histidine-rich, calcium-binding protein. Am J Physiol Heart Circ Physiol 2004;287(4):H1705-11.

27.   Farrell EF, Antaramian A, Rueda A, Gomez AM, Valdivia HH. Sorcin inhibits calcium release and modulates excitation-contraction coupling in the heart. J Biol Chem 2003;278(36):34660-6.

28.   Feldman AM, Ray PE, Silan CM, Mercer JA, Minobe W, Bristow MR. Selective gene expression in failing human heart. Quantification of steady-state levels of messenger RNA in endomyocardial biopsies using the polymerase chain reaction. Circulation 1991;83(6):1866-72.

29.   Feldman AM, Weinberg EO, Ray PE, Lorell BH. Selective changes in cardiac gene expression during compensated hypertrophy and the transition to cardiac decompensation in rats with chronic aortic banding. Circ Res 1993;73(1):184-92.

30.   Frank K, Bolck B, Bavendiek U, Schwinger RH. Frequency dependent force generation correlates with sarcoplasmic calcium ATPase activity in human myocardium. Basic Res Cardiol 1998;93(5):405-11.

31.   Frank K, Kranias EG. Phospholamban and cardiac contractility. Ann Med 2000;32(8):572-8.

32.   Frank K, Tilgmann C, Shannon TR, Bers DM, Kranias EG. Regulatory role of phospholamban in the efficiency of cardiac sarcoplasmic reticulum Ca2+ transport. Biochemistry 2000;39(46):14176-82.

33.   Frank KF, Mesnard-Rouiller L, Chu G, Young KB, Zhao W, Haghighi K, Sato Y, Kranias EG. Structure and expression of the mouse cardiac calsequestrin gene. Basic Res Cardiol 2001;96(6):636-44.

34.   Frank KF, Bolck B, Brixius K, Kranias EG, Schwinger RH. Modulation of SERCA: implications for

the failing human heart. Basic Res Cardiol 2002;97 Suppl 1:I72-8.

35.   Frank KF, Bolck B, Erdmann E, Schwinger RH. Sarcoplasmic reticulum Ca2+-ATPase modulates cardiac contraction and relaxation. Cardiovasc Res 2003;57(1):20-7.

36.   Frank KF, Bolck B, Ding Z, Krause D, Hattebuhr N, Malik A, Brixius K, Hajjar RJ, Schrader J, Schwinger RH.. Overexpression of sorcin enhances cardiac contractility in vivo and in vitro. J Mol Cell Cardiol 2005;38(4):607-15.

37.   Go LO, Moschella MC, Watras J, Handa KK, Fyfe BS, Marks AR. Differential regulation of two types of intracellular calcium release channels during end-stage heart failure. J Clin Invest 1995;95(2):888-94.

38.   Gomez AM, Valdivia HH, Cheng H, Lederer MR, Santana LF, Cannell MB, McCune SA, Altschuld RA, Lederer WJ. Defective excitation-contraction coupling in experimental cardiac hypertrophy and heart failure. Science 1997;276(5313):800-6.

39.   Gwathmey JK, Copelas L, MacKinnon R, Schoen FJ, Feldman MD, Grossman W, Morgan JP. Abnormal intracellular calcium handling in myocardium from patients with end-stage heart failure. Circ Res 1987;61(1):70-6.

40.   Gyorke S, Gyorke I, Terentyev D, Viatchenko-Karpinski S, Williams SC. Modulation of sarcoplasmic reticulum calcium release by calsequestrin in cardiac myocytes. Biol Res 2004;37(4):603-7.

41.   Hajjar RJ, Kang JX, Gwathmey JK, Rosenzweig A. Physiological effects of adenoviral gene transfer of sarcoplasmic reticulum calcium ATPase in isolated rat myocytes. Circulation 1997;95(2):423-9.

42.   Hajjar RJ, Schmidt U, Matsui T, Guerrero JL, Lee KH, Gwathmey JK, Dec GW, Semigran MJ, Rosenzweig A. Modulation of ventricular function through gene transfer in vivo. Proc Natl Acad Sci U S A 1998;95(9):5251-6.

43.   Hajjar RJ. The promise of gene therapy as a therapeutic modality in heart failure. J Med Liban 2000;48(2):86-8.

44.   Hasenfuss G, Reinecke H, Studer R, Meyer M, Pieske B, Holtz J Holtz J, Holubarsch C, Posival H, Just H, Drexler H. Relation between myocardial function and expression of sarcoplasmic reticulum Ca(2+)-ATPase in failing and nonfailing human myocardium. Circ Res 1994;75(3):434-42.

45.   Hautala N, Tokola H, Luodonpaa M, Puhakka J, Romppanen H, Vuolteenaho O, Vuolteenaho O, Ruskoaho H. Pressure overload increases GATA4 binding activity via endothelin-1. Circulation 2001;103(5):730-5.

46.   He H, Giordano FJ, Hilal-Dandan R, Choi DJ, Rockman HA, McDonough PM, Bluhm WF, Meyer M, Sayen MR, Swanson E, Dillmann WH. Overexpression of the rat sarcoplasmic reticulum Ca2+ ATPase gene in the heart of transgenic mice accelerates calcium transients and cardiac relaxation. J Clin Invest 1997;100(2):380-9.

47.   He TC, Zhou S, da Costa LT, Yu J, Kinzler KW, Vogelstein B. A simplified system for generating recombinant adenoviruses. Proc Natl Acad Sci U S A 1998;95(5):2509-14.

48.   Hunt SA, Baker DW, Chin MH, Cinquegrani MP, Feldman AM, Francis GS. ACC/AHA guidelines for the evaluation and management of chronic heart failure in the adult: executive summary. A report of the American College of Cardiology/American Heart Association Task Force on Practice Guidelines. J Am Coll Cardiol 2001;38(7):2101-13.

49.   Hunter JJ, Chien KR. Signaling pathways for cardiac hypertrophy and failure. N Engl J Med 1999;341(17):1276-83.

50. Ji Y, Lalli MJ, Babu GJ, Xu Y, Kirkpatrick DL, Liu LH, Chiamvimonvat N, Walsh RA, Shull GE, Periasamy M. Disruption of a single copy of the SERCA2 gene results in altered Ca2+ homeostasis and cardiomyocyte function. J Biol Chem 2000;275(48):38073-80.

51. Jones LR, Suzuki YJ, Wang W, Kobayashi YM, Ramesh V, Franzini-Armstrong C, Cleemann L, Morad M. Regulation of Ca2+ signaling in transgenic mouse cardiac myocytes overexpressing calsequestrin. J Clin Invest 1998;101(7):1385-93.

52. Kadambi VJ, Ponniah S, Harrer JM, Hoit BD, Dorn GW, 2nd, Walsh RA, Kranias EG. Cardiac-specific overexpression of phospholamban alters calcium kinetics and resultant cardiomyocyte mechanics in transgenic mice. J Clin Invest 1996;97(2):533-9.

53. Kentish JC, McCloskey DT, Layland J, Palmer S, Leiden JM, Martin AF, Solaro RJ. Phosphorylation of troponin I by protein kinase A accelerates relaxation and crossbridge cycle kinetics in mouse ventricular muscle. Circ Res 2001;88(10):1059-65.

54. Koss KL, Kranias EG. Phospholamban: a prominent regulator of myocardial contractility. Circ Res 1996;79(6):1059-63.

55. Laemmli UK. Cleavage of structural proteins during the assembly of the head of bacteriophage T4. Nature 1970;227(5259):680-5.

56. Lehrach H, Diamond D, Wozney JM, Boedtker H. RNA molecular weight determinations by gel electrophoresis under denaturing conditions, a critical reexamination. Biochemistry 1977;16(21):4743-51.

57. Li L, Satoh H, Ginsburg KS, Bers DM. The effect of Ca(2+)-calmodulin-dependent protein kinase II on cardiac excitation-contraction coupling in ferret ventricular myocytes. J Physiol 1997;501 (Pt 1):17-31.

58. Liang Q, De Windt LJ, Witt SA, Kimball TR, Markham BE, Molkentin JD. The transcription factors GATA4 and GATA6 regulate cardiomyocyte hypertrophy in vitro and in vivo. J Biol Chem 2001;276(32):30245-53.

59. Liang Q, Wiese RJ, Bueno OF, Dai YS, Markham BE, Molkentin JD. The transcription factor GATA4 is activated by extracellular signal-regulated kinase 1- and 2-mediated phosphorylation of serine 105 in cardiomyocytes. Mol Cell Biol 2001;21(21):7460-9.

60. Liang Q, Molkentin JD. Divergent signaling pathways converge on GATA4 to regulate cardiac hypertrophic gene expression. J Mol Cell Cardiol 2002;34(6):611-6.

61. Lim HW, Molkentin JD. Calcineurin and human heart failure. Nat Med 1999;5(3):246-7.

62. Lim HW, De Windt LJ, Steinberg L, Taigen T, Witt SA, Kimball TR, Molkentin JD. Calcineurin expression, activation, and function in cardiac pressure-overload hypertrophy. Circulation 2000;101(20):2431-7.

63. Lindner M, Erdmann E, Beuckelmann DJ. Calcium content of the sarcoplasmic reticulum in isolated ventricular myocytes from patients with terminal heart failure. J Mol Cell Cardiol 1998;30(4):743-9.

64. Lindner M, Brandt MC, Sauer H, Hescheler J, Bohle T, Beuckelmann DJ. Calcium sparks in human ventricular cardiomyocytes from patients with terminal heart failure. Cell Calcium 2002;31(4):175-82.

65. Lokuta AJ, Meyers MB, Sander PR, Fishman GI, Valdivia HH. Modulation of cardiac ryanodine receptors by sorcin. J Biol Chem 1997;272(40):25333-8.

66. Loukianov E, Ji Y, Baker DL, Reed T, Babu J, Loukianova T, Greene A, Shull G, Periasamy M. Sarco(endo)plasmic reticulum Ca2+ ATPase isoforms and their role in muscle physiology and

pathology. Ann N Y Acad Sci 1998;853:251-9.

67. Luo W, Grupp IL, Harrer J, Ponniah S, Grupp G, Duffy JJ, Doetschman T, Kranias EG. Targeted ablation of the phospholamban gene is associated with markedly enhanced myocardial contractility and loss of beta-agonist stimulation. Circ Res 1994;75(3):401-9.

68. Luo W, Chu G, Sato Y, Zhou Z, Kadambi VJ, Kranias EG. Transgenic approaches to define the functional role of dual site phospholamban phosphorylation. J Biol Chem 1998;273(8):4734-9.

69. Maier LS, Zhang T, Chen L, DeSantiago J, Brown JH, Bers DM. Transgenic CaMKIIdeltaC overexpression uniquely alters cardiac myocyte Ca2+ handling: reduced SR Ca2+ load and activated SR Ca2+ release. Circ Res 2003;92(8):904-11.

70. Marks AR. Cardiac intracellular calcium release channels: role in heart failure. Circ Res 2000;87(1):8-11.

71. Marks AR. Clinical implications of cardiac ryanodine receptor/calcium release channel mutations linked to sudden cardiac death. Circulation 2002;106(1):8-10.

72. Marx SO, Reiken S, Hisamatsu Y, Jayaraman T, Burkhoff D, Rosemblit N, Marks AR. PKA phosphorylation dissociates FKBP12.6 from the calcium release channel (ryanodine receptor): defective regulation in failing hearts. Cell 2000;101(4):365-76.

73. Marx SO, Marks AR. Regulation of the ryanodine receptor in heart failure. Basic Res Cardiol 2002;97 Suppl 1:I49-51.

74. Matsumoto T, Hisamatsu Y, Ohkusa T, Inoue N, Sato T, Suzuki S, Ikeda Y, Matsuzaki M. Sorcin interacts with sarcoplasmic reticulum Ca(2+)-ATPase and modulates excitation-contraction coupling in the heart. Basic Res Cardiol 2005;100(3):250-62.

75. Meguro T, Hong C, Asai K, Takagi G, McKinsey TA, Olson EN, Vatner SF. Cyclosporine attenuates pressure-overload hypertrophy in mice while enhancing susceptibility to decompensation and heart failure. Circ Res 1999;84(6):735-40.

76. Meyers MB, Schneider KA, Spengler BA, Chang TD, Biedler JL. Sorcin (V19), a soluble acidic calcium-binding protein overproduced in multidrug-resistant cells. Identification of the protein by anti-sorcin antibody. Biochem Pharmacol 1987;36(14):2373-80.

77. Meyers MB, Pickel VM, Sheu SS, Sharma VK, Scotto KW, Fishman GI. Association of sorcin with the cardiac ryanodine receptor. J Biol Chem 1995;270(44):26411-8.

78. Meyers MB, Puri TS, Chien AJ, Gao T, Hsu PH, Hosey MM, Fishman GI. Sorcin associates with the pore-forming subunit of voltage-dependent L-type Ca2+ channels. J Biol Chem 1998;273(30):18930-5.

79. Meyers MB, Fischer A, Sun YJ, Lopes CM, Rohacs T, Nakamura TY Zhou YY, Lee PC, Altschuld RA, McCune SA, Coetzee WA, Fishman. Sorcin regulates excitation-contraction coupling in the heart. J Biol Chem 2003;278(31):28865-71.

80. Minamisawa S, Hoshijima M, Chu G, Ward CA, Frank K, Gu Y, Martone ME, Wang Y, Ross J Jr, Kranias EG, Giles WR, Chien KR. Chronic phospholamban-sarcoplasmic reticulum calcium ATPase interaction is the critical calcium cycling defect in dilated cardiomyopathy. Cell 1999;99(3):313-22.

81. Minamisawa S, Sato Y, Cho MC. Calcium cycling proteins in heart failure, cardiomyopathy and arrhythmias. Exp Mol Med 2004;36(3):193-203.

82. Mohiddin SA, Farrel F, Valdivia HH. A Naturally-occurring sorcin missense mutation (F112L) is associated with hypertrophic cardiomyopathy, hypertension, and impaired modulation of cardiac

ryanodine receptors. (abstract) In: Circulation; 2002; 2002. p.: 120.

83. Molkentin JD, Lu JR, Antos CL, Markham B, Richardson J, Robbins J, Grant SR, Olson EN. A calcineurin-dependent transcriptional pathway for cardiac hypertrophy. Cell 1998;93(2):215-28.

84. Molkentin JD, Dorn IG, 2nd. Cytoplasmic signaling pathways that regulate cardiac hypertrophy. Annu Rev Physiol 2001;63:391-426.

85. Munch G, Bolck B, Sugaru A, Schwinger RH. Isoform expression of the sarcoplasmic reticulum Ca2+ release channel (ryanodine channel) in human myocardium. J Mol Med 2000;78(6):352-60.

86. Netticadan T, Temsah RM, Kawabata K, Dhalla NS. Sarcoplasmic reticulum Ca(2+)/Calmodulin-dependent protein kinase is altered in heart failure. Circ Res 2000;86(5):596-605.

87. Neumann J, Schmitz W, Scholz H, von Meyerinck L, Doring V, Kalmar P. Increase in myocardial Gi-proteins in heart failure. Lancet 1988;2(8617):936-7.

88. Orkin SH. Transcription factors and hematopoietic development. J Biol Chem 1995;270(10):4955-8

89. Pack-Chung E, Meyers MB, Pettingell WP, Moir RD, Brownawell AM, Cheng I, Cheng I, Tanzi RE, Kim TW. Presenilin 2 interacts with sorcin, a modulator of the ryanodine receptor. J Biol Chem 2000;275(19):14440-5.

90. Packer M. Lack of relation between ventricular arrhythmias and sudden death in patients with chronic heart failure. Circulation 1992;85(1 Suppl):I50-6.

91. Periasamy M, Reed TD, Liu LH, Ji Y, Loukianov E, Paul RJ, Nieman ML, Riddle T, Duffy JJ, Doetschman T, Lorenz JN, Shull GE. Impaired cardiac performance in heterozygous mice with a null mutation in the sarco(endo)plasmic reticulum Ca2+-ATPase isoform 2 (SERCA2) gene. J Biol Chem 1999;274(4):2556-62.

92. Periasamy M, Huke S. SERCA pump level is a critical determinant of Ca(2+)homeostasis and cardiac contractility. J Mol Cell Cardiol 2001;33(6):1053-63.
     Pickel VM, Clarke CL, Meyers MB. Ultrastructural localization of sorcin, a 22 kDa calcium binding protein, in the rat caudate-putamen nucleus: association with ryanodine receptors and intracellular calcium release. J Comp Neurol 1997;386(4):625-34.

93. Prestle J, Janssen PM, Janssen AP, Zeitz O, Lehnart SE, Bruce L, Smith GL, Hasenfuss G. Overexpression of FK506-binding protein FKBP12.6 in cardiomyocytes reduces ryanodine receptor-mediated Ca(2+) leak from the sarcoplasmic reticulum and increases contractility. Circ Res 2001;88(2):188-94.

94. Reiken S, Lacampagne A, Zhou H, Kherani A, Lehnart SE, Ward C, Huang F, Gaburjakova M, Gaburjakova J, Rosemblit N, Warren MS, He KL, Yi GH, Wang J, Burkhoff D, Vassort G, Marks AR. PKA phosphorylation activates the calcium release channel (ryanodine receptor) in skeletal muscle: defective regulation in heart failure. J Cell Biol 2003;160(6):919-28.

95. Ritter O, Hack S, Schuh K, Rothlein N, Perrot A, Osterziel KJ, Schulte HD, Neyses L. Calcineurin in human heart hypertrophy. Circulation 2002;105(19):2265-9.

96. Rockman HA, Koch WJ, Lefkowitz RJ. Seven-transmembrane-spanning receptors and heart function. Nature 2002;415(6868):206-12.

97. Sacchetto R, Damiani E, Turcato F, Nori A, Margreth A. Ca(2+)-dependent interaction of triadin with histidine-rich Ca(2+)-binding protein carboxyl-terminal region. Biochem Biophys Res Commun 2001;289(5):1125-34.

98. Salzer U, Hinterdorfer P, Hunger U, Borken C, Prohaska R. Ca(++)-dependent vesicle release from erythrocytes involves stomatin-specific lipid rafts, synexin (annexin VII), and sorcin. Blood 2002;99(7):2569-77.

99. Sato Y, Ferguson DG, Sako H, Dorn GW, 2nd, Kadambi VJ, Yatani A, Hoit BD, Walsh RA, Kranias EG. Cardiac-specific overexpression of mouse cardiac calsequestrin is associated with depressed cardiovascular function and hypertrophy in transgenic mice. J Biol Chem 1998;273(43):28470-7.

100. Schwinger RH, Bohm M, Koch A, Erdmann E. Force-frequency relation in human heart failure. Circulation 1992;86(6):2017-8.

101. Schwinger RH, Bohm M, Schmidt U, Karczewski P, Bavendiek U, Flesch M, Krause EG, Erdmann E. Unchanged protein levels of SERCA II and phospholamban but reduced Ca2+ uptake and Ca(2+)-ATPase activity of cardiac sarcoplasmic reticulum from dilated cardiomyopathy patients compared with patients with nonfailing hearts. Circulation 1995;92(11):3220-8.

102. Schwinger RH, Munch G, Bolck B, Karczewski P, Krause EG, Erdmann E. Reduced Ca(2+)-sensitivity of SERCA 2a in failing human myocardium due to reduced serin-16 phospholamban phosphorylation. J Mol Cell Cardiol 1999;31(3):479-91.

103. Schwinger RH, Wang J, Frank K, Muller-Ehmsen J, Brixius K, McDonough AA, Erdmann E.. Reduced sodium pump alpha1, alpha3, and beta1-isoform protein levels and Na+,K+-ATPase activity but unchanged Na+-Ca2+ exchanger protein levels in human heart failure. Circulation 1999;99(16):2105-12.

104. Scott BT, Simmerman HK, Collins JH, Nadal-Ginard B, Jones LR. Complete amino acid sequence of canine cardiac calsequestrin deduced by cDNA cloning. J Biol Chem 1988;263(18):8958-64.

105. Seidler T, Miller SL, Loughrey CM, Kania A, Burow A, Kettlewell S, Teucher N, Wagner S, Kogler H, Meyers MB, Hasenfuss G, Smith GL. Effects of adenovirus-mediated sorcin overexpression on excitation-contraction coupling in isolated rabbit cardiomyocytes. Circ Res 2003;93(2):132-9.

106. Solaro RJ, Varghese J, Marian AJ, Chandra M. Molecular mechanisms of cardiac myofilament activation: modulation by pH and a troponin T mutant R92Q. Basic Res Cardiol 2002;97 Suppl 1:I102-10.

107. Suarez J, Belke DD, Gloss B, Dieterle T, McDonough PM, Kim YK, Brunton LL, Dillmann WH. In vivo adenoviral transfer of sorcin reverses cardiac contractile abnormalities of diabetic cardiomyopathy. Am J Physiol Heart Circ Physiol 2004;286(1):H68-75.

108. Sussman MA, Lim HW, Gude N, Taigen T, Olson EN, Robbins J, Colbert MC, Gualberto A, Wieczorek DF, Molkentin JD. Prevention of cardiac hypertrophy in mice by calcineurin inhibition. Science 1998;281(5383):1690-3.

109. Takeshima H, Komazaki S, Hirose K, Nishi M, Noda T, Iino M. Embryonic lethality and abnormal cardiac myocytes in mice lacking ryanodine receptor type 2. Embo J 1998;17(12):3309-16.

110. Terentyev D, Viatchenko-Karpinski S, Gyorke I, Volpe P, Williams SC, Gyorke S. Calsequestrin determines the functional size and stability of cardiac intracellular calcium stores: Mechanism for hereditary arrhythmia. Proc Natl Acad Sci U S A 2003;100(20):11759-64.

111. Ungerer M, Bohm M, Elce JS, Erdmann E, Lohse MJ. Altered expression of beta-adrenergic receptor kinase and beta 1-adrenergic receptors in the failing human heart. Circulation 1993;87(2):454-63.

112. Valdivia HH. Cardiac ryanodine receptors and accessory proteins: augmented expression does not necessarily mean big function. Circ Res 2001;88(2):134-6.

113. Van der Bliek AM, Meyers MB, Biedler JL, Hes E, Borst P. A 22-kd protein (sorcin/V19) encoded by an amplified gene in multidrug-resistant cells, is homologous to the calcium-binding light chain of calpain. Embo J 1986;5(12):3201-8.

114. van der Heyden MA, Wijnhoven TJ, Opthof T. Molecular aspects of adrenergic modulation of cardiac L-type Ca2+ channels. Cardiovasc Res 2005;65(1):28-39.

115. Ver Heyen M, Heymans S, Antoons G, Reed T, Periasamy M, Awede B, Lebacq J, Vangheluwe P, Dewerchin M, Collen D, Sipido K, Replacement of the muscle-specific sarcoplasmic reticulum Ca(2+)-ATPase isoform SERCA2a by the nonmuscle SERCA2b homologue causes mild concentric hypertrophy and impairs contraction-relaxation of the heart. Circ Res 2001;89(9):838-46.

116. Verzili D, Zamparelli C, Mattei B, Noegel AA, Chiancone E. The sorcin-annexin VII calcium-dependent interaction requires the sorcin N-terminal domain. FEBS Lett 2000;471(2-3):197-200.

117. Wehrens XH, Lehnart SE, Huang F, Vest JA, Reiken SR, Mohler PJ, Sun J, Guatimosim S, Song LS, Rosemblit N, D'Armiento JM, Napolitano C, Memmi M, Priori SG, Lederer WJ, Marks AR. FKBP12.6 deficiency and defective calcium release channel (ryanodine receptor) function linked to exercise-induced sudden cardiac death. Cell 2003;113(7):829-40.

118. Wehrens XH, Marks AR. Altered function and regulation of cardiac ryanodine receptors in cardiac disease. Trends Biochem Sci 2003;28(12):671-8.

119. Wehrens XH, Marks AR. Molecular determinants of altered contractility in heart failure. Ann Med 2004;36 Suppl 1:70-80.

120. Wei SK, Ruknudin A, Hanlon SU, McCurley JM, Schulze DH, Haigney MC. Protein kinase A hyperphosphorylation increases basal current but decreases beta-adrenergic responsiveness of the sarcolemmal Na+-Ca2+ exchanger in failing pig myocytes. Circ Res 2003;92(8):897-903.

121. Wilkins BJ, Molkentin JD. Calcium-calcineurin signaling in the regulation of cardiac hypertrophy. Biochem Biophys Res Commun 2004;322(4):1178-91.

122. Xie X, Dwyer MD, Swenson L, Parker MH, Botfield MC. Crystal structure of calcium-free human sorcin: a member of the penta-EF-hand protein family. Protein Sci 2001;10(12):2419-25.

123. Xin HB, Senbonmatsu T, Cheng DS, Wang YX, Copello JA, Ji GJ, Collier ML, Deng KY, Jeyakumar LH, Magnuson MA, Inagami T, Kotlikoff MI, Fleischer S. Oestrogen protects FKBP12.6 null mice from cardiac hypertrophy. Nature 2002;416(6878):334-8.

124. Zamparelli C, Ilari A, Verzili D, Giangiacomo L, Colotti G, Pascarella S, Chiancone E. Structure-function relationships in sorcin, a member of the penta EF-hand family. Interaction of sorcin fragments with the ryanodine receptor and an Escherichia coli model system. Biochemistry 2000;39(4):658-66.

6 Erklärung

Hiermit erkläre ich, dass ich die vorliegende Dissertation selbstständig und ohne unzulässige Hilfe angefertigt, die benutzten Quellen und Hilfsmittel vollständig angegeben und die Stellen der Arbeit, die anderen Werken in Wortlaut oder dem Sinn nach entnommen sind, in jedem Einzelfall als Entlehnung kenntlich gemacht habe; dass die Dissertation noch keiner anderen Fakultät oder Universität vorgelegt und noch nicht veröffentlicht worden ist sowie, dass ich eine solche Veröffentlichung vor Ablauf des Promotionsverfahrens nicht vornehmen werde. Die Bestimmungen der geltenden Promotionsordnung sind mir bekannt. Die von mir vorgelegte Dissertation ist von Herrn Prof. Dr. Jens Brüning und Herrn Prof. Dr. Robert H. G. Schwinger betreut worden.

Köln, 1. Dezember 2005

7 Acknowledgements

8 Publication and Abstracts

Publication

1. K.F. Frank, B. Bölck. Ding, D. Krause, N. Hattebuhr, **A. Malik**, K. Brixius, R.J. Hajjar, J. Schrader and R.H.G. Schwinger. Overexpression of sorcin enhances cardiac contractility in vivo and in vitro.J Mol Cell Cardiol 38(4): 606-614.

Abstracts

1. Frank KF, Malik AS**, Bölck B, Hajjar RJ, Schwinger RHG. Reduced sorcin expression results in decreased cardiac function, altered Ca^{2+} homeostasis and enhanced calcineurin signaling. Circulation 110: 1536 (2005)**

2. Frank KF, Bölck B, **Malik AS**, Bebernik O, Hattebuhr N, Schwinger RHG: Reduced expression but increased binding of Sorcin with the ryanodine receptor in human atrial failing myocardium. Eur Heart J 25 (Abstr. Suppl): 541 (2005).

3. Frank KF, Bölck B, **Malik AS**, Ding Z, Brixius K, Schrader J, Hajjar RJ , Schwinger RHG: Reduced sorcin expression induces decreased cardiac contractility and dilated cardiomyopathy. Eur Heart J25 (Abstr. Suppl): 2637 (2005).

4. Frank KF, Bölck B**, Malik AS**, Ding Z, Krause D, Brixius K, Hajjar RJ, Schrader J, Schwinger RHG: Adenoviral-induzierte Reduktion der Sorcin Expression resuliert in einer dilatativen Kardiomyopathie. Z Kardiol 94: Suppl 1: 749 (2005).

5. Frank KF, Hattebuhr N, **Malik AS**, Bölck B: Reduzierte Expression, jedoch erhöhte Bindung von Sorcin an den Ryanodin-Rezeptor am humanen insuffizienten, atrialen Myokard. Z Kardiol 94: Suppl 1: 1294 (2005).

6. Frank KF, Bölck B, Hattebuhr N, **Malik AS**, Schwinger RH: Verminderte Expression und verstärkte Bindung von Sorcin an den Ryanodin-Rezeptor Kanal von menschlichem insuffizientem Myokard. Z Kardiol 93(Suppl 3): P712 (2004)

7. Frank KF, Bölck B, Hattebuhr N, **Malik AS**, Schwinger RH: Decreased Ca2+-dependent binding of sorcin to annexin VII and Ca2+-release channel in human failing myocardium. Eur Heart J 24 (Abstr. Suppl): 426 (2004).

8. Frank KF, Bölck B, Hattebuhr N, **Malik AS**, Schwinger RH: Verminderte Expression und verstärkte Bindung von Sorcin an den Ryanodin-Rezeptor Kanal von menschlichem insuffizientem Myokard. Z Kardiol 93(Suppl 3): 712 (2004).

9. Frank KF, Bölck B, Ding Z, Krause D, **Malik AS**, Hajjar RJ, Schwinger RHG: Reduced Sorcin Expression Results in Dilated Cardiomyopathy. Circulation 109: 60 (2004).

9 Lebenslauf

Persönliche Daten

Name	Malik Alock Suchitra
Anschrift	Berrenrather Str, 133, Köln 50937
Heimataddresse	2/84 Sector II, Rajendra Nagar, Ghaziabad Uttar Pradesh, 20001 India
Geburtsdatum/-ort	08.07.1977 /Muzaffar Nagar, India
Staatsangehörigkeit	Indisch

Schulbildung

1982-1992	Little flowers public School, Delhi, India
1992-1994	Guru harkrishan public School, Delhi, India

Studium (Universität)

1995-1999	B. Pharm, Bangalore University, K L E College of Pharmacy, Bangalore, India
2001-2002	M.A.S (Biotechnology), University of Western Sydney, Sydney, Australia.

Doktorarbeit

Oktober 2002- Januar 2006	Promotion an der Mathematisch-Naturwissenschaftlichen Fakultät der Universität zu Köln im Fach Genetik am bei Prof. Dr. Jens Brüning und Prof. Dr. R.H.G. Schwinger

Köln, 01. Dezember 2005

10 Appendix

a. Sorcin cDNA sequence used in the present study: NM_003130

```
   1 ggcggagagg cctggcgcac agggcgaggg cggctgcggc gcagtctgca gcatggcgta
  61 cccggggcat cctggcgccg gcggcgggta ctacccaggc gggtatggag gggctcccgg
 121 agggcctgcg tttcccggac aaactcagga tccgctgtat ggttactttg ctgctgtagc
 181 tggacaggat gggcagatag atgctgatga attgcagaga tgtctgacac agtctggcat
 241 tgctggagga tacaaacctt ttaacctgga gacttgccgg cttatggttt caatgctgga
 301 tagagatatg tctggcacaa tgggtttcaa tgaatttaaa gaactctggg ctgtactgaa
 361 tggctggaga caacacttta tcagttttga cactgacagg agtggaacag tagacccaca
 421 agaattgcag aaggccctga caacaatggg atttaggttg agtccccagg ctgtgaattc
 481 aattgcaaaa cgatacagca ccaatggaaa gatcaccttc gacgactaca tcgcctgctg
 541 cgtcaaactg agggctctta cagacagctt tcgaagacgg gatactgctc agcaaggtgt
 601 tgtgaatttc ccatatgatg atttcattca atgtgtcatg agtgtttaaa tcaagaggaa
 661 gctgcatgaa tgtaatcaac attccaactg gagctctcct ttgcttgtcc tctttgcctt
 721 cggtaatatg tataaactta catcacgact ttctcttaac agctgttgta aagtttatta
 781 ctttatgtac aactgaagtt ttgttttagt tttgataata aattctttgg aactttaata
 841 agatctagtc tgttacacca tttagaactt tcctgagcca ttatcagtca tgccttattt
 901 tcttgctaaa actctatgta aatttaagta tgcaaaatgt ttaagtcaca ttatttattt
 961 ttcattgtga gacactaaaa actgttaatc agactacagc tgttatcttt cctctcctac
1021 aaagaatact ccacacataa aaacttaggt aaatgacata gacgcacttg ggtgaaataa
1081 aacaacaaaa aaggtaatcc agtaatccac gtcaggattc accttagaag tttagcacac
1141 gcccttcaaa acctgttgaa taatttgatt ggcaaatact atctgtcacc aagtcccttt
1201 ttgtcatcta tttaaacctt tgttaactct ccttaaaaat cttgtacatt ataagcttaa
1261 ctatataaaa agaaaattga tagaaaaaga ctaagggaat atatggaaat attaacaatg
1321 tttattttgg atgaatggaa ttctagatga cttttaatttt ctttatatca gtatttttca
1381 gattttctat atgctttcct tttaaaatca gattttagtt tttaaaatac tgatacatcc
1441 attttgatat accatgtatt cacactttaa aaaatacaca tagcagagta tcggaaagta
1501 tgtaccaaaa cattgatctg ctaccactg ggagtcagga tcatgagttc atcttcttcc
1561 ttcttactgc ttttccaaac attctccagt aagcaggtac tacatttata atggaaggaa
1621 tttttttaaaa aattttaagc tgtacacttt caagtaagat ctgaattcta atgctggctt
1681 gtgcctctta ctatgtggtt tggtcattat agataatgcc cagtttcagt ttccccatct
1741 ttgaaaagga gataatatgt tatctcttgg gagtagttct gaatatgaag tgtgttgata
1801 caagaagcac tgacaatgtt tctgtttctt aaatttaaaa ctggcctggt ttgccttttt
1861 tatcaagaga gcttaacaga taaaaaatga aattagtcta ttttctactt gccagcagag
1921 tatctgtctt attttaggat gcagtgtgaa acttaccatt caactgaaca actagttgtc
1981 aactaatgaa aataaaacat tttctctaag aaaaaaaaaa aaaaaaaaaa
```

b. Sorcin protein sequence: accession NM_003130.2

```
   1 maypghpgag ggyypggygg apggpafpgq tqdplygyfa avagqdgqid adelqrcltq
  61 sgiaggykpf nletcrlmvs mldrdmsgtm gfnefkelwa vlngwrqhfi sfdtdrsgtv
 121 dpqelqkalt tmgfrlspqa vnsiakryst ngkitfddyi accvklralt dsfrrrdtaq
 181 qgvvnfpydd fiqcvmsv
```